



**MODULATION DER EXPRESSION VON ENZYMEN DER  
ISOPRENOIDSYNTHESE: EFFEKTE AUF DIE V $\gamma$ 9V $\delta$ 2 T  
ZELLAKTIVIERUNG UND DAS TUMORZELLWACHSTUM**

**MODULATING THE EXPRESSION OF ENZYMES OF  
ISOPRENOID SYNTHESIS: EFFECTS ON V $\gamma$ 9V $\delta$ 2 T CELL  
ACTIVATION AND TUMOR CELL GROWTH**

Doctoral thesis for a doctoral degree at the Graduate School of  
Life Sciences, Julius-Maximilians-Universität Würzburg,  
Section of Infection and Immunity

Submitted by  
*JIANQIANG LI*  
From Hebei, China

Würzburg, 2009

Submitted on: .....

Office stamp

**Members of the *Promotionskomitee*:**

Chairperson: Prof. Thomas Müller

Primary Supervisor: Prof. Thomas Herrmann

Supervisor (Second): Prof. Roland Benz

Supervisor (Third): Prof. Alexander Steinle

Date of Public Defence: .....

Date of Receipt of Certificates: .....

谨将此论文献给我亲爱的妻子和女儿!

*This work is dedicated to my wife Haiming and my daughter  
Zhiyu whose sacrifices, which were realized by our loss of  
precious time together, were for me the most painful and  
humbling of all!*

## **ACKNOWLEDGMENTS**

First of all, I would like to gratefully acknowledge the enthusiastic supervision of Prof. Dr. Thomas Herrmann during this work. With his enthusiasm and inspiration, he helped to make science research fun for me. Throughout my PhD work, he provided encouragement, sound advice, good teaching, good company, and lots of good ideas.

I also would like to express my deep gratitude to Prof. Dr. Thomas Hünig for his great support and nice organization which create a positive work atmosphere and luxuriant study resources. Thanks a lot for his useful suggestions and interesting discussions during my work.

I must also acknowledge Dr. Volker Kunzmann for his stimulating suggestions, and provision of the crucial cell lines and chemical materials in this study.

Many special thanks go out to all our group members for their kindly help in both lab work and daily life, particularly Ingrid Müller, Elisa Monzon-Casanova, Lisa Starick, Bladimiro Rincon-Orozco, Martina Roilo, Ronald Rudolf, and Julian Redzek. Despite my handicap in German language they helped to make life much easier.

I acknowledge with utmost sincerity, the friendly atmosphere I have enjoyed, with other staffs of the institute, and with all students of graduate college for nice friendship and interesting discussions.

## SUMMARY

In all jawed vertebrates, three classes of antigen receptors have been conserved throughout the last 480 million years: Immunoglobulins (Ig),  $\alpha\beta$  T cell antigen receptors ( $\alpha\beta$  TCR) and  $\gamma\delta$  T cell antigen receptors ( $\gamma\delta$  TCR).  $\gamma\delta$  T cells respond to some danger signals such as stress, infection, and tumor malignancies and possess immunomodulatory activity. The ligands of their antigen receptors are largely unknown. TCR composition defines two major populations of human  $\gamma\delta$  T cells: V $\delta$ 1 T cells and V $\gamma$ 9V $\delta$ 2 T cells, which recognize different types of antigens and home to different tissues.

This study focuses on phosphoantigen specific V $\gamma$ 9V $\delta$ 2 T cells which only exist in human and non-human primates. This population accounts for 1%-5% of peripheral blood T-lymphocytes but their frequency can rise to 50% of total blood T cells upon infection. V $\gamma$ 9V $\delta$ 2 T cells can be activated by nonpeptide compounds with critical phosphate moieties which are termed as phosphoantigens. These include isopentenyl pyrophosphate (IPP), a key compound of isoprenoid synthesis in all organisms, and (E)-4-Hydroxy-3-methyl-but-2-enyl pyrophosphate (HMBPP), a direct precursor of IPP in DOXP pathway which only exist in eubacteria, plants, apicomplexan parasites. Its activity as phosphoantigen is at least 1000 fold higher than that of IPP. However, direct structural evidence of phosphoantigen binding to the TCR is missing so far. Moreover, V $\gamma$ 9V $\delta$ 2 T cells have potent anti-tumor activity e.g. against the B-cell lymphoma Daudi, whose V $\gamma$ 9V $\delta$ 2 T cell activating properties have been suggested to result from sensing of abnormal intracellular IPP levels by the V $\gamma$ 9V $\delta$ 2 TCR or V $\gamma$ 9V $\delta$ 2 TCR binding to other postulated ligands such as an ectopically expressed F1-ATPase or UL-16 binding protein 4 (ULBP4). Aminobisphosphonates and alkylamines were hypothesized to activate V $\gamma$ 9V $\delta$ 2 T cells indirectly by inhibiting the IPP consuming enzyme farnesyl pyrophosphates synthesis (FPPS) although off target effects of these drugs or a direct

interaction with the V $\gamma$ 9V $\delta$ 2 TCR could not be excluded.

This thesis presents new approaches for the mechanistic analysis of V $\gamma$ 9V $\delta$ 2 T cell activation. By employing retroviral transduction of FPPS specific shRNA, it shows that specific shRNA reduces expression of FPPS and is sufficient to convert hematopoietic and non-hematopoietic tumor cell lines into V $\gamma$ 9V $\delta$ 2 T cell activators. FPPS knockdown cells activated V $\gamma$ 9V $\delta$ 2 T cells as measured by increased levels of CD69 and CD107a, kill of FPPS knockdown cells and induction of IFN- $\gamma$  secretion. The IPP-synthesis-inhibiting drug mevastatin reduced V $\gamma$ 9V $\delta$ 2 T cell activation by FPPS knockdown cells or aminobisphosphonate treated cells but not activation by the phosphoantigen bromohydrin pyrophosphate (BrHPP). A reduced growth of the FPPS knockdown cells has not been observed which is different to what has been reported for aminobisphosphonate treated cells. Finally, the human B-cell lymphoma RAJI has been transduced with Tetracyclin-inducible FPPS specific shRNA and proven to gain and lose the capacity to activate V $\gamma$ 9V $\delta$ 2 TCR transductants upon doxycyclin provision or removal.

Another approach for the analysis of V $\gamma$ 9V $\delta$ 2 T cell activation is V $\gamma$ 9V $\delta$ 2 TCR transduced mouse cell lines with specificity for phosphoantigens. In contrast to the previously used V $\gamma$ 9V $\delta$ 2 TCR transduced Jurkat cells, these cells do not present phosphoantigens, and are therefore specially suited for analysis of phosphoantigen presentation. The response of the new TCR transductants to presumed V $\gamma$ 9V $\delta$ 2 TCR ligands/activators such as phosphoantigens, aminobisphosphonates or FPPS knockdown cells, depended strongly on the expression of a rat/mouse CD28 molecule by the transductants and its ligation by the (CD80) counter receptor on the ligand-presenting cell. The response is likely to reflect recognition of cognate V $\gamma$ 9V $\delta$ 2 TCR antigens since mutations in the TCR- $\delta$  chain CDR2 and 3 abolished this response but activation by TCR or CD3 specific antibodies. A major difference between TCR transductants and primary  $\gamma\delta$  T cells, was the lacking response of TCR transductants to Daudi or IPP. In addition their sensitivity to other soluble phosphoantigens was about 100 fold weaker than that of primary cells, stimulation of both cell type to CD80 expressing FPPS knock down or

aminobisphosphonates was similar. Finally, the transductants have also been used to analyze effects of over-expression or knockdown of enzymes of isoprenoid synthesis such as 3-hydroxy-3-methyl-glutaryl-CoA reductase (HMG-CoA reductase or HMGR), mevalonate-5-pyrophosphate decarboxylase (MVD), isopentenyl pyrophosphate isomerase (IDI), geranyl-geranyl pyrophosphate synthase (GGPPS) but no clear effects have been found.

In conclusion, this thesis supports the concept of V $\gamma$ 9V $\delta$ 2 T cells being sensors of a dysregulated isoprenoid metabolism and established new tools to study ligand recognition and TCR mediated activation of this T cell population. These tools will be most useful to address following questions: 1) How does the dysregulation of isoprenoid metabolism affect tumor growth? 2) What is the correlation between the modulation of IPP levels and the V $\gamma$ 9V $\delta$ 2 TCR binding or expression of other postulated ligands? 3) Are there any mevalonate pathway enzymes other than FPPS and HMGR, which play an important role in V $\gamma$ 9V $\delta$ 2 T cells activation? 4) What is/are the putative phosphoantigen-presenting molecule(s)?

## ZUSAMMENFASSUNG

In allen Kiefermäulern (Gnathostoma) haben sich drei Arten von Antigenrezeptoren über die letzten 480 Millionen Jahre erhalten: Immunglobuline (Ig),  $\alpha\beta$  T Zellantigenrezeptoren ( $\alpha\beta$  TCR) und  $\gamma\delta$  T Zellantigenrezeptoren ( $\gamma\delta$  TCR).  $\gamma\delta$  T Zellen antworten auf Gefahrensignale wie Stress, Infektion, und Tumorbildung und wirken immunmodulatorisch wobei die Liganden der  $\gamma\delta$  TCR Antigenrezeptoren weitgehend unbekannt sind. Im Menschen werden je nach Antigenrezeptorzusammensetzung zwei Hauptgruppen von humanen  $\gamma\delta$  T Zellen unterschieden, V $\delta$ 1 T Zellen und V $\gamma$ 9V $\delta$ 2 T Zellen, die unterschiedliche Antigenklassen erkennen und in unterschiedlichen Geweben zu finden sind.

Die vorliegende Arbeit widmet sich den phosphoantigenspezifischen V $\gamma$ 9V $\delta$ 2 T Zellen, die nur im Menschen und nicht-humanen Primaten zu finden ist. Diese Population stellt 1-5% der peripheren Blut T-Zellen aber ihre Frequenz kann bei Infektionen auf bis zu 50% steigen. V $\gamma$ 9V $\delta$ 2 T Zellen können durch nicht Peptid-Moleküle aktiviert werden, die sich durch eine essentielle Phosphatkomponente auszeichnen. Hierzu gehören das Isopentenyl-pyrophosphat (IPP), ein Schlüsselmolekül der Isoprenoidsynthese aller Organismen, sowie das bezüglich seiner  $\gamma\delta$  T zellaktivierenden Eigenschaften mehr als 1000fach stärkere (E)-hydroxy-3-methyl-but-2-enyl-pyrophosphat (HMBPP), dass der direkte Vorläufer des IPP im DOXP Stoffwechselweg ist, der nur bei Eubakterien, Pflanzen und apikomplexen Bakterien zu finden ist. Direkte strukturelle Belege für die Bindung von Phosphoantigenen an den  $\gamma\delta$  TCR stehen jedoch aus. Darüber hinaus besitzen V $\gamma$ 9V $\delta$ 2 T Zellen eine direkte gegen Tumoren wie das B-Zelllymphom Daudi gerichtete Aktivität, für deren Erklärung ein „Erspüren“ eines abnormal erhöhten



intrazellulären IPP Spiegels durch den V $\gamma$ 9V $\delta$ 2 TCR oder Bindung des V $\gamma$ 9V $\delta$ 2 TCR an Liganden, wie einer ectopisch exprimierten F1-ATPase oder des UL-16 bindenden Proteins 4 (ULBP4) herangezogen wurde. Die V $\gamma$ 9V $\delta$ 2 T Zell Aktivierung durch Aminobisphosphonate und Alkylamine wurde hingegen auf die Inhibition des IPP verbrauchenden Enzyms Farnesylpyrophosphatsynthase (FPPS) zurückgeführt, obgleich Wirkungen auf andere Moleküle oder eine direkte Bindung an den TCR nicht ausgeschlossen werden konnten.

Die vorgelegte Dissertationsschrift beschreibt neue Ansätze der Analyse der Mechanismen der V $\gamma$ 9V $\delta$ 2 T Zell Aktivierung. Sie zeigt, dass eine mittels retroviraler Transduktion von shRNA erzielte Reduktion der FPPS Expression ausreicht, um hematopoietische und nicht-hematopoietische Tumorzellen zu V $\gamma$ 9V $\delta$ 2 T Zellaktivatoren zu machen. Die FPPS knockdown zellvermittelte Aktivierung der V $\gamma$ 9V $\delta$ 2 T Zellen zeigte sich in erhöhter Expression von CD69, CD107a, Zytotoxizität gegen FPPS knockdown Zellen und Induktion der IFN $\gamma$  Sekretion. Die, die IPP-Synthese inhibierende Substanz Mevastatin, reduzierte die V $\gamma$ 9V $\delta$ 2 T Zellaktivierung durch FPPS knockdown Zellen oder Aminobisphosphonat behandelte Zellen, aber nicht die Aktivierung durch das Phosphoantigen Bromhydrin Pyrophosphat. Ein vermindertes Wachstum der FPPS knockdown Zellen wurde nicht nachgewiesen was im Gegensatz zur Literatur über Aminobisphosphonat behandelte Zellen steht. Weiterhin wurde ein Tetracyclin-induzierbares FPPS spezifische shRNA kodierendes lentivirales Konstrukt in humane B-Zelllymphom Raji Zellen transduziert, die anschließend die durch Zugabe bzw. Entfernung von doxycyclin gesteuerte Fähigkeit erhielten, V $\gamma$ 9V $\delta$ 2 T Zellen zu aktivieren.

Ein anderer Ansatz zur Analyse der V $\gamma$ 9V $\delta$ 2 T-zellvermittelten Aktivierung war die Entwicklung phosphoantigenspezifischer V $\gamma$ 9V $\delta$ 2 TCR transduzierter Mauszelllinien. Diese Zellen unterscheiden sich von den bisher benutzten humanen V $\gamma$ 9V $\delta$ 2 TCR transduzierten Jurkat Zellen dadurch, dass sie keine Phosphoantigene präsentieren, und sind daher für Analyse der Phosphoantigenpräsentation besonders geeignet. Die Antwort

der neuen TCR Transduktanten auf wahrscheinliche V $\gamma$ 9V $\delta$ 2 TCR Zellliganden bzw. V $\gamma$ 9V $\delta$ 2 T-Zellaktivatoren wie Phosphoantigene, Aminobisphosphonate oder FPPS knockdown Zellen hing im hohen Maße von der Expression eines Ratten/Maus CD28 Moleküls auf den Transduktanten und dessen Bindung an den (CD80) Gegenrezeptor auf der antigenpräsentierenden Zelle ab. Höchstwahrscheinlich reflektiert die Antwort auf eine spezifische Antigenerkennung, da Mutationen in den CDR2 und 3 der TCR $\delta$  Kette die Antwort verschwinden ließen, aber keine Effekte auf die Stimulation durch CD3 oder TCR spezifische Antikörper hatten. Ein gravierender Unterschied der TCR-Transduktanten zu primären  $\gamma\delta$  T Zellen lag auch darin, dass die TCR Transduktanten weder durch Daudi Zellen noch durch IPP stimuliert wurden und ihre Empfindlichkeit gegenüber löslichen Phosphoantigenen ungefähr 1000fach geringer als bei primären V $\gamma$ 9V $\delta$ 2 T-Zellen war, während sich die Antwort der beiden Zelltypen auf FPPS knockdown oder Aminobisphosphonate-behandelte Zellen ähnelten. Schließlich wurden die Transduktanten verwendet, um Effekte der Überexpression oder des knockdown von Enzymen der Isoprenoidsynthese wie 3-Hydroxy-3-Methyl-Glutaryl-CoA reductase (HMG-CoA reductase or HMGR), Mevalonat-5-Pyrophosphat decarboxylase (MVD), Isopentenyl Pyrophosphat Isomerase (IDI), Geranylgeranyl Pyrophosphate Synthase (GGPPS) zu analysieren, wobei keine eindeutigen Effekte beobachtet wurden.

Zusammengefasst kann gesagt werden, dass die vorgelegte Arbeit die Vorstellung von V $\gamma$ 9V $\delta$ 2 TCR Zellen als Sensoren eines entgleisten Isoprenoidstoffwechsel unterstützt und neue Werkzeuge zur Analyse der Ligandenerkennung und TCR vermittelten Aktivierung dieser Zellpopulation vorstellt. Diese Werkzeuge sollten bei der Beantwortung folgender Fragen helfen: 1) Wie beeinflusst die Fehlregulation des Isoprenoidstoffwechsels das Tumorwachstum. 2) Welche Korrelation besteht zwischen der Modulation der IPP Spiegel und der V $\gamma$ 9V $\delta$ 2 TCR vermittelten Aktivierung bzw. der Expression anderer vorgeschlagener V $\gamma$ 9V $\delta$ 2 Liganden. 3) Gibt es Enzyme außer der FPPS und der HMG-CoA Reduktase, die eine wichtige Rolle bei der V $\gamma$ 9V $\delta$ 2 T-Zellaktivierung spielen und schließlich 4) Welche(s) Molekül(e) präsentiert bzw. präsentieren Phosphoantigene ?

## Index

ACKNOWLEDGMENTS.....	i
SUMMARY.....	ii
ZUSAMMENFASSUNG.....	v
LIST OF TABLES.....	xi
LIST OF FIGURES.....	xii
1 INTRODUCTION.....	1
1.1 The Unique TCR Repertoire of Human $\gamma\delta$ T Cells.....	1
1.2 Unique Conservation and Evolution of $\gamma\delta$ T Cells.....	3
1.3 Prenyl Pyrophosphates: Unique Antigens of V $\gamma$ 9V $\delta$ 2 T cells.....	4
1.4 DOXP and Mevalonate Pathways for Isoprenoid Biosynthesis.....	5
1.5 Indirect Stimulation of V $\gamma$ 9V $\delta$ 2 T Cells By Aminobisphospho-nates Or Alkylamines.....	8
1.6 Activation Requirements of V $\gamma$ 9V $\delta$ 2 T Cells.....	10
1.7 Effector Functions of V $\gamma$ 9V $\delta$ 2 T cells.....	11
1.7.1 Functions of V $\gamma$ 9V $\delta$ 2 T cells in microbial infections.....	11
1.7.2 Functions of V $\gamma$ 9V $\delta$ 2 T cells in tumor immunosurveillance.....	12
1.7.3 Functions of V $\gamma$ 9V $\delta$ 2 T cells as a bridge between innate and adaptive immunity.....	13
1.8 Clinical Perspective of V $\gamma$ 9V $\delta$ 2 T cells.....	13
1.9 Retroviral/Lentiviral Delivery of Short Haipin RNAs.....	14
2 MATERIALS AND METHODS.....	17
2.1 MATERIALS.....	17
2.1.1 Chemical reagents.....	17
2.1.2 Media, solutions and buffers.....	19
2.1.3 Cell lines.....	21
2.1.4 Vectors.....	22

2.1.5	Antibodies .....	24
2.1.6	Cloning reagents .....	24
2.1.7	Kits.....	25
2.1.8	Apparatus.....	25
2.1.9	Consumables .....	26
2.1.10	Softwares .....	26
2.1.11	Primers.....	27
2.2	METHODS.....	31
2.2.1	Routine cell culture methods.....	31
2.2.2	Gene clone and Transfer.....	31
2.2.3	Preparation of competent cells .....	36
2.2.4	Human V $\gamma$ 9V $\delta$ 2 TCR Transduced BW58 Reporter Cell lines .....	36
2.2.5	Retrovirus Mediated Over-expression of Enzymes.....	37
2.2.6	MiR-30 Based shRNA Mediated Knockdown of Enzymes.....	37
2.2.7	Lentivirus Mediated Inducible FPPS Knockdown in Tumor Cells.....	40
2.2.8	Isolation of peripheral blood mononuclear cells (PBMCs) .....	41
2.2.9	Establishment of V $\gamma$ 9V $\delta$ 2 T cell lines by stimulation of fresh V $\gamma$ 9V $\delta$ 2 T cells from peripheral blood .....	41
2.2.10	Activation analysis of primary or enriched V $\gamma$ 9V $\delta$ 2 T cells.....	41
3	RESULTS .....	44
3.1	Generation of V $\gamma$ 9V $\delta$ 2 TCR Transduced BW58 Reporter Cell Lines.....	44
3.1.1	Cell surface expression of $\gamma\delta$ TCR and mouse CD3 in TCR <sup>-</sup> hybridoma BW58 cells.....	44
3.1.2	Activation of BW58 $\gamma\delta$ T cells by phosphoantigens or aminobisphosphonates depends on CD28 mediated signal. ....	46
3.1.3	The activation of BW58r/mCD28 $\gamma\delta$ cells requires presentation of the TCR-ligands by human cells .....	47
3.1.4	Mevastatin blocks the response of BW58r/mCD28 $\gamma\delta$ T cells to aminobisphosphonates but not to phosphoantigens.....	48
3.1.5	Mutations in V $\delta$ 2 region abrogate the reactivity of the TCR transductants.....	49
3.1.6	Comparison of the response of short term $\gamma\delta$ T cell lines and $\gamma\delta$ TCR transduced BW58 cells to different V $\gamma$ 9V $\delta$ 2 activators .....	50
3.1.7	Daudi cells alone do not induce IL-2 production by BW58r/mCD28 $\gamma\delta$ cells .....	52

3.1.8	Primary $\gamma\delta$ T cells and $\gamma\delta$ TCR transductants differ in their response to Ecto-ATPase coated beads .....	54
3.2	Reduced FPPS Expression Unveils Recognition of Tumor Cells by V $\gamma$ 9V $\delta$ 2 T Cells .....	55
3.2.1	Reduction of FPPS expression in RAJI cells by retrovirally expressed shRNAs .....	55
3.2.2	FPPS knockdown in RAJI cells induces activation of primary V $\gamma$ 9V $\delta$ 2 T cells .....	56
3.2.3	RAJI-FPPS knockdown cells induce activation of V $\gamma$ 9V $\delta$ 2 T cell lines .....	58
3.2.4	Activation of V $\gamma$ 9V $\delta$ 2 T cells by aminobisphosphonates and RAJI-FPPS knockdown cells is inhibited by mevastatin .....	60
3.2.5	FPPS knockdown in RAJI directly activated $\gamma\delta$ TCR transduced BW58r/mCD28 cells. . . . .	61
3.2.6	FPPS knockdown in RAJI had no effects on Ecto-ATPase expression .....	62
3.2.7	FPPS knockdown in RAJI cells had no effects on growth of tumor cells .....	63
3.2.8	FPPS specific shRNA converts Jurkat cells to V $\gamma$ 9V $\delta$ 2 T cell activators .....	64
3.2.9	FPPS specific shRNA converts also tumor cells of non-hematopoietic origin to V $\gamma$ 9V $\delta$ 2 T cell activators .....	65
3.2.10	Comparison of $\gamma\delta$ -T-cell activation by FPPS knockdown cells versus Daudi cells ...	69
3.3	Conditional Knockdown of FPPS by a Tet-Inducible Lentiviral shRNA Expression System. . . . .	69
3.4	Regulating Expression of Other Enzymes of Isoprenoid Synthesis .....	72
4	DISCUSSION .....	75
4.1	A new tool for the analysis of ligand recognition by V $\gamma$ 9V $\delta$ 2 TCR .....	75
4.2	Reduced expression of the farnesylpyrophosphate synthase unveils recognition of tumor cells by V $\gamma$ 9V $\delta$ 2 T cells .....	81
4.3	Work in progress and outlook .....	83
	REFERENCE .....	85
	ABBREVIATION .....	95
	CURRICULUM VITAE .....	98
	AFFIDATIV .....	102

## LIST OF TABLES

Table 1-1 Utilization of DOXP and mevalonate pathways by selected organisms. ....	7
Table 2-1 Monoclonal Antibodies for FACS staining or Immuno-blot. ....	24
Table 2-2 Primers for constructs of retroviral vectors encoding TCR $\gamma$ gene and $\delta$ gene .....	27
Table 2-3 Primers for constructs of retroviral vectors encoding CD28 and CD80 .....	28
Table 2-4 Primers for constructs of retroviral vectors encoding mevalonate pathway enzymes' genes .	29
Table 2-5 Hairpin sequences for constructs of retroviral vectors expressing different shRNAs.....	30

## LIST OF FIGURES

Figure. 1-1 Schematic representation of human TCR- $\gamma$ genes and TCR- $\delta$ genes .....	3
Figure. 1-2 Structure and activity of prenyl pyrophosphate antigens and analogs .....	5
Figure. 1-3 The biosynthesis pathway of isoprenoides. ....	6
Figure. 1-4 Structures of the bisphosphonates .....	9
Figure. 1-5 Schematic of non-replicating retroviral/lentiviral vector mediated shRNAmir expression and processing.....	16
Figure 3-1 Cells surface expression of mCD3 $\epsilon$ and V $\delta$ 2 TCR after BW58 transduction of V $\gamma$ 9V $\delta$ 2 TCR ....	45
Figure 3-2 ELISA analysis of IL-2 production by BW58 cells expressing $\gamma\delta$ TCR.....	46
Figure 3-3 BW58r/mCD28 cells expressing $\gamma\delta$ TCR response to Jurkat, Jurkat/rCD80 or Jurkat/huCD80	47
Figure 3-4 BW58r/mCD28 $\gamma\delta$ T cells respond only to BrHPP presented by cell lines of human origin ....	48
Figure 3-5 Mevastatin reduced IL-2 production of BW58r/mCD28 $\gamma\delta$ Mop in the response to aminobisphosphonates, but not to phosphoantigens .....	48
Figure 3-6 Comparison of the IL-2 production by WT $\gamma\delta$ Mop, D51 and D96 in response to different stimuli.....	50
Figure 3-7 A comparison of the response of BW58r/mCD28 $\gamma\delta$ T cells and enriched short-term $\gamma\delta$ lines .....	51
Figure 3-8 BW58r/mCD28 cells expressing $\gamma\delta$ TCR Mop, Buk and G115 indicated no response to Daudi cells alone .....	52
Figure 3-9 Amino acid sequence alignment of TCR- $\gamma$ chain (left) and TCR- $\delta$ chain (right) from different $\gamma\delta$ TCR genes Buk, G115 and Mop.....	53
Figure 3-10 activation analysis of primary $\gamma\delta$ T cells and $\gamma\delta$ TCR transduced cells by Ecto-ATPase coated beads .....	54
Figure 3-11 The RAJI cell line expressing FPPS-EYFP fusion protein (RAJI-FPPSYFP) was transfected, with either empty vector control (AS) or control shRNA (ASGr2) or FPPS-specific shRNA (AS22 or AS11) .....	56
Figure 3-12 FPPS knockdown in RAJI cells increases CD69 and CD107a expression and IFN- $\gamma$ production by primary V $\delta$ 2 T cells.....	57
Figure 3-13 FPPS knockdown in RAJI cells induces effector-functions in V $\gamma$ 9V $\delta$ 2 T cells .....	59
Figure 3-14 FPPS knockdown in RAJI cells induces effector-functions in highly purified V $\gamma$ 9V $\delta$ 2 T cells..	60

Figure 3-15 Effects of mevastatin treatment on induction of IFN- $\gamma$ secretion by FPPS knockdown RAJI and zoledronate-treated RAJI cells.....	61
Figure 3-16 FPPS knockdown in RAJI cells induces IL-2 production by BW58r/mCD28 $\gamma\delta$ cells .....	62
Figure 3-17 FACS staining with F1-ATPase MoAb .....	63
Figure 3-18 Flow cytometry analysis of cell growth.....	64
Figure 3-19 FPPS knockdown in Jurkat cells increase the IFN- $\gamma$ secretion and CD107a expression by short-term enriched $\gamma\delta$ line while both were reduced by 10nM mevastatin .....	65
Figure 3-20 FACS analysis of CD107a expression in short-term enriched $\gamma\delta$ T cell line in response to various non-hematopoietic tumor targets transduced with AS or AS22.....	67
Figure 3-21 FACS analysis of CD69 upregulation in fresh isolated PBLs in response to various non-hematopoietic tumor lines transduced with AS or AS22 .....	68
Figure 3-22 Comparison of the response of a short term $\gamma\delta$ T cell line to Daudi and FPPS knockdown cells .....	69
Figure 3-23 Lentiviral system for inducible FPPS knockdown .....	70
Figure 3-24 Inducible and reversible IL-2 production of BW58r/mCD28 $\gamma\delta$ TCR in response to RAJI/FH1t(SR22)UTG cells. ....	71
Figure 3-25 Immunoblot analysis of FPPS expression levels .....	72
Figure 3-26 Comparing analysis of IL-2 production by transduced BW58 cells in response to RAJI cells up-regulating different enzymes .....	73
Figure 3-27 Comparison of induction of IFN $\gamma$ in a short term $\gamma\delta$ T cell line by RAJI cells transduced with constructs containing different shRNAs .....	74
Figure 4-1 Amino acid sequence alignment of human, mouse and rat CD28 and crucial cytoplasmic tails for signal transduction. ....	77



# 1 INTRODUCTION

$\gamma\delta$  T cells represent a unique population of T lymphocytes which express a distinct T cell receptor (TCR) composed of two glycoprotein chains called TCR- $\gamma$  and TCR- $\delta$ . Early studies demonstrated that  $\gamma\delta$  T cells do not respond to peptide antigens presented by major histocompatibility complex (MHC) class I and class II molecules that stimulate the majority of CD4 and CD8  $\alpha\beta$  T cells. Instead, they often respond to stress, infection, or destruction of tissue integrity, and exert similar functions as cells of the innate immune system (1). Currently the only well defined ligands of  $\gamma\delta$  TCR are the stress induced gut epithelium class Ib molecule T22 and T10 (2). Self and foreign small nonpeptide prenyl pyrophosphates, so called phosphoantigens, are very likely putative ligands of human V $\gamma$ 9V $\delta$ 2 TCR despite lacking biochemical or structural evidence for a direct binding to the TCR.  $\gamma\delta$  T cells also express Toll-like receptors and NK receptors that allow them to respond to other nonpeptide microbial components or to alterations in the expression of normal cell surface ligands such as MHC class I chain-related gene A/B (MICA/B) or UL16-binding proteins (ULBPs) (3, 4). Both TCR and non-TCR receptors dependent activation plays a major role in determining the unique role of  $\gamma\delta$  T cells in immunity.

## 1.1 The Unique TCR Repertoire of Human $\gamma\delta$ T Cells

Somatic recombination of Ig-domain antigen receptor genes occurs in all jawed vertebrates and generates a diverse repertoire of T cell receptor (TCR) and immunoglobulin (Ig) molecules that allow them to recognize diverse antigens from bacterial, viral, and parasitic invaders, and from dysfunctional cells such as tumor cells.

In mammals, TCR- $\delta$  and TCR- $\alpha$  gene segments are always closely linked and located in a single chromosomal locus in which TCR- $\delta$  segments are situated between TCR- $\alpha$

## INTRODUCTION

segments (1). In human they map on chromosome 14 (5). As shown in Figure. 1-1A, human TCR- $\delta$  locus is composed of single C $\delta$  gene segment, four J $\delta$  segments preceded by three diversity (D $\delta$ ) elements (6-8) and V $\delta$  segments, which in some cases are used both as V $\delta$  and V $\alpha$ : V $\delta$ 4/V $\alpha$ 14, V $\delta$ 6/V $\alpha$ 23, V $\delta$ 5/V $\alpha$ 29 (8, 9). Although eight distinct V $\delta$  genes have been localized, only six of them were found expressed on the cell surface (10, 11). Human TCR- $\gamma$  genes are located on chromosome 7 (12) and composed of two constant gene segments (C $\gamma$ ), five joining elements (J $\gamma$ ) and fourteen variable (V $\gamma$ ) genes of which six encode functional proteins and eight are pseudogenes (13) (Figure. 1-1B). These six genes can be subdivided into two families: the V $\gamma$ I family composed of V $\gamma$ 2, 3, 4, 5 and 8 genes and V $\gamma$ II consisting of V $\gamma$ 9 (V $\gamma$ 2 in other nomenclature) gene.

During somatic recombination, the enormous diversity of the  $\gamma\delta$  T cell repertoires can be generated either via random combinations of multiple germline V(D)J gene segments or by addition of P and N nucleotides between V and D, D and J, or V and J segments at the time of joining. In particular, the variability of TCR- $\delta$  chain can be extremely high owing to the D $\delta$  segments that can undergo tandem rearrangement and flexible reading frame usage creating diverse length and composition of the joining regions. Therefore, despite the limited numbers of available TCR V $\gamma$  and V $\delta$  elements, the potential repertoire of this  $\gamma\delta$  TCR is at least three orders of magnitude higher than TCR  $\alpha\beta$  repertoire due to the extremely high variability in the CDR3 regions (14, 15). Paradoxically, however, the actual diversity of expressed  $\gamma\delta$  TCRs is limited because only a few of the available V, D, and J segments are used in mature  $\gamma\delta$  T cells.

The distinct assemble pattern of TCR  $\gamma\delta$  chains is the preferential association of V $\delta$  chains with certain V $\gamma$  chains (Figure. 1-1). In human, there are two main populations of  $\gamma\delta$  T cells based on TCR composition. In peripheral blood, the majority of  $\gamma\delta$  T lymphocytes express the TCR variable regions V $\delta$ 2 and V $\gamma$ 9. In healthy adults, the total size of the population accounts for 1-5% of blood T lymphocytes. By contrast, the second major subset of  $\gamma\delta$  T cells always expresses V $\delta$ 1 segment, which are paired with various V $\gamma$  segments from V $\gamma$ I gene family. V $\delta$ 1 T cell is resident mainly within epithelial

## INTRODUCTION

tissues, where these cells might provide a first line of defense against infections or malignancies (1).

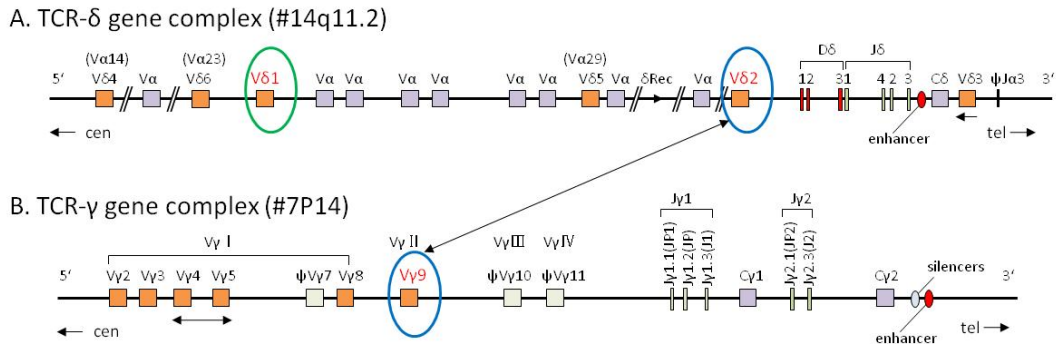


**Figure. 1-1 Schematic representation of human TCR- $\gamma$  genes and TCR- $\delta$  genes.** Only representative gene segments or pseudogenes are shown. V $\delta$ 1 segment and V $\delta$ 2/V $\gamma$ 9 segments were highlighted in red texts and green circle or blue circles. (modified from (16))

### 1.2 Unique Conservation and Evolution of $\gamma\delta$ T Cells

Throughout the last 400-500 millions years, TCR gene families have been strongly conserved in all jawed vertebrates (1).  $\gamma\delta$  TCR conserves the following features (reviewed in (1)): 1) TCR- $\alpha$  and TCR- $\delta$  loci are closely linked; 2) The somatic VJ ( $\gamma$  chain) and VDJ ( $\delta$  chain) rearrangements occur during lymphocyte development; 3) The structural conservation includes “Ig folds” and subdivision of V regions into CDRs based on V-gene encoded (CDR1 and CDR2) and V(D)J-gene encode (CDR3); 4) Some amino acid sequences are conserved in different organisms, like the serine residue at position 8 of V $\gamma$ , the IHWY motif at positions 34–37 of V $\gamma$ , the highly charged cytoplasmic tail of C $\gamma$  and the uncharged tail of C $\delta$ .

Despite the respective conservation of the  $\gamma\delta$  TCR in above features,  $\gamma\delta$  T cells differ remarkably between species in features such as TCR-V genes, cell frequencies, tissue distribution, phenotype and function. Furthermore in a given individual they show a high degree of specialization which is often associated with a certain TCR-V genes usage. Some examples for this diversification is given as follows: Frequencies of  $\gamma\delta$  T cells in circulating T cells range only between 1%–5% in adult primates and rodents, in avian and ruminants like chicken, sheep, cow and pig 20%-50% of circulating T cells are  $\gamma\delta$  T cells

## INTRODUCTION

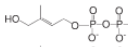
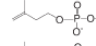
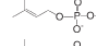
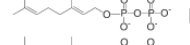
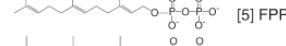
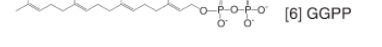
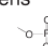
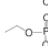
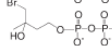
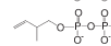
(1). In addition to circulating distribution, human  $\gamma\delta$  T cells are also localized in tissues like epithelium of the intestine where they comprise the majority of intraepithelial lymphocytes (IELs) (17). In mice and rats, there is a typical cell population in the skin named as dendritic epidermal T cells (DETCs) which express a canonical  $\gamma\delta$  TCR composed of V $\gamma$ 3 and V $\delta$ 1 (18). Classically,  $\gamma\delta$  TCR expression is mandatorily associated with CD3 even in a recent report regarding to the identification of a  $\gamma\delta$  TCR expressing human eosinophils (19). By contrast, CD4 or CD8 associated expression with  $\gamma\delta$  TCR cannot be observed in most species with exception of the rat whose  $\gamma\delta$  T cells are to 90% CD8 positive and most of for the CD8 $\alpha\beta$  heterodimer (20-22). In cattle and avian, the CD8 antigen expression has been used as useful parameter for the definition of  $\gamma\delta$  T cell subpopulations (23, 24). More recently, CD56 and CD27 molecular expression have been reported as the promising phenotypes to define different functional subpopulations of human V $\gamma$ 9V $\delta$ 2 T cells, respectively (25, 26).

### **1.3 Prenyl Pyrophosphates: Unique Antigens of V $\gamma$ 9V $\delta$ 2 T cells**

Since the first observations that human peripheral  $\gamma\delta$  T cells responded to mycobacterial components which were suggested as small nonpeptide antigens owing to their resistance to protease digestion (27), large numbers of intensive studies were undertaken for identification and purification of the natural ligands from mycobacterium. In 1994, Tanaka and colleagues reported that synthetic alkyl phosphates, especially monoethyl phosphate, which are chemically similar to natural mycobacterial ligands (28), selectively activated V $\gamma$ 9V $\delta$ 2 T cells. Sequentially, isopentenyl pyrophosphate (IPP) and related prenyl pyrophosphate derivatives were identified as natural antigens produced by mycobacteria to specifically activate human V $\gamma$ 9V $\delta$ 2 T cells (29). IPP is a central intermediate in isoprenoid biosynthesis, which is produced either by the mevalonate pathway or the recently discovered 1-Desoxy-D-xylulose-5 phosphate (DOXP) pathway (30) which will be discussed in section 1.4. Another defined natural activator of V $\gamma$ 9V $\delta$ 2 T cells is immediate precursor of IPP in the DOXP pathway of IPP synthesis, (E)-4-Hydroxy-3-methyl-but-2-enyl pyrophosphate (HMBPP) (31, 32), which occurs in many eubacteria, plants and in apicomplexan parasites. HMBPP is  $10^4$  times more potent in activating human V $\gamma$ 9V $\delta$ 2 T cells than IPP and is probably causative for massive

## INTRODUCTION

expansion of V $\gamma$ 9V $\delta$ 2 T cells found in many infectious diseases. Phosphorylated bromohydrin (BrHPP) is synthetic structural analogue of physiological pyrophosphates which mimics the biological properties of IPP and HMBPP (33). BrHPP is nearly as efficient as HMBPP in its capacity to stimulate V $\gamma$ 9V $\delta$ 2 T cells (Figure. 1-2). Although functional evidences of pyrophosphates recognition by V $\gamma$ 9V $\delta$ 2 TCR were provided by the transfection of V $\gamma$ 9V $\delta$ 2 TCR into TCR<sup>-</sup> Jurkat cells which confer reactivity to phosphoantigens (29), direct structural evidences of binding between TCR and ligands are still missing.

Natural Prenyl pyrophosphates	Compound	1/2 Max. Stim. (μM)
	[1] HMBPP	0.000032
	[2] IPP	1
	[3] DMAPP	30
	[4] GPP	50
	[5] FPP	300
	[6] GGPP	300
Synthetic phosphoantigens		
	[7] MP	~30000
	[8] EPP	1
	[9] BrHPP	0.001
	[10] 2M3BPP	0.4

**Figure. 1-2 Structure and activity of prenyl pyrophosphate antigens and analogs.** Structural and biological activity of various prenyl pyrophosphates is shown. Values are the concentration required for half-maximum stimulation of proliferation for the V $\gamma$ 9V $\delta$ 2 T cells (modified from (34)).

### 1.4 DOXP and Mevalonate Pathways for Isoprenoid Biosynthesis

Isoprenoids are a most ancient and diverse class of natural compounds with carbon skeleton built of branched C5 isoprenoid units. They play many important biological roles such as photosynthesis, hormonal metabolism, growth regulation, intracellular signal transduction, vesicular transport within the cell, membrane structure maintain, and so on (35). Isopentenyl pyrophosphate (IPP) is the essential precursor for isoprenoid synthesis in all organisms including eubacteria, archaebacteria and eukaryotes. However, there are two distinct and independent biosynthetic routes to produce IPP: the mevalonate pathway (MVA pathway) and the 1-Desoxy-D-xylulose-5 phosphate (DOXP) pathway

## INTRODUCTION

(also termed as methylerythritol phosphate pathway, MEP pathway). The former is found in most eukaryotes where IPP is synthesized from the condensation of three acetyl-CoA molecules; in contrast, in the DOXP pathway IPP is synthesized via the condensation of pyruvate and D-glyceraldehyde 3-phosphate. It is present in most eubacteria, apicomplexan protozoa, cyanobacteria, and plant chloroplasts (Table 1-1).

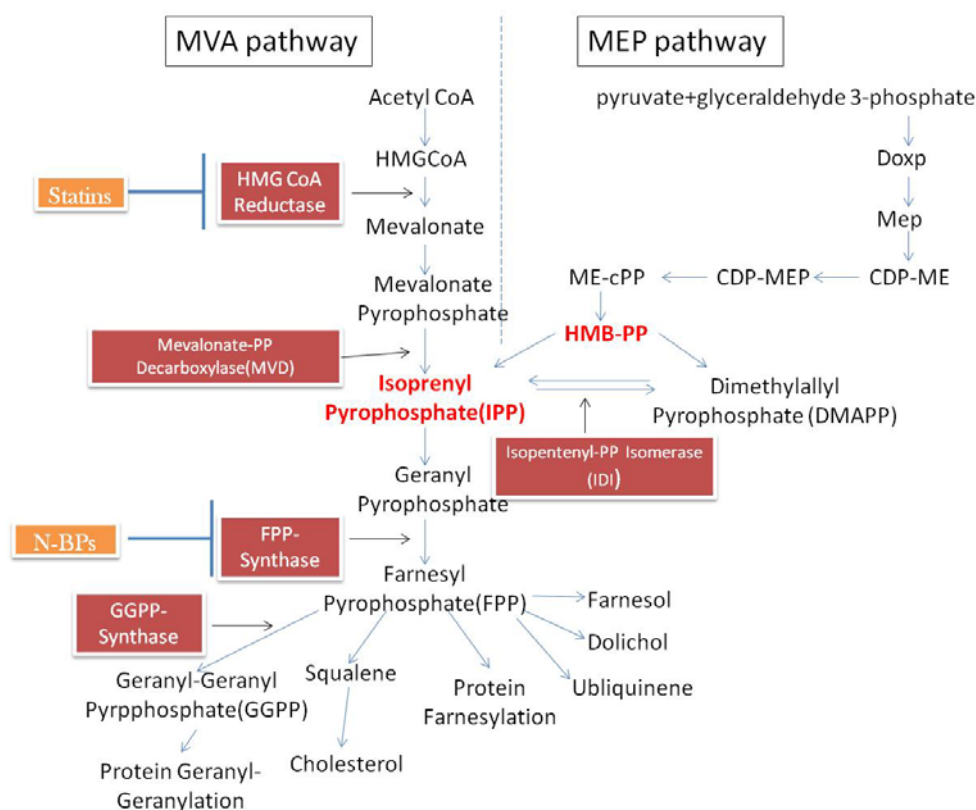


**Figure. 1-3 The biosynthesis pathway of isoprenoids. (according to (34)).** Mevalonate Pathway (MVA) is shown in left and pathway 1-deoxy-D-xylulose-5-phosphate (DOXP) in right. DOXP, 1-deoxy-D-xylulose 5-phosphate; MVA, 3R-Mevalonic acid; Mep, 2-C-methyl-D-erythritol 4-phosphate; CDP-ME, 4-(cytidine 5'-diphospho)-2C-methyl-D-erythritol; CDP-MEP, 4-(cytidine 5'-diphospho)-2C-methyl-D-erythritol 2-phosphate; ME-cPP, 2C-methyl-D-erythritol 2,4-cyclodiphosphate.

The key enzymes involved in both biosynthesis pathways were identified and investigated. In human, HMG-CoA reductase (HMGR) is the rate-controlling enzyme of mevalonate pathway. The activity of this enzyme is competitively inhibited by statins which are widely prescribed drugs for hypercholesterolemia (36). The other crucial enzymes surrounding IPP production or metabolism include mevalonate pyrophosphate decarboxylase (MVD), isopentenyl pyrophosphate isomerase (IDI), farnesyl pyrophosphate synthase (FPPS) and geranyl-geranyl pyrophosphate synthase (GGPPS).

## INTRODUCTION

Modulating the expression of those enzymes is of especial interests owing to their potent roles in regulation of endogenous IPP level subsequently the conversion of IPP to downstream products.

**Table 1-1 Utilization of DOXP and mevalonate pathways by selected organisms, adapted from (37).**

Organism	MEP pathway	Mevalonate pathway
<b>Prokaryotes</b>		
Eubacteria		
<i>Mycobacterium tuberculosis</i>	+	-
<i>Mycobacterium leprae</i>	+	-
<i>Escherichia coli</i>	+	-
<i>Haemophilus influenzae</i>	+	-
<i>Chlamydia pneumoniae</i>	+	-
<i>Pseudomonas aeruginosa</i>	+	+
<i>Listeria monocytogenes</i>	+	+
<i>Staphylococcus aureus</i>	-	+
<i>Streptococcus pneumoniae</i>	-	+
<i>Borrelia burgdorferi</i>	-	+
Archaeobacteria		
<i>Pyrococcus horikowskii</i>	-	+
<i>Methanobacterium</i>	-	+
<b>Eukaryotes</b>		
Apicomplexan parasites		
<i>Plasmodium falciparum</i>	+	-
Plants		
<i>Arabidopsis thaliana</i>	+	+
Fungi		
<i>Saccharomyces cerevisiae</i>	-	+
Mammals	-	+

Moreover, inhibition of mevalonate pathway perhaps leads to apoptosis of tumor or normal cells due to the importance of core human isoprenoid biosynthesis for diverse cellular processes related to cancer cell growth and metastasis. Particularly, there are two

## INTRODUCTION

explanations for the apoptosis caused by inhibition of mevalonate pathway: 1) a loss or decrease of prenylated small signaling proteins (Rho, Ras) which are important for respective cellular signal transduction or regulating cell motility, and consequently, apoptosis (38, 39); 2) the accumulation of a cytotoxic ATP analog, APPPi, formed by conjugation of IPP and AMP leads to cell apoptosis due to inhibiting mitochondrial adenine nucleotide translocase (ANT) (40, 41).

### **1.5 Indirect Stimulation of V $\gamma$ 9V $\delta$ 2 T Cells By Aminobisphosphonates Or Alkylamines**

In addition to the direct response of V $\gamma$ 9V $\delta$ 2 T cells to phosphoantigens like IPP, HMBPP or BrHPP, there are other compounds including aminobisphosphonates and alkylamines which were capable of activating V $\gamma$ 9V $\delta$ 2 T cells (42, 43). However, they were proposed as the indirect activators of V $\gamma$ 9V $\delta$ 2 T cells via increasing the endogenous IPP level (34).

Bisphosphonates are pyrophosphate analogs. Prenyl pyrophosphates connect two phosphates through an oxygen atom while bisphosphonates through a carbon atom (Figure. 1-4A). There are two classes of bisphosphonates: non-nitrogen containing (Non-N-BPs) and nitrogen containing bisphosphonates (N-BPs). The former include etidronate, clodronate and tiludronate while the latter include pamidronate (APD, Aredia), alendronate (Fosamax), neridronate, olpadronate, ibandronate (Boniva), risedronate (Actonel), zoledronate (Zometa, Aclasta), etc (44) (Figure. 1-4B, C). Nitrogen containing bisphosphonates, also termed as aminobisphosphonates, inhibit the activity of FPP synthase and also GGPP synthase (45) but non-nitrogen-containing bisphosphonates do not (46). Moreover, most recently, Zhang et al. developed a class of lipophilic bisphosphonates which were demonstrated as the dual inhibitors of FPPS and GGPPS by X-ray and NMR (47). Kunzmann et al. observed the increased numbers of V $\gamma$ 9V $\delta$ 2 T cells in patients after pamidronate treatment for the first time (43). Further investigations demonstrated that these compounds indeed induce V $\gamma$ 9V $\delta$ 2 T cell activation and proliferation in vitro and in vivo, trigger V $\gamma$ 9V $\delta$ 2 TCR mediated lysis of tumor lines and



## INTRODUCTION

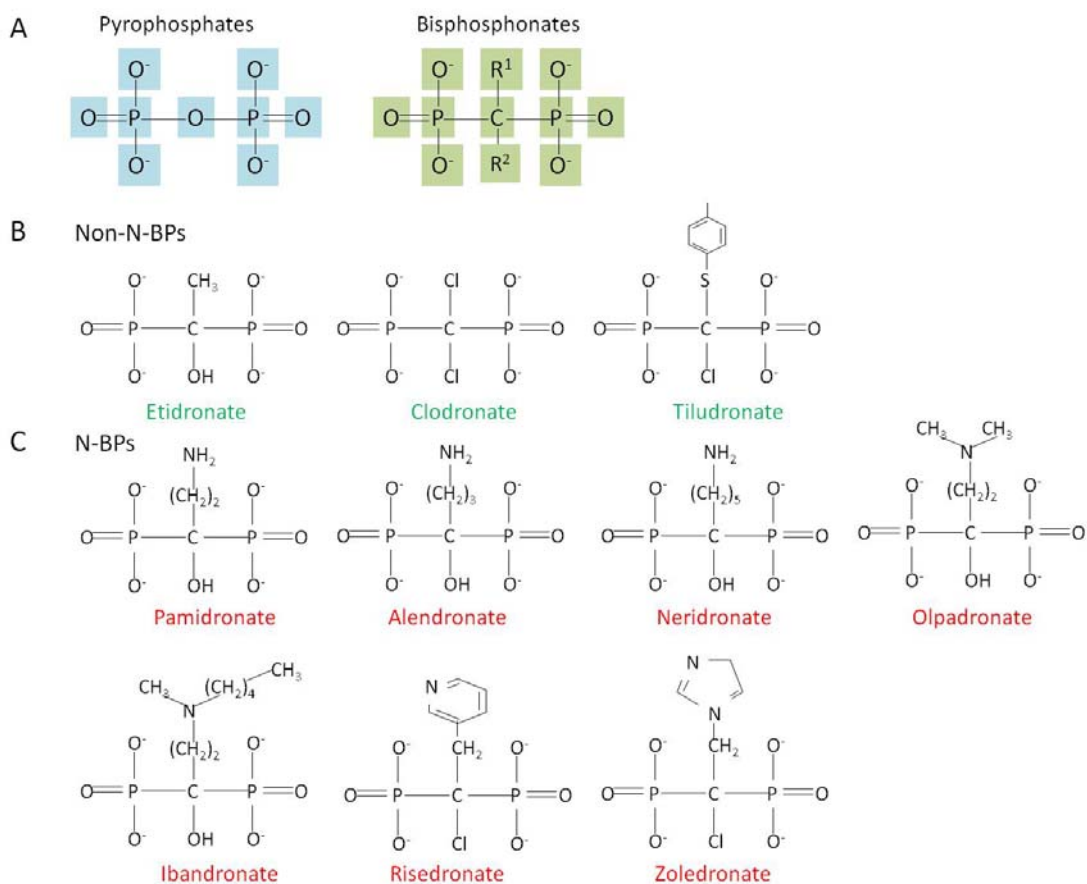


**Figure. 1-4 Structures of the bisphosphonates (according to (44)).** A) Comparison of pyrophosphates and bisphosphonates; B) Non-nitrogen containing bisphosphonates (Non-N-BPs) and C) Nitrogen containing bisphosphonates (N-BPs).

reduce survival of autologous myeloma cells in bone marrow biopsy specimens (43, 48, 49). The evidences from structural study demonstrated that aminobisphosphonates were capable of inhibiting the binding of FPPS to its substrates subsequently leading to the accumulation of IPP and DMAPP (50-52). Functionally, the activation of V $\gamma$ 9V $\delta$ 2 T cells by aminobisphosphonates could be blocked by the HMG-CoA reductase inhibitor mevastatin which decreases the accumulation of IPP production (53, 54). Similar to phosphoantigens, V $\gamma$ 9V $\delta$ 2 T cell activation by aminobisphosphonates requires cognate recognition by the TCR (55) but it recognizes only cells pulsed with aminobisphosphonates and not cells pulsed with phosphoantigens. These findings led to the concept that aminobisphosphonates are indirect activators of V $\gamma$ 9V $\delta$ 2 T cells. However, a direct

## INTRODUCTION

interaction between V $\gamma$ 9V $\delta$ 2 TCR and aminobisphosphonate or aminobisphosphonate-modified cellular compounds cannot be excluded.

FPPS-inhibition has also been suggested as mechanisms behind the V $\gamma$ 9V $\delta$ 2 T cell activation by alkylamines which were identified as a new stimulator to V $\gamma$ 9V $\delta$ 2 T cells (56). Alkylamines are a class of compounds composed of non-phosphate short alkyl chains bearing a terminal amino group which are chemically distinct from prenyl pyrophosphates and bisphosphonates. They are secreted by certain commensal and pathogenic bacteria and are also produced from L-theanine found in tea and are present in wine, mushrooms and apples (57). The indirect response of V $\gamma$ 9V $\delta$ 2 T cells by alkylamines most likely occurs through FPPS-inhibition and intracellular IPP accumulation as it suggested demonstrated by mevastatin blocking experiment (42).

### **1.6 Activation Requirements of V $\gamma$ 9V $\delta$ 2 T Cells**

So far V $\gamma$ 9V $\delta$ 2 T cells have been found only in human and non-human primates, and there is accumulating evidence that activation of V $\gamma$ 9V $\delta$ 2 T cell by phosphoantigens absolutely requires cell-cell contact with cells of human origin. There are two mutually non-exclusive explanations for the need of this species-specific interaction: 1) activation of V $\gamma$ 9V $\delta$ 2 T cell requires a species-specific presentation by unknown factors which are unique in cells of human origin and 2) activation of V $\gamma$ 9V $\delta$ 2 T cell requires a human specific co-receptor element or co-stimulatory signals. More and more evidences support the existence of some unknown presenting “factors” which are not classical MHC class I, MHC class II or MHC like molecules such as CD1 (58-60). Very recently, the group of Chen developed a soluble V $\gamma$ 9V $\delta$ 2 TCR tetramer of primate origin which strongly bond to M. tuberculosis infected or HMBPP incubated human or non-human primate cells but not all of other species (61). Interestingly, V $\gamma$ 9V $\delta$ 2 TCR tetramer binding was diminished after protease treatment of the cells. The other new class of tools are photoaffinity analogues of HMBPP such as meta/para-benzophenone-(methylene)-prenyl pyrophosphates (m/p-BZ-(C)-C5-OPP) which have been shown to crosslink to the surface of tumor cells which again were restricted to human or non-human primate origin (60). However, the identification of the putative presenting molecular is still a

## INTRODUCTION

conundrum. A number of functional studies suggest for the presenting molecular seem common characteristics such as lack of a functional polymorphism, wide and constitutive expression and conservation between human and non-human primates (34). But such characteristics could also be explained by a species-specific co-stimulatory signal which cannot be excluded by far. Although some reports demonstrated MICA/NKG2D interaction (62, 63), LFA-1/ICAM-1-mediated cell adhesion (64) and also CD6/CD166 engagement (65) are likely to play a role in the activation of V $\gamma$ 9V $\delta$ 2 T cells, they may not represent the dominant host factors required for the activation of V $\gamma$ 9V $\delta$ 2 T cells owing to either relatively limited types of tumor cells expresses these molecules or that they are not essential for the activation of V $\gamma$ 9V $\delta$ 2 T cells.

The structural requirements of phosphoantigen recognition by the V $\gamma$ 9V $\delta$ 2 TCR are still poorly understood. V $\gamma$ 9V $\delta$ 2 TCR dependent recognition of pyrophosphates can be well demonstrated through transfection of TCR into TCR<sup>-</sup> Jurkat cells which confer responsiveness of the transductants to phosphoantigens (29, 66). Further TCR mutation studies based on TCR gene transfer demonstrated that residues K108 of CDR3 $\gamma$  and residues R51 of CDR2 $\delta$  as well as the starting hydrophobic residues of the CDR3 $\delta$  were putative binding sites for pyrophosphates (67).

### **1.7 Effector Functions of V $\gamma$ 9V $\delta$ 2 T cells**

#### ***1.7.1 Functions of V $\gamma$ 9V $\delta$ 2 T cells in microbial infections***

Human V $\gamma$ 9V $\delta$ 2 T cells which in healthy adults make up 1%-5% of peripheral blood lymphocytes, can be massively expanded in vivo to than 50% in toxoplasmosis, malaria, ehrlichiosis, legionellosis, tularemia and mycobacterial infections (34). The large expansion of this population can be seen at the first week after infection and as it has been shown for tularaemia and last for as long as 1 year (68). The expanded V $\gamma$ 9V $\delta$ 2 T cells produce type 1 cytokines such as IFN- $\gamma$  and TNF- $\alpha$  as well as some chemokines including CCL3 (MIP-1 $\alpha$ ), CCL4(MIP-1 $\beta$ ) and CCL5 (RANTES) (69-71). They are also potent killer cells of infected cells and intracellular bacteria through perforin or Fas/Fas ligands interactions as well as through granulysin release (72-74). Some animal models also support an important role of V $\gamma$ 9V $\delta$ 2 T cells in infections of tuberculosis and other

## INTRODUCTION

bacteria including the humanized–SCID mice (75) and monkeys with BCG infection (76). Moreover, through secretion of growth-promoting molecules and growth factors such as MMP-7 (matrilysin) and fibroblast growth factor-9 in response to IPP and connective tissue growth factor in response to IL-15 and TGF- $\beta$ 1, V $\gamma$ 9V $\delta$ 2 T cells also play a role for in the maintenance of the integrity of the epithelium during epithelial infection or injury consequently limiting the spread of infections within the host (34).

### ***1.7.2 Functions of V $\gamma$ 9V $\delta$ 2 T cells in tumor immunosurveillance***

Human V $\gamma$ 9V $\delta$ 2 T cells can directly recognize and lyse human tumor cell lines like Daudi (Burkitt's lymphoma) and RPMI 8226 (plasmacytoma) (77, 78) which are dependent on V $\gamma$ 9V $\delta$ 2 TCR but not other receptors like NKG2D (66). IPP levels in Daudi cells are higher than in non-stimulating tumor cells and Daudi cell mediated V $\gamma$ 9V $\delta$ 2 T cell activation is inhibited by mevastatin, which is a blocker of HMG-CoA reductase, and consequently of the synthesis of downstream metabolites such as IPP (53). Moreover, the patients with lymphoid malignancies show increasing numbers of  $\gamma\delta$  T cells in vivo (79) which suggests a role of  $\gamma\delta$  T cells in tumor immunosurveillance. Alternatively, several cell surface molecules have been suggested to act as direct V $\gamma$ 9V $\delta$ 2 TCR ligands or modifiers of V $\gamma$ 9V $\delta$ 2 TCR ligand interactions (80-82). Scotet et al. reported that an ectopically expressed F1-ATPase complex, which, in conjunction with apolipoprotein A, binds recombinant V $\gamma$ 9V $\delta$ 2 TCR (80). The group of He reported that the NKG2D ligand ULBP4 binds to a soluble chimeric protein containing V $\gamma$ 9V $\delta$ 2 TCR and activates TCR<sup>+</sup> Jurkat T cells transfected with V $\gamma$ 9V $\delta$ 2 TCR (81). How far the modulation of IPP levels may affect the V $\gamma$ 9V $\delta$ 2 TCR binding or expression of these postulated ligands has not been investigated. Furthermore, there is modulation of the TCR mediated activation through the innate immune receptors such as KIRs and NKG2D. For NKG2D, even a TCR independent triggering of cellular cytotoxicity and TNF $\alpha$  production has been demonstrated by our group (63).

### ***1.7.3 Functions of V $\gamma$ 9V $\delta$ 2 T cells as a bridge between innate and adaptive immunity***

The classical boundary of innate immunity and adaptive immunity becomes more and more obscure due to the continuous breakdown in conventional hallmarks of each system.  $\gamma\delta$  T cells have been classed to innate immunity owing to the quick response and unspecific activation in microbial infections or cancer surveillance. Interestingly, V $\gamma$ 9V $\delta$ 2 T also display the hallmark features of professional antigen presenting cells (APCs) for naive  $\alpha\beta$  T cells (83, 84): 1) activated V $\gamma$ 9V $\delta$ 2 T cells upregulate the surface expression of MHC class II and costimulatory molecules CD80/CD86; 2) they have the capacity to take up and process soluble antigens, such as tetanus toxoid, consequently present to CD4<sup>+</sup> T cells (83); 3)  $\gamma\delta$  T-APCs are also capable of cross-presenting microbial and tumor antigens to CD8<sup>+</sup>  $\alpha\beta$  T cells. Moreover,  $\gamma\delta$  T cells also provide potent B-cell help. IPP stimulating V $\gamma$ 9V $\delta$ 2 T cells rapidly upregulate CCR7 which allow them to migrate to lymph nodes through attraction by CCR21 (85). Activated  $\gamma\delta$  T cells also upregulate the surface expression of CD40, OX40, CD70, and ICOS which may provide strong help to B cell response (85). Eberl et al. reported a rapid crosstalk between human V $\gamma$ 9V $\delta$ 2 T cells and monocytes which not only confer V $\gamma$ 9V $\delta$ 2 T stronger responsiveness to microbial infections but also drive monocytes survival and differentiation into inflammatory immature dendritic cells (86). In the presence of toll like receptors (TLRs) signal, these immature DCs further differentiate into CCR7<sup>+</sup> DCs which are capable of inducing Th17 cells response (86).

### **1.8 Clinical Perspective of V $\gamma$ 9V $\delta$ 2 T cells**

Large numbers of in vitro studies demonstrated that phosphoantigen-activated V $\gamma$ 9V $\delta$ 2 T cells are capable of killing tumor cells derived from bladder cancers, breast cancers, colon carcinomas, lymphomas, melanomas, myelomas, nasopharyngeal carcinomas, neuroblastomas, pancreatic carcinomas, prostate cancers, renal cell carcinomas, and lung cancers (34). The well documented potent broad anti-tumor activities of V $\gamma$ 9V $\delta$ 2 T cells have recently aroused great interests in V $\gamma$ 9V $\delta$ 2 T cells based cancer immunotherapy. In a pilot study, Wilhelm et al. (48) treated patients with low-grade non-Hodgkin lymphoma and multiple myeloma via intravenous pamidronate and low-dose recombinant IL-2. This

## INTRODUCTION

type of immunotherapy was well tolerated by patients and no dose-limiting toxicity could be defined besides self-limiting fever and local thrombophlebitis. More significantly, this clinical trial showed for the first time that the administration of pamidronate induces a selective activation and proliferation of V $\gamma$ 9V $\delta$ 2 T cells in vivo and also provided the first evidence that the selective stimulation of  $\gamma\delta$  T cells can be accompanied by anti-lymphoma activity in vivo. Another clinical study indicated that in vivo treatment with zoledronate without IL-2 did not change the percentage and absolute numbers of V $\gamma$ 9V $\delta$ 2 T cells in peripheral blood lymphocytes. However, this type of treatment could expand an IFN- $\gamma$ -producing effector V $\gamma$ 9V $\delta$ 2 T cells (CD45RA<sup>-</sup>CD27<sup>-</sup>), while decreasing the naive (CD45RA<sup>+</sup>CD27<sup>-</sup>) and central memory (CD45RA<sup>-</sup>CD27<sup>+</sup>) subsets (87). In another phase I clinical trial, Dieli et al. reported the treatment with zoledronate plus IL-2 as a safe and feasible approach for immunotherapy of patients with metastatic carcinomas (88). Furthermore, intravenous infusion of BrHPP with low dose of IL-2 in patients with renal carcinomas was also conducted in a phase I clinical trial (89). There are also a number of clinical or preclinical trials in progress using adoptive transfer of V $\gamma$ 9V $\delta$ 2 T cells expanded ex vivo with either bisphosphonates or phosphoantigens for immunotherapy of renal carcinomas (90, 91) and breast cancers (92).

Despite the promising perspective of V $\gamma$ 9V $\delta$ 2 T cells in cancer immunotherapy, there are some potential problems to be solved such as anergy induction, immune exhaustion, and activation-induced cell death (ACID) (34).

### **1.9 Retroviral/Lentiviral Delivery of Short Haipin RNAs**

In 1998, Andrew Fire and Craig Mello reported their break-through study on the mechanism of RNA interference (RNAi) in *Nature* (93). Since then, the research on RNAi revealed its enormous potential not only in basic biological research but also in therapeutic drugs discovery. In brief, generation of RNAi is a conserved biological response to double-stranded RNA (dsRNA) that permits the sequence-specific gene silencing. In a bit more detail, dsRNA is cleaved by the Rnase III enzyme Dicer into short interfering RNAs (siRNAs; 21-23 nucleotides in length). The sense strand of the siRNA is rapidly cleaved while the antisense strand is incorporated into the RNA-induced

## INTRODUCTION

silencing complex (RISC) and targets the specific genes owing to sequence complement. As a consequence, the specific gene is silenced (94, 95).

RNAi can be induced by three types of small RNA: synthetic short interfering RNA (siRNA), short hairpin RNA (shRNA) and microRNA-adapted short hairpin RNA (shRNAmir) (96). Synthetic siRNA are short dsRNAs that are typically 19-22 bps in length. Introduction of this kind of RNA resembling the Dicer-processed siRNA into cells induces specific gene silencing (97). There are two limitations using siRNA: low transfection efficiencies and short-term silencing effects (3-5 days). Since the discovery of microRNA (miRNA) and its endogenous biogenesis pathway, an alternative vector-based RNAi triggers including shRNA and shRNAmir were developed (96). As shown in Figure. 1-5, there are three distinct RNA intermediates during miRNA biogenesis pathway: a primary miRNA (pri-miRNA) transcript, a precursor miRNA (pre-miRNA) and the mature miRNA. shRNA is modeled based on the structure of pre-miRNA and shRNAmir mimics the structure of pri-miRNA through replacing the stem of the primary miR-30 transcript with gene-specific sequences (98-100).

shRNA and shRNAmir can be endogenously expressed through plasmid or viral vectors mediated oligonucleotide delivery. The latter method is commonly used for shRNAs expression owing to its easy delivery, high expressing efficiencies and long-term effects. Especially, retroviral and lentiviral vectors provide a means for life-long shRNA expression and target gene silencing since the viral DNA gets incorporated in the host genome. Due to the serious unsafety using native viruses, non-replicating recombinant viruses are used for transgene expression. The retroviral vectors were produced using transient transfection of three different plasmids into 293T cells (101). In addition to the transfer plasmid containing the backbone of the 5' and 3' long terminal repeats (LTRs), the packaging signal ( $\psi$ ), and the inserted gene of interest, there are two more plasmids comprising gag-pol genes and env gene coding for capsid proteins, reverse transcriptase and integrase, and the envelope proteins, respectively. Currently, the HIV-based lentiviral vectors are predominantly used owing to their particular traits in infecting non-dividing cells and the accommodation of large segments of transgenes. However, it must be

## INTRODUCTION

cautioned that the potential high risks are the core issue in the development of lentiviral vectors. To obviate all potential risks, the steady improvements in the lentiviral vector design and production were made over time. The current lentiviral vectors are produced using four separate plasmids with minimal sequence homology comprising the gag-pol genes, the rev gene, the VSV-G envelope, and the transfer plasmid (102). Drug-inducible control of gene expression would be desirable in many circumstances such as in vivo based RNAi. Most recently, conditional expression of shRNA in a signal lentiviral vector improved significantly (103-107). The combination of retroviral/lentiviral vectors and RNAi, will probably develop novel targets and therapeutic strategies on the basis of new insights into complex genetic pathways.

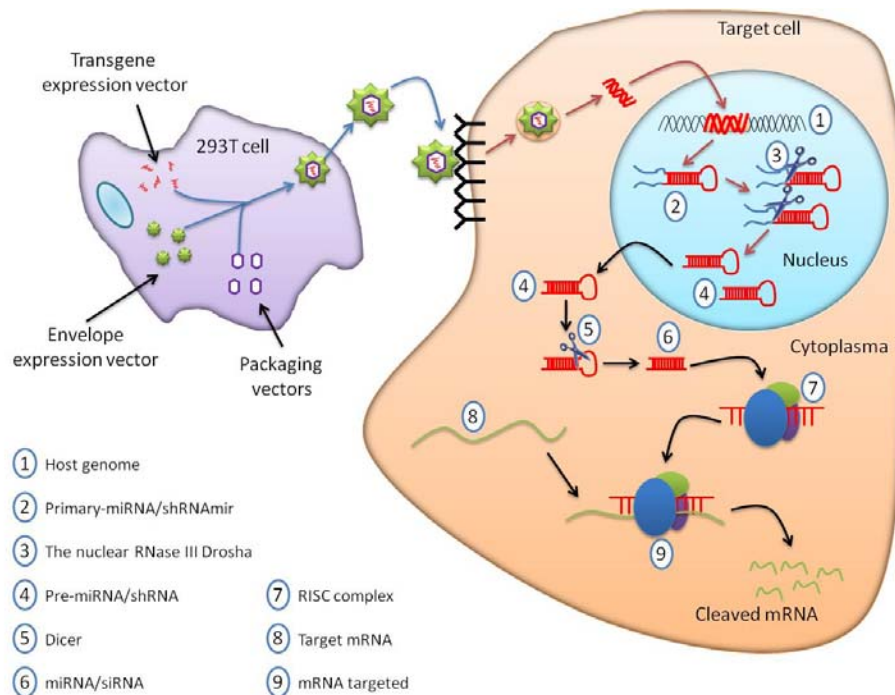


**Figure. 1-5 Schematic of non-replicating retroviral/lentiviral vector mediated shRNA expression and processing.** 293T cells are transfected with a mixture of 3 or 4 plasmids. The generated virus is then used to transduce the desired cell type and the inserted shRNA sequences are incorporated into host genome. shRNA triggers are modeled on primary miRNA and processed by Drosha and Dicer to produce mature siRNA that targets a complementary mRNA in a RISC complex. mRNA is then cleaved and subsequently expression of target gene is arrested.



## 2 MATERIALS AND METHODS

### 2.1 MATERIALS

#### 2.1.1 *Chemical reagents*

Agar-agar	Roth (Karlsruhe, Germany)
Agarose	Roth (Karlsruhe, Germany)
Acrylamide	Roth (Karlsruhe, Germany)
Ammoniumchloride	Roth (Karlsruhe, Germany)
Ampicillin	Gibco BLR (Eggenstein, Germany)
Aprotinin	Calbiochem (Darmstadt, Germany)
APS (Ammoniumpersulfat)	Roth (Karlsruhe, Germany)
$\beta$ -mercaptoethanol	Gibco BLR (Eggenstein, Germany)
Boric acid	Roth (Karlsruhe, Germany)
BrHPP	Innate Pharma (Marseille, France)
Calcium Chloride (CaCl <sub>2</sub> )	Roth (Karlsruhe, Germany)
5-(and-6)-carboxyfluorescein diacetate	
Succinimidyl ester (CFSE)	Molecular Probes (Eugene, Oregon)
DEPC (Diethylpyrocarbonate)	Sigma (Deisenhofen, Germany)
Diatomaceous earth	Sigma (Deisenhofen, Germany)
DMSO (Dimethyl sulfoxide)	Sigma (Taufkirchen, Germany)
5,5'-dithio-bis-2-nitrobenzoic acid	Pierce (Bonn, Germany)
dNTP Set	Peqlab Biotechnologie (Erlangen, Germany)
Doxycycline hyclate	Sigma (Steinheim, Germany)

## MATERIALS AND METHODS

EDTA	AppliChem GmbH (Darmstadt, Germany)
Ethanol	AppliChem GmbH (Darmstadt, Germany)
Ethidium bromide	Roth (Karlsruhe, Germany)
Ficoll-Paque	Amersham (Piscataway, N.J. USA)
Formaldehyde	Roth (Karlsruhe, Germany)
Formamide	Roth (Karlsruhe, Germany)
FPPS antibody blocking peptide	ABGENT (San Diego, USA)
G418 (Geneticin solution)	Biochrom AG (Berlin, Germany)
Glycerol	Sigma (Schnelldorf, Germany)
Glycine	Roth (Karlsruhe, Germany)
HMBPP	Labor Jomaa (Giessen, Germany)
Ionomycin	Sigma (Deisenhofen, Germany)
IPP (Isopentenyl pyrophosphate ammonium)	Sigma (Deisenhofen, Germany)
Isopropanol	AppliChem GmbH (Darmstadt, Germany)
LB (Broth Base medium)	Gibco BLR (Eggenstein, Germany)
Leupeptin	Calbiochem (Darmstadt, Germany)
Magnesium Chloride	Roth (Karlsruhe, Germany)
Mevastatin	Dr. Kunzmann (Würzburg, Germany)
Methanol	AppliChem GmbH (Germany)
Na-Butyrate	Sigma (Deisenhofen, Germany)
NaF (Sodium fluoride)	Calbiochem (Darmstadt, Germany)
Na <sub>3</sub> VO <sub>4</sub> (Sodium vanadate)	Calbiochem (Darmstadt, Germany)
N-benzyloxycarbonyl lysine thiobenzyl	Calbiochem (Darmstadt, Germany)
NaN <sub>3</sub> (Sodium Azide)	Merck (Darmstadt, Germany)
Sodium Chloride	Roth (Karlsruhe, Germany)
Sodium Butyrate	Sigma (Deisenhofen, Germany)
Pamidronate	Novartis (Basel, Switzerland)
PEG (Polyethylenglycol)	Boehringer Mannheim (Mannheim, Germany)

## MATERIALS AND METHODS

PKH-26	Sigma (St Louis, Mo, USA)
Penicillin	Gibco BRL (Eggenstein, Germany)
Pepstatin	Calbiochem (Darmstadt, Germany)
PMA (Phorbol myristate acetate)	Sigma (Deisenhofen, Germany)
Polybrene (Hexadimethrinbromide)	Sigma (Deisenhofen, Germany)
Puromycine	Cayla (Toulouse Cedex, France)
rhuIL-2 (recombinant human IL-2)	Miltenyi Biotec (Bergisch Gladbach, Germany)
SDS (Sodium dodecyl sulfate)	Sigma (Deisenhofen, Germany)
Tris (Tris(hydroxymethyl)-aminomethan)	AppliChem GmbH (Darmstadt, Germany)
Trypan blue	Sigma (Deisenhofen, Germany)
Tween 20	Sigma (Deisenhofen, Germany)
Zeocin	Cayla (Toulouse Cedex, France)
Zoledronate	Novartis (Basel, Switzerland)

### **2.1.2 Media, solutions and buffers**

Media used for cell cultures were obtained from Gibco-BRL (Eggenstein, Germany):

DMEM	with Pyruvate, without HEPES (#41966-029)
(Dulbecco's Modified Eagle's Medium)	without Pyruvate, with HEPES (#41966-027)
RPMI	RPMI 1640 + L-Glutamine (#21875-034)
SC (supplement complete)	500 ml heat-deactivated FCS
(50ml SC/500ml Medium)	100 ml Na pyruvate 100 mM
	100 ml non-essential amino acids
	100 ml Penicillin-Streptomycin (10000U/ml)
	5 ml $\beta$ -Mercaptoethanol 50 mM
	58.4 ml L-Glutamine solution 5%
ATV	0.05% Trypsin, 0.02% EDTA in PBS
2 $\times$ HBS(pH7.05)	50 mM HEPES pH 7.05, 10 mM KCl, 12 mM Glucose, 280 mM NaCl, 1.5 mM NaH <sub>2</sub> PO <sub>4</sub>

## MATERIALS AND METHODS

LB- medium		20 g LB, in 1 L dH <sub>2</sub> O, autoclaved and stored at 4°C
PBS (Phosphate buffered saline)		4 mM KH <sub>2</sub> PO <sub>4</sub> , 16 mM Na <sub>2</sub> HPO <sub>4</sub> , 115mM NaCl, pH 7.3
PBS/BSA/Azide		0.2% BSA, 0.02% Na-Azide in PBS
TAC (Tris-Ammoniumchlorid)		20 mM Tris-HCl pH 7.2, 0.82% NH <sub>4</sub> Cl
10× TBE		890 mM Tris pH 8.0, 890 mM Boric acid, 20 mM EDTA
FACS buffer		0.1% BSA, 0.05% NaN <sub>3</sub> in PBS
Modified RIPA buffer		50 mM pH 7.4 Tris-HCl, 1% NP-40, 0.25% Na-deoxycholate, 150 mM NaCl, 1 mM EDTA, 1 mM PMSF, 1 µg/ml Aprotinin, Leupeptin and Pepstatin, 1 mM Na <sub>3</sub> VO <sub>4</sub> , 1 mM NaF.
Tris-glycine-SDS electrophoresis buffer (1×)	protein	25 mM Tris, 250 mM glycine, 0.1% SDS, pH 8.3
6×SDS Protein electrophoresis loading buffer		300 mM Tris.Cl (pH 6.8), 600 mM DTT, 12% SDS, 0.6% Trypanblau, 60% Glycerol
Protein transfer buffer for Western-blot		
Anode Buffer I		0.3 M Tris, pH 10.4, 10% Methanol
Anode Buffer II		25 mM Tris, pH 10.4, 10% Methanol
Cathode Buffer		25 mM Tris, 40 mM Glycine, 10% Methanol, pH 9.4,
HRP substrate for western-blot		ECL (Amersham. Freiburg, Germany)
1×TSS (transformation and storage solution)		20.0g PEG3350, 2.03g MgCl <sub>2</sub> .6H <sub>2</sub> O, 5.0g LB, supplement water to 180 ml, pH6.5. Autoclaved, add 20ml DMSO (sterile) when cooled, keep at 4°C.

## MATERIALS AND METHODS

(1L)BSS (Hanks balanced salt solution)

(125ml) BSS I (8×) 50 g Glucose, 3 g KH<sub>2</sub>PO<sub>4</sub>, 11.9 g NaH<sub>2</sub>PO<sub>4</sub>  
0.4 g Phenol red, Water to 5 L

(125ml) BSS II(8×) 9.25 g CaCl<sub>2</sub>, 20 g KCl, 320 g NaCl, 10 g  
MgCl<sub>2</sub>, 10 g MgSO<sub>4</sub>, Water to 5 L

(750ml) dH<sub>2</sub>O

BSS/BSA 0.2 % BSA in BSS

Cell freezing solution 50% FCS, 40% RPMI, 10% DMSO

Buffer for ELISA

Coating Buffer (1L) 7.13g NaHCO<sub>3</sub>, 1.59g Na<sub>2</sub>CO<sub>3</sub>, pH to 9.5 with  
(0.1 M Sodium Carbonate, pH 9.5) 10 N NaOH

Assay Dilute PBS with 10% FCS, pH 7.0

Wash Buffer PBS with 0.05% Tween-20

Stop Solution 2N H<sub>2</sub>SO<sub>4</sub>

### **2.1.3 Cell lines**

293T transformed primary human embryonic kidney cells;  
ATCC#CRL-1573

58C (BW58) Do-11.10.7 hybridoma derived AKR/J mouse  $\alpha\beta$  TCR-negative cell  
lymphoma (108); ATCC#TIB-233. Kindly provided by Dr Palmer  
(Basel Institute, Switzerland).

721.221 EBV-transformed MHC class I-deficient human B cell line, kindly  
provided by Prof. Champagne (INSERM, Toulouse, France)

A549 Human lung adenocarcinoma epithelial cell line, kindly provided by  
Dr. Kunzmann (Wuerzburg University)

AsPC-1 Human pancreatic carcinoma cell line, kindly provided by Dr.  
Kunzmann (Wuerzburg University)

BW58r/mCD28 BW58 cells that have been transfected with r/mCD28 (109)

## MATERIALS AND METHODS

Daudi	$\beta$ 2-microglobulin-deficient human B cell lymphoma, ATCC#CTL-213
HepG-2	Human hepatocellular liver carcinoma cell line
J.K7	The line was cloned from J.RT3-T3.5 by our group before
J.RT3-T3.5	Mutant line derived from Jurkat that lacks the beta chain of the T cell antigen receptor. The cells express neither CD3 nor the $\alpha\beta$ TCR on the surface; ATCC#TIB-153
Jurkat	Human T lymphoma; ATCC#TIB-152
K562-Ctl	human erythroleukemia line K562(ATCC#CCL-243) that have been transfected with pcDNA empty vector, kindly provided by Prof. Champagne (INSERM, Toulouse, France)
L929	mouse fibroblast cell line; ATCC#CCL-1
LBB	mouse B cell hybridoma (110)
RAJI	human Burkitt lymphoma; ATCC#CCL-86
RMA	mouse T cell lymphoma
RMA-S	RMA-derived TAP2-deficient mouse T lymphoma

### 2.1.4 Vectors

pVSV-g	pCZVSV-g wt, containing <i>env</i> from Vesicular Stomatitis Virus (111)
pHIT60	-CMV-MVV- <i>gag-pol</i> -SV40ori; containing <i>gag</i> and <i>pol</i> from Moloney Murine Leukemia Virus (MoMLV) under the control of human Cytomegalovirus (CMV) promoter (101)
pMDL-RRE (MDL)	Lentiviral packaging plasmid containing <i>gag</i> , <i>pol</i> and RRE, a binding site for the Rev protein which facilitates export of the RNA from the nucleus (112)
pRSV-REV (REV)	Rev cDNA expressing plasmid in which the joined second and third exons of HIV-1 rev are under the transcriptional control of RSV U3 promoter (112)
pczCG5IEGZ (EGZ)	IRES bicistronic retroviral vector for the MuLV driven constitutive expression of the interesting gene and IRES mediated EGFP reporter

## MATERIALS AND METHODS

	and zeocin resistant marker expression.
pczCG5IEGN (EGN)	IRES bicistronic retroviral vector for the MuLV driven constitutive expression of the interesting gene and IRES mediated EGFP reporter and neomycin resistant marker expression.
pczCFG5IZ (pIZ)	Retroviral vector for the MuLV driven constitutive expression of the interesting gene with resistant marker zeocin
pIZ/EYFP	Retroviral vector for the MuLV driven constitutive fusion protein expression of the interesting gene and EYFP with resistant marker zeocin.
SFG GFP (S65T)	Retroviral vector for constitutive expression of the interesting gene inserted in the Polylinker (Nco I/BamH I) to replace the GFP gene between these two restriction sites (113).
MSCV-LTRmir30-Pig (LMP)	A MSCV mediated retroviral vector to enable the efficient expression of shRNAmir constructs from RNA Polymerase II (Pol II) promoters containing puromycin resistance and GFP marker (OpenBiosystem).
LMP/ASred (AS)	The red fragment of pred/MCS which contains the AsRed fluorescent protein (red) was ligated into the NcoI and PacI sites of MSCV-LMP to replace GFP gene (114).
pH1tet-flex	Lentiviral vector consists of the human H1 promoter with a tet-operator and cloning sites (BbsI/XhoI) for the insertion of the shRNA-oligos. Kindly provided by Dr. Herold (Walter and Eliza Hall Institute of Medial Research, Melbourne, Australia).
FH1t(INSR)UTG	Lentiviral vector consists of the H1tet-shIR5 cassette (shIR5 is a shRNA specific for the insulin receptor) and the UbiquitinP-TetR-T2A-eGFP cassette. The H1tet-shIR5 cassette can be excised with PacI and replaced by an H1tet-shRNA cassette with the required specificity amplified from the pH1tet-flex vector (107). Kindly provided by Dr. Herold (Melbourne, Australia).

## MATERIALS AND METHODS

### 2.1.5 Antibodies

**Table 2-1 Monoclonal Antibodies for FACS staining or Immuno-blot.**

Antigen	Clone	Conjugated	Isotype	Offer
mCD3e	145-2C11	Purified	Hamster IgG1, $\kappa$	BD Pharmingen
mCD3e	145-2C11	Bio	Hamster IgG1, $\kappa$	BD Pharmingen
huCD69	FN50	FITC	m IgG1, $\kappa$	BD Pharmingen
huCD69	FN50	APC	m IgG1, $\kappa$	BD Pharmingen
huCD107a	H4A3	FITC	m IgG1, $\kappa$	BD Pharmingen
huCD107a	H4A3	PE	m IgG1, $\kappa$	BD Pharmingen
huCD107a	H4A3	PE-Cy5	m IgG1, $\kappa$	BD Pharmingen
huCD80	L307.4	FITC	m IgG1, $\kappa$	BD Pharmingen
huCD3	UCHT1	PE	m IgG1, $\kappa$	BD Pharmingen
huCD28	CD28.2	PE.Cy5	m IgG1, $\kappa$	BD Pharmingen
hu $\gamma\delta$ TCR	B1	FITC	m IgG1, $\kappa$	BD Pharmingen
huV $\delta$ 2 chain	B6	PE	m IgG1, $\kappa$	BD Pharmingen
huIFN- $\gamma$	4S.B3	PE	m IgG1, $\kappa$	BD Pharmingen
Rat CD28	JJ319	Bio	m IgG1, $\kappa$	BD Pharmingen
Rat CD80	3H5	Purified	m IgG1, $\kappa$	BD Pharmingen
Hu $\beta$ -Tubulin	5H1	Purified	m IgM	BD Pharmingen
Hu $\beta$ -ATPase	3D5	Purified	m IgG1, $\kappa$	Molecular Probes
mIgG2b, $\kappa$	187.1	HRP	rat IgG1, $\kappa$	BD Pharmingen
Rabbit IgG		HRP	goat IgG	Santa Cruz
FPP Synthase		Purified	Rabbit IgG	ABGENT

#### **Other secondary staining reagents:**

FITC/RPE/APC conjugated affinipure F(ab')<sub>2</sub> fragments donkey anti mouse IgG (H+L) polyclonal antibodies, Dianova, Hamburg, Germany.

PE.Cy5/APC conjugated with Streptavidin, BD Pharmingen.

### 2.1.6 Cloning reagents

T4-DNA-Ligase

Promega (Heidelberg, Germany)



## MATERIALS AND METHODS

Phusion High-Fidelity DNA Polymerase	Finnzymes (Finland)
Taq-DNA Polymerase	MBI Fermentas (St.Leon-Rot, Germany)
CIAP	MBI Fermentas (St.Leon-Rot, Germany)
Restriction Enzymes	MBI Fermentas (St.Leon-Rot, Germany)

### **2.1.7 Kits**

JETsorb Gel Extraction Kit	# 110150	Genomed (Löhne, Germany)
JETquick DNA Clean Up Spin Kit	# 430050	Genomed (Löhne, Germany)
RNeasy MiniKit	# 74104	QIAGEN (Hilden, Germany)
QIAquick PCR Purification Kit	# 28104	QIAGEN (Hilden, Germany)
First Strand cDNA Synthesis Kit	# K1612	MBI Fermentas(St.Leon-Rot, Germany)
BigDye Terminator Cycle Sequencing	# 4303152	Applied Biosystem (Warrington, United Kingdom)
OPTEIA mouse IL-2 Set	# 555148	BD (Heidelberg, Germany)
Human IFN- $\gamma$ ELISPOT kit	# 3420–2APW-2	Mabtech (Hamburg, Germany)

### **2.1.8 Apparatus**

FACS-Calibur	Becton Dickinson (USA)
Power supply unit (protein electrophoresis and transfer)	Pharmacia Biotech (USA)
UV/Visible Spectrophotometer:Ultraspe 2000	Pharmacia Biotech (USA)
Transmenbrane apparatus Hofer	Scientific Instrument (USA)
Eppendorf centrifuge 5417R	Eppendorf AG (Hamburg, Germany)
Hettich centrifuge Rotixa 50 RS	Hettich (Tuttlingen, Germany)
Microcentrifuge Biofuge pico	Hereaus (Osterode, Germany)
Cell incubator	Forma Scientific (USA)
Heating block	VWR (Germany)
Water bath	Lauda (Lauda, Germany)
Liquid Scintillation Counter Microbeta Trilux	Perkin Elmer (Turku, Finland)
ELR03 ELISPOT reader	AID Gmbh (Straßberg, Germany)
PCR Cycler	Eppendorf AG (Hamburg, Germany)

## MATERIALS AND METHODS

### **2.1.9 Consumables**

6 well flat bottom culture plates	Greiner-Bio-One (Germany)
12 well flat bottom culture plates	Greiner-Bio-One (Germany)
24 well flat bottom culture plates	Greiner-Bio-One (Germany)
48 well flat bottom culture plates	Greiner-Bio-One (Germany)
96 well flat bottom culture plates	Greiner-Bio-One (Germany)
96 well U bottom culture plates	Greiner-Bio-One (Germany)
6 cm tissue culture dish	Greiner-Bio-One (Germany)
50 ml cell culture flask	Greiner-Bio-One (Germany)
1.5 ml Eppendorf centrifuge tube	Eppendorf GmbH (Germany)
15 ml centrifuge tube	Greiner-Bio-One (Germany)
50 ml centrifuge tube	Greiner-Bio-One (Germany)
Cuvette	Bio-Rad (USA)
10 µL tips	Molecular Bioproducts (USA)
200 µL yellow tips	Roth (Karlsruhe, Germany)
1000 µL blue tips	Roth (Karlsruhe, Germany)
Syringe: 2ml and 5ml single-use syringe	Braun (Melsungen, Germany)
96 well flat bottom microplate	Nunc (Denmark)
Absorbent paper for Western-Blot	Whatman (USA)
PVDF membrane for Western-Blot	Roth (Karlsruhe, Germany)

### **2.1.10 Softwares**

Scion Image, density analysis software for western blot bands  
Cell Quest, flow cytometry data analysis software  
FlowJo, flow cytometry data analysis software  
Endnote, software tool for publishing and managing bibliographies  
Origin, graphing and data analysis software

## MATERIALS AND METHODS

### 2.1.11 Primers

All primers and DNA oligos were synthesized by MWG- Biotech AG (Ebersberg, Germany) or Sigma (Taufkirchen, Germany).

**Table 2-2 Primers for constructs of retroviral vectors encoding TCR  $\gamma$  gene and  $\delta$  gene**

<b>TCR<math>\gamma\delta</math> chain</b>	<b>Cloning vectors</b>	<b>Restriction sites</b>	<b>Primers</b>
$\gamma$ Mop	EGN	EcoR I, BamH I/Bgl II	Fwd: 5'-GCTACGAATTCACCATGCTGTCACTGCTGCTC-3' Rev: 5'-AGCATAGATCTTTATGATTTCTCTCCATTGCAGC-3'
$\delta$ Mop	pIZ	EcoR I/Mfe I, BamH I	Fwd: 5'-GCTACCAATGGACCATGATCTCCTCCCTCATCC-3' Rev: 5'-AGCATGGATCCTTACAAGAAAATAACTTGGCAG-3'
D51	pIZ	EcoR I/Mfe I, BamH I	5' Rev: 5'-GATGTCCTTTTCTGCGTATATG-3' 3' Fwd: 5'-CGCAGAAAAGGACATCTATGG-3'
D96	pIZ	EcoR I/Mfe I, BamH I	5' Rev: 5'-AGCGGTATCGGGGTCACAGGCACAGTAGTAAG-3' 3' Fwd: 5'-GATACCGCTTACACCGATAAACTCATCTTTGG-3'
$\gamma$ Mop-T2A- $\delta$ Mop	EGN	BamH I/Bgl II	V $\gamma$ Mop Bgl Fwd: 5'-GCTACAGATCTACCATGCTGTCACTGCTGCTC-3' V $\gamma$ 2A Rev: 5'- CCAGGATTCTCCTCGACGTCACCGCATGTTAGCAGACTTCCTCTG CCCTCTGATTTCTCTCCATTGCAGCAG-3' 2A V $\delta$ Fwd: 5'- GAGGGCAGAGGAAGTCTGCTAACATGCGGTGACGTCGAGGAGAATC CTGGCCAATGATCTCCTCCCTCATCCATC-3' V $\delta$ Mop Bgl Rev: 5'-AGCATAGATCTTTACAAGAAAATAACTTGGCAGTCG-3'

## MATERIALS AND METHODS

**Table 2-3 Primers for constructs of retroviral vectors encoding CD28 and CD80**

Gene	Vectors	Restriction sites	Primers
Mouse CD28	S65T	Nco I, BamH I	Fwd: 5'-GCTACCCATGGACCATGACACTCAGGCTGCTG-3' Rev: 5'-AGCATGGATCCTCAGGGGCGGTACGCTGC-3'
Human CD28	S65T	Nco I, BamH I	Fwd: 5'-CTACCCATGGATGCTTCAGGCTGCTCTTGG-3' Rev: 5'-GCATGGATCCTCAGGAGCGATAGGCTGC-3'
Rat/mouse CD28	S65T	Nco I, BamH I	Fwd: 5'-GCTACCCATGGACCATGACACTCAGACTGCTATTC-3' Rev: 5'-AGCATGGATCCTCAGGGGCGGTACGCTGC-3'
Human/mouse CD28 1 <sup>st</sup>	S65T	Nco I, BamH I	hu/mCD28 Nco fwd: GCTACCCATGGACCATGCTCAGGCTGCTCTTG hu/mCD28 OL rev: CACGACCAGTGCCCAAAGGGCTTAGAAGG hu/mCD28 OL fwd: AAGCCCTTTTGGGCACTGGTCGTGGTTGCTG hu/mCD28 Bam rev: AGCATGGATCCTCAGGGGCGGTACGCTGC
Human/mouse CD28 2 <sup>nd</sup>	S65T	Nco I, BamH I	New hu/mCD28 OL rev: GTTCCATTGCTCTTCTCATTG New hu/mCD28 OL fwd: GAAGAGCAATGGA ACTATTATTCAC
Human CD80	S65T	Nco I, BamH I	Fwd: 5'-GCTACCCATGGACCATGGGCCACACACGGAGG-3' Rev: 5'-AGCATGGATCCTTATACAGGGCGTACACTTTC-3'

## MATERIALS AND METHODS

**Table 2-4 Primers for constructs of retroviral vectors encoding mevalonate pathway enzymes' genes.**

<b>Gene of interest</b>	<b>Accession Nr.</b>	<b>Cloning vectors</b>	<b>Restriction sites</b>	<b>Primers</b>
FPPS	<a href="#">NM_002004</a>	EGZ	EcoR I/Mfe I, BamH I	Fwd: 5'- <i>CACAATTG</i> ACCATGCCCCTGTCCCGCTGG-3' Rev: 5'- <i>ACGGATCCTTACTTTCTCCGCTTGTAGAT</i> -3'
		pIZYFP	EcoR I/Mfe I, BamH I	Fwd: 5'-TAGCCCAATTGGCCGCCACCATGCCCCTGTCCCGCT-3' Rev: 5'-AGTCCGGATCCCGCTTTCTCCGCTTGTAGAT-3'
GGPPS	<a href="#">NM_004837</a>	EGN	BamH I	Fwd: 5'-GCTACGGATCCACCATGGAGAAGACTCAAGAAAC-3' Rev: 5'-AGCATGGATCCTTATTCATTTTCTTCTTTGAACATC-3'
		pIZYFP	EcoR I/Mfe I, BamH I	Fwd: 5'-GCTACCAATTGACCATGGAGAAGACTCAAGAAACAG-3' Rev: 5'-AGCATGGATCCCCTTCATTTTCTTCTTTGAACATC-3'
IDI	<a href="#">NM_004508</a>	EGN	EcoR I/Mfe I, BamH I	Fwd: 5'-GCTACCAATTGACCATGATGCCTGAAATAAACAC-3' Rev: 5'-GCTACGGATCCCCTACATATTCACATTCTG-3'
		pIZYFP	EcoR I/Mfe I, BamH I	Fwd: 5'-GCTACCAATTGACCATGATGCCTGAAATAAACAC-3' Rev: 5'-AGCATGGATCCCCCATTCTGTATATTTTCTCATGG-3'
MVD	<a href="#">NM_002461</a>	EGN	EcoR I, BamH I	Fwd: 5'-TGGGGGAATTCACCATGGCCTCGGAGAAG-3' Rev: 5'-CGGTCCCTGAGGCAGGGATCCTCAGGCAG-3'
		pIZYFP	EcoR I, BamH I	Fwd: 5'-TGGGGGAATTCACCATGGCCTCGGAGAAG-3' Rev: 5'-CGGTCCCTGCTGAGGCAGGGATCCGGCAG-3'
HMGR	<a href="#">NM_000859</a>	EGN	EcoR I, BamH I	Fwd: 5'-GGAGGAATTCGCCGCCACCATGTTGTCAAGACTTTTTCGAATGC-3' Rev: 5'-GTAATGGATCCTCAGGCTGTCTTCTTGGTG

## MATERIALS AND METHODS

**Table 2-5 Hairpin sequences for constructs of retroviral vectors expressing different shRNAs.**

<b>Gene</b>	<b>Openbiosystem Nr.</b>	<b>Abbrev.</b>	<b>Hairpin sequence</b>
FPPS	V2HS_228248	AS22	AAGGTATATTGCTGTTGACAGTGAGCGACCAGCAGTGTTCCTTGCAATATTAGTGAAGCC ACAGATGTAATATTGCAAGAACAACACTGCTGGCTGCCTACTGCCTCGGAATATAACCTT
	V2HS_113816	AS11	AAGGTATATTGCTGTTGACAGTGAGCGCCCTCCTGGAAGCATGTATCTATAGTGAAGCC ACAGATGTATAGATACATGCTTCCAGGAGGTTGCCTACTGCCTCGGAATATAACCTT
GGPPS	V2HS_68130	AS30	TGCTGTTGACAGTGAGCGAACTCCAAAGAATATAGTGAAATAGTGAAGCCACAGATGT ATTTCACTATATTCTTTGGAGTGTGCCTACTGCCTCGGA
	V2HS_68132	AS32	TGCTGTTGACAGTGAGCGCGCAGTTGTTCTCTGATTACAATAGTGAAGCCACAGATGTA TTGTAATCAGAGAACAACACTGCATGCCTACTGCCTCGGA
IDI	V2HS_48970	AS70	TGCTGTTGACAGTGAGCGCAGGTTGAATCTTCTTGTAATAGTGAAGCCACAGATGTA ATTTACAAGAAGATTCAACCTATGCCTACTGCCTCGGA
	V2HS_67395	AS95	TGCTGTTGACAGTGAGCGCGGTTCTCCAGAAGAAATTAATAGTGAAGCCACAGATGT ATTAATTTCTTCTGGAGGAACCTTGCCTACTGCCTCGGA
HMGR	V2HS_130980	AS80	TGCTGTTGACAGTGAGCGCCCTACCTTACAGGGATTATAATAGTGAAGCCACAGATGTA TTATAATCCCTGTAAGGTAGGTTGCCTACTGCCTCGGA
	V2HS_130983	AS83	TGCTGTTGACAGTGAGCGAGGTTCTAAAGGACTAACATAATAGTGAAGCCACAGATGT ATTATGTTAGTCCTTTAGAACCCTGCCTACTGCCTCGGA
MVD	TRCN0000078480	AS00	TGCTGTTGACAGTGAGCGCCATCTCTTACCTCAATGCCATAGTGAAGCCACAGATGTA TGGCATTGAGGTAAGAGATGGTGCCTACTGCCTCGGA
	TRCN0000078482	AS02	TGCTGTTGACAGTGAGCGGAATGGAGACACGTTTCTGAATAGTGAAGCCACAGATGTA TTCAGAAACGTGTCTCCATTCTGCCTACTGCCTCGGA

### 2.2 METHODS

#### ***2.2.1 Routine cell culture methods***

Cells were cultured in sterile conditions in CO<sub>2</sub> cell culture incubator at 37°C with 5% CO<sub>2</sub> and H<sub>2</sub>O-saturated atmosphere. Almost all suspended cells were cultivated in RPMI medium while DMEM medium was always used for adherent cells. The cells were maintained in 6/12/24-well tissue culture plates or 50/250 ml culture flasks. Depending on cell growth, cells were split every 3-7 days. For adherent cells ATV or trypsin were used to detach cells from the plates.

Frozen cells were stored at -70°C /-140°C in freezing medium (mixture with 50% FCS, 40% RPMI and 10% DMSO). Cells in a proliferative stage of growth were harvested, diluted in 0.5ml of growth medium and stored on the ice for 30 min. Then 0.5 ml of freezing medium was added to each vial and cells were frozen at -70°C.

To thaw cells, cells were quickly put in pre-warmed 37°C water bath until whole solution thawed. The cell suspension was transferred by dropping into a 15 ml tube containing 5 ml medium and centrifuged at 1600 rpm (400 g) for 5 min. The medium was discarded and cell pellet was resuspended in culture medium and plated onto a fresh tissue culture plate.

To determine the percentage of viable cells within population, the cells were diluted with a trypan blue solution and counted in a Neubauer Chamber under the microscope. Only unstained, living cells were counted.

#### ***2.2.2 Gene clone and Transfer***

##### **2.2.2.1 Total RNA extraction and quantification**

RNA was isolated from cytoplasmic extracts of  $\sim 5 \times 10^6$  PBMCs or cell lines according to the protocol of Rneasy<sup>®</sup> MiniKit (QIAGEN#74104). All steps of the procedure were carried with precautions to minimize RNAase activity. The concentration of eluted RNA

## MATERIALS AND METHODS

was determined by measuring the absorbance at 260 nm (A<sub>260</sub>) in a spectrophotometer. The evaluation of RNA purity was made by the ratio between the absorbance values at 260 and 280 nm.

### 2.2.2.2 The first strand cDNA synthesis

The synthesis of the first cDNA suitable as template for PCR amplification was usually performed according to manufacturer's RT-PCR protocol supplied with the First Strand cDNA Synthesis Kit (Fermentas#K1612).

### 2.2.2.3 PCR amplification

Phusion high-fidelity DNA polymerase (Finnzymes) was used when PCR products were cloned or sequenced while *Taq* DNA polymerase (2×PCR Master Mix, Fermentas) was only used for the purpose of clones identification. Both Polymerases were different in either reaction system or cycle program which was listed as follows:

Phusion DNA Polymerase PCR system		<i>Taq</i> DNA Polymerase PCR reaction system	
DNA template	0.1~0.5μg	DNA template	0.1~0.5μg
Forward Primer(10μM)	5μl	Forward Primer(10μM)	2.5μl
Reverse Primer(10μM)	5μl	Reverse Primer(10μM)	2.5μl
dNTP(10mM)	1μl	2×PCR Master Mix	12.5μl
5×Phusion Buffer	10μl	Supplement water to 25 μl	
Phusion Polymerase	0.5μl		
Supplement water to 50 μl			
Cycle program as follows:		Cycle program as follows:	
1, 98 °C	30s (initial denaturation)	1, 94 °C	5min (initial denaturation)
2, 98 °C	10s (denaturation)	2, 94 °C	1min (denaturation)
3, *55 °C	*20s (annealing)	3, *55 °C	*30s (annealing)
4, 72 °C	*30s (extention)	4, 72 °C	*1min (extention)
Step 2~4 30cycle		Step 2~4 30cycle	
5, 72 °C	10min (final extention)	5, 72 °C	10min (final extention)
4 °C hold		4 °C hold	



## MATERIALS AND METHODS

(\*): The annealing temperature ( $T_a$ ) chosen for a PCR varied between 45°C and 62°C based on length and composition of the primer(s). The optimal annealing temperature was calculated as:  $T_a$  (°C) = [4(G+C) + 2(A+T)]-5°C. Annealing and extension time was also variable which depends directly on the estimated size of PCR products.

### 2.2.2.4 Gel electrophoresis

5µl PCR products were mixed with 1µl 6×loading buffer. The mixture and suitable DNA marker (1Kb/100bp) were loaded in agarose gel with ethidium bromide. Agarose concentrations varied between 1% and 2% depending on the estimated size of the DNA fragments. Electrophoresis was run and the gel was visualized in UV scanner.

### 2.2.2.5 Digestion and ligation of PCR products and plasmid

PCR products were purified with QIAquick PCR Purification Kit (Qiagen) according to its protocol. Purified products and empty vector (2µg) were digested by corresponding restriction endonucleases. DNA fragments were separated by electrophoresis on an agarose gel. The right size bands were cut out and extracted with Gel Extraction Kit (Genomed GMBH) following the protocol.

Mixture with 5µl insert, 1µl vector, 1µl T4 ligase, 1 µl 10×buffer (Fermentas) and 2µl H<sub>2</sub>O were incubated at 16°C /overnight or 22°C /2 hours.

### 2.2.2.6 Transformation

Mixture of 100 µl competent cells with 5 µl of the ligation reaction in a sterial EP tube was incubated on ice for at least 5 min. Subsequently the tubes were removed from the ice and immediately put them in the 42° bath for 90 seconds. The tubes were return to ice and incubate for ~ 5 mins. Then add 150 µl fresh LB/SOC medium and shak at 37 °C, 180 rpm for 1 hr. The entire cultures were plated onto a LB agar plate containing 100µg/ml ampicillin. After overnight 37 °C incubation, the resultant colonies were picked up and plasmid were prepared with miniprep.

## MATERIALS AND METHODS

### 2.2.2.7 Miniprep and Positive clones identification

Usually we picked six colonies from each agar plates, transferred them into 5 ml of LB medium containing 100µg/ml of ampicillin. After incubation overnight at 37 °C with 180rpm shaking, 3 ml of bacterial cultures were used to prepared plasmid DNAs with the Miniprep Kit following the protocol. 2 µl plasmid DNAs were digested with corresponding endonucleases. Digested products were resolved on 1% agarose gel to identify positive clones.

### 2.2.2.8 Sequencing

PCR mixture containing:		25 cycles with:
Sequencing primer	1µl	96°C 10s
DNA	3µl	50°C 5s
BD (big dye)	1µl	60°C 4min

### 2.2.2.9 Midiprep of plasmid DNA

Plasmid DNA was extracted with JETSTAR 2.0 MIDI columns (GENOMED) following the protocol. The concentration and purity of prepared plasmid DNA were measured with UV/Visible Spectrophotometer.

### 2.2.2.10 Viral particles package and infection

To express the gene of interest in mammalian cells, virus particles were produced by transfection of 293T cells with calcium phosphate precipitate technique. Then virus supernatants were used for infection of target cells. A transient three-plasmid expression system (retrovirus)\* was used (101):

#### Day 1:

293T cells were plated into 6 cm dishes with 5ml DMEM containing  $1.5 \times 10^6$  cells.

Mixture of plasmid DNA (5µg recombinant plasmid + 5µg pHIT60 + 5µg pVSV-G)\* were precipitated with 500µl of isopropanol, washed once with 70% of ethanol dried at RT and resuspended in 100 µl of sterile H<sub>2</sub>O. DNA samples were stored in the fridge (4°C).

#### Day 2:

## MATERIALS AND METHODS

Medium from 6 cm dishes was aspirated and 4 ml of fresh media without HEPES was gently added. The plates were kept in incubator for 1hr to equilibrate the pH value of medium. 338µl sterile water was added into the DNA tubes and subsequently 62µl CaCl<sub>2</sub> solution (2M). Afterwards, the mixture of DNA and CaCl<sub>2</sub> was given to 500µl 2×HBS solution and carefully mixed by “bubbling”. Immediately, added the mixture in all over the dish. Shake carefully a couple times to distribute the precipitate evenly. Incubate the dishes 6-8 hrs at 37°C, 5% CO<sub>2</sub>. Replace the media to DMEM with Hepes very gently. Incubate overnight at 37°C, 5%CO<sub>2</sub>.

### Day 3:

In order to activate the CMV Promoter media from the plates were replaced with 5 ml of fresh normal DMEM medium containing 10 mM Na-Butyrate. Plates were incubated at 37°C, 5% CO<sub>2</sub> for 6~8 hours and then Na-Butyrate containing media were aspirated, fresh medium were added for overnight incubation at 37°C, 5% CO<sub>2</sub>.

### Day 4:

The 293T cell supernatant containing viral particles was harvested with a syringe and pushed through a 0.45 µm filter into a 15 ml Falcon tube containing Polybrene (the final concentration was 4 µg/ml). Viral supernatants were plated onto 12 well plate and  $1 \times 10^5$  target cells per well were added. Plates were returned into incubator and incubated for 1h. To increase the efficiency of infection, plates were centrifuged in 2000 rpm for 3h at 37°C. After centrifugation plates were incubated at 37°C for 1h. Infection supernatants were then replaced by fresh growth medium.

(\*): For lentivirus(FUTG vector), plasmid mixture was prepared with 10µg recombinant plasmid+5µg pMDL-RPE+2.5µg pRSV-REV+5µg pVSV-G (107).

### 2.2.2.11 Identification and selection of transduced cells

2~3 days after infection, the expression level of transduced gene was tested by FACS analysis of fluorescence marker GFP/YFP/ASred or specific Ab staining. Transduced cells were selected by supplementing the culture medium with neomycin, zeocin or puromycin, which depends on the used plasmid. Alternatively, cells were selected by FACS sorter dependent on the fluorescence marker or specific surface staining.

## MATERIALS AND METHODS

### **2.2.3 Preparation of competent cells**

The competent cells or *E. coli* DH5 $\alpha$  were directly plated on an agar plate (no antibiotics). The colony was picked from plate to grow in 5ml LB medium (no antibiotic) overnight at 37°C shaking. Then the fresh overnight culture of bacterial were diluted (ratio=1:100) into 50ml LB medium. Bacterial were incubate at 37°C, 180rpm, about 2-3hours, detect the A600=0.3~0.4. The cells were pelleted at 3,000rpm/4°C /10min. After discarded the supernatant, the tubes were reversed on sterile paper for 1 min and subsequently put on ice. Cell pellet were resuspended at 5ml (1/10 volume of original volume) in 1 $\times$ TSS (icy cold) and mixed them gently on ice. Finally, the competent cells were aliquoted (200ul/tube) and saved in -70°C freezer.

### **2.2.4 Human V $\gamma$ 9V $\delta$ 2 TCR Transduced BW58 Reporter Cell lines**

#### **2.2.4.1 Human V $\gamma$ 9V $\delta$ 2 TCR Cloning**

In our work, three V $\gamma$ 9V $\delta$ 2 TCRs were analyzed.  $\gamma\delta$  TCR Mop was cloned by Dr. Kreiss in our group before (115),  $\gamma\delta$  TCR Buk was kindly provided by Dr. Bukowski (Harvard Medical School, Boston) (66),  $\gamma\delta$  TCR G115 was kindly provided by Prof. Champagne (Toulouse, France) (116). We used two different cloning and transduction strategies:

① Double vector transfection:

V $\gamma$ 9 chain was inserted into MCS of retrovirus vector EGN and V $\delta$ 2 chain was inserted into MCS of vector pIZ. Specific primers with restriction site were used as shown in Table 2-4. After virus particle package by 293T cells, both virus supernatant co-infected BW58 cells. Positive cells were selected with antibiotic resistance marker neomycin and zeocin.

② Single vector transfection with bicistronic construct containing 2A:

Bicistronic expression plasmid EGN was used as the cloning vector. The nucleotide segments  $\gamma$ Mop-T2A- $\delta$ Mop with restriction site was amplified with overlap PCR by specific primers containing T2A nucleotide sequence. Afterwards the segment was inserted into MCS of EGN to form construct of: 5'—LTR— $\gamma$ MopT2A $\delta$ Mop—IRES—EGFP-Neo—3'. Subsequent transfection was performed like before.

## MATERIALS AND METHODS

### **2.2.4.2 Stimulation of $\gamma\delta$ TCR transduced BW58**

In 96 well plate (U bottom),  $5 \times 10^4$  different types of transduced BW58 effector cells were cocultured with  $5 \times 10^4$  APC (cell lines, PBLs or DCs) in the presence of different concentration of phosphoantigens or aminobisphosphonate or only medium. Plate was incubated overnight at 37°C, 5% CO<sub>2</sub>.

For anti-CD3 antibody stimulation, 96 well plate was pre-coated with titrated mCD3 antibody in pH9.6 coating buffer for 2 hours. Afterwards coated wells were washed with medium.  $5 \times 10^4$  BW58 effector cells were added. Plate was incubated overnight at 37°C, 5% CO<sub>2</sub>.

### **2.2.4.3 Mouse IL-2 ELISA Assays**

In order to detect mouse IL-2 production after overnight incubation, the supernatants were harvested and mIL-2 concentration was measured using Mouse IL-2 ELISA Set (BD Biosciences, #555148) according to the manufacturer's instructions.

### **2.2.5 Retrovirus Mediated Over-expression of Enzymes**

Genes were PCR amplified from cDNAs of RAJI or PBMCs with indicated relevant primers listed in Table 2-4. Subsequently PCR products were inserted into the multiple cloning site of the retroviral vectors. Recombinant vectors were transduced with three-plasmid-package system mentioned above. Positive cells were selected with FACS sorter or antibiotics.

### **2.2.6 MiR-30 Based shRNA Mediated Knockdown of Enzymes**

#### **2.2.6.1 Target sequence selection and oligonucleotides synthesis**

Specific target sequence of RNA interference for gene of interest was acquired from the database of RNAi Codex (<http://codex.cshl.edu/scripts/newmain.pl>) by searching for the keyword or the accession number of the favorite gene. Based on the selected sequence, two shRNA oligonucleotides were synthesized from Sigma. The sense oligonucleotide tailed with *XhoI* cohesive end and mir-30 context sequence (tcgagAAGGTATAT) at the

## MATERIALS AND METHODS

5' end while the antisense sequence with *EcoRI* cohesive end at the 5' end (aatT) and the complementary mir-30 sequence (ATATACCTTc) at the 3' end.

For example, the shRNA sequence of FPPS designated V2HS\_228248 was acquired from RNAi Codex as follows:

TGCTGTTGACAGTGAGCGACCAGCAGTGTCTTGCAATATTAGTGAAGCCAC  
AGATGTAATATTGCAAGAACAACACTGCTGGCTGCCTACTGCCTCGGA

Depend on above sequence, two oligos were synthesized:

Sense: 5'-  
tcgagAAGGTATATTGCTGTTGACAGTGAGCGACCAGCAGTGTCTTGCAATAT  
TAGTGAAGCCACAGATGTAATATTGCAAGAACAACACTGCTGGCTGCCTACTGCC  
TCGGA

Anti-sense: 5'-  
aatTTCCGAGGCAGTAGGCAGCCAGCAGTGTCTTGCAATATTACATCTGTGGC  
TTCACATAATATTGCAAGAACAACACTGCTGGTCGCTCACTGTCAACAGCA  
ATATACCTTc

### 2.2.6.2 Annealing of shRNA oligos

Set up annealing mixture:

Sense Oligo (100 $\mu$ M)	3 $\mu$ l
Antisense Oligo(100 $\mu$ M)	3 $\mu$ l
3M NaCl	0.5 $\mu$ l
1M MgCl <sub>2</sub>	2 $\mu$ l
1M pH7.5 Tris	2 $\mu$ l
TE	9.5 $\mu$ l

Anneal mixture by PCR machine using the following parameters:

96°C	5 min	1 cycle
80°C	1 hour	1 cycle
4°C	hold	

## MATERIALS AND METHODS

### **2.2.6.3 Preparation of cloning vector (LMP/AsRed)**

To transfer shRNA oligos, we developed a new cloning vector designated LMP/AsRed dependent on the Expression ArrestLMP microRNA-adapted retroviral shRNAmir Vector (MSCV-LMP, Open Biosystems). For construction of LMP/AsRed, the red fragment of pred/MCS which contains the AsRed fluorescent protein (red) was cloned from MSCV-LMP with specific primers containing restriction sites of *NcoI* and *PacI* afterwards was ligated into the corresponding sites of MSCV-LMP, to replace the GFP coding region.

### **2.2.6.4 Generation of target gene knockdown in tumor cell lines**

shRNA oligos were inserted into *XhoI* and *EcoRI* restriction site of LMP/AsRed. Positive clones were selected and identified with routine gene clone technique.

To transfer the shRNA constructs into target cells, calcium phosphate precipitate technique and three-plasmid expression system were used. To select positive cells, infected cells were cultured 1-2 weeks with medium containing 3µg/ml puromycin.

Afterwards, flow-cytometry analysis was performed to test the fluorescent intensity of FL2 and FL1.

### **2.2.6.5 Western Blot Analysis of FPPS Knockdown in RAJI**

Whole-cell lysates were prepared by lysing  $1.5 \times 10^6$  cells in 50 µl lysis buffer (50mM pH7.4 Tris-HCL, 1% NP-40, 0.25% Na-deoxycholate, 150 mM NaCl, 1mM EDTA, 1 µg/ml aprotinin, leupeptin and pepstatin, 1mM Na<sub>3</sub>VO<sub>4</sub>, 1mM NaF) combined with a protease inhibitor cocktail, Complete Mini (Roche Applied Science). Proteins were separated by 12% SDS-PAGE, and transferred to a Roti-PVDF membrane (Carl Roth). FPPS expression levels were determined using rabbit anti-FPPS polyclonal antibody (ABGENT, Animal ID: RB4786). As loading control, β-tubulin expression was detected by anti-β-tubulin monoclonal antibody (Biosciences Pharmingen, Clone: 5H1).

## MATERIALS AND METHODS

### 2.2.7 *Lentivirus Mediated Inducible FPPS Knockdown in Tumor Cells*

#### 2.2.7.1 Cloning strategy

Cloning lentiviral vectors pH1tet-flex and FH1t(INSR)UTG were kindly provided by Dr. Herold (Melbourne, Australia) (107). Dependent on the specific target sequence of V2HS\_228248 (ACCAGCAGTGTCTTGCAATAT), we designed two oligos with the BbsI/XhoI overhangs as follows:

Sense: 5'-tccc ACCAGCAGTGTCTTGCAATAT ttcaagaga ATATTGCAAGAACACTGCTGGT ttttc-3'

Antisense: 5'-tcgagaaaa ACCAGCAGTGTCTTGCAATAT tctcttgaaATATTGCAAGAACACTGCTGGT-3'

The two oligos were annealed to generate shRNA22:

5'-tcccACCAGCAGTGTCTTGCAATATttcaagagaATATTGCAAGAACACTGCTGGCttttctcgag-3',

subsequently the annealing products were inserted into the *BbsI* and *XhoI* sites of pH1tet-flex.

Amplification of the H1tet-shRNA cassette from the construct was done using a proof-reading polymerase with the following two primers:

H1tetflex-fwd: 5'-cgtgtaTTAATTAAccatggaattcgaacgctgac-3'

H1tetflex-rev: 5'-cgatcTTAATTAAcaggctagcctaggacgcg-3'

PCR products were digested with *PacI* to purify the H1tet-shRNA cassette and FH1t(INSR)UTG plasmid DNA were digested with *PacI* to purify the vector (FUTG) without the original H1tet-shIR5 insert. H1tet-shRNA22 were cloned into the FUTG vector to generate the construct designated as FH1t(SR22)UTG.

#### 2.2.7.2 Virus Production and Transduction of Cells

Lentiviral particles were produced by transfecting 293T cells seeded in 6-cm dishes with 10 µg of vector DNA together with three helper plasmids (5 µg of pMDL-RRE, 2.5 µg of pRSV-REV, and 3 µg of pVSV-g) using CaPO<sub>4</sub> precipitation according to above protocol. Afterwards RAJI cells were infected and positive percentage were detected by flow-cytometry analysis of GFP expression.



## MATERIALS AND METHODS

### ***2.2.8 Isolation of peripheral blood mononuclear cells (PBMCs)***

PBMCs were isolated from fresh blood samples collected from healthy donors by the following procedure: 10 ml of Heparin treated blood were collected with the vacutainer system, and diluted with an equal volume of phosphate buffered saline (PBS). Blood samples were carefully layered over 10 ml of Ficoll-Hypaque in a 50 ml tube and centrifuged at 400g for 30 minutes at 20 °C. The upper layer containing the platelets was drawn off with a pipette, taking care not to disturb the PBMCs layer at the interface. The PBMCs layer was subsequently transferred to a clean centrifuge tube using a sterile Pasteur pipette, washed twice with 3 volumes of PBS and then centrifuged at 400g for 10 minutes at 20 °C. The PBMCs were finally resuspended in 1 ml of RPMI medium (10% FCS).

### ***2.2.9 Establishment of V $\gamma$ 9V $\delta$ 2 T cell lines by stimulation of fresh V $\gamma$ 9V $\delta$ 2 T cells from peripheral blood***

PBLs from blood of adult healthy donors were isolated by Ficoll-Hypaque density gradient centrifugation. The PBLs ( $1 \times 10^6$ /ml) in RPMI medium (10% FCS) were stimulated with Bromohydrin pyrophosphate (BrHPP) (1 $\mu$ M) or IPP (1 $\mu$ g/ml) in the presence of 100 U/ml rhIL-2 and incubated in a 24 well plate for 15 days at 37°C and 5% CO<sub>2</sub>. Half of the medium was replaced by fresh medium on days 3, 7, 10 and 14. After day 10, the cells were analyzed by flow cytometry. At this time point approximately 40-70% of all the CD3<sup>+</sup> cells comprised V $\gamma$ 9V $\delta$ 2 T cells.

### ***2.2.10 Activation analysis of primary or enriched V $\gamma$ 9V $\delta$ 2 T cells***

#### **2.2.10.1 IFN- $\gamma$ ELISpot Assay**

A commercially available IFN- $\gamma$  ELISPOT kit (Mabtech) containing a pre-coated 96-well plate was used. After 2 hours blocking of unspecific binding sites with cell culture medium containing 5% FCS (200 $\mu$ l/well), medium was removed. Subsequently,  $5 \times 10^3$  V $\gamma$ 9V $\delta$ 2 T cells (numbers were calculated from staining of short term lines with FITC-anti-human V $\delta$ 2 TCR antibody) were co-cultured with  $2.5 \times 10^4$  tumor cells and different

## MATERIALS AND METHODS

stimulator. The final reaction volume was 150  $\mu$ l per well. Plates were incubated for 16~18 hours in 37°C, 5% CO<sub>2</sub>.

After incubation, the cells were removed and the wells were washed 5 times with PBS. Subsequently the one-step detection reagent (alkaline phosphatase-conjugated detection anti-IFN $\gamma$  mAb 7-B6-1) was added in a dilution 1:200 in filtered PBS-FSC (0.5% fetal calf serum), and incubated for 2 h at RT. After incubation the wells were washed 5 times with PBS, and 100  $\mu$ l of filter ready-to-use substrate solution (BCIP/NBT-plus) was added to the wells, and developed for 10-15 min until spots emerge. Color development was stopped by washing extensively in tap water. After the washes, the plate was dried and the spots counted in an ELISpot Reader.

### **2.2.10.2 FACS staining of surface markers CD69 and CD107a/LAMP-1**

Cytometric analysis was performed on a FACSCalibur instrument using Cell-Quest or FlowJo software. For evaluation of CD69 expression,  $1 \times 10^5$  effector cells (fresh PBL) were cocultured with  $1 \times 10^5$  target cells in 96 wells tissue culture plates. After 16~18 hours of incubation, cells were harvested and stained for 30 min with FITC-anti-human V $\delta$ 2 TCR antibody plus PE-conjugated mouse anti-Human CD69 (Beckman Coulter, Clone: TP1.55.3).

For evaluation of the CD107a expression, effector cells ( $1 \times 10^5$  fresh PBL or  $3 \times 10^4$  primary  $\gamma\delta$  T cell line) were cocultured with  $1 \times 10^5$  target cells plus 10  $\mu$ l conjugated mouse anti-human CD107a/LAMP-1 (BD Biosciences, Pharmingen, Clone: H4A3) in 96 wells tissue culture plates. After 16~18 hours or 4 hours incubation, cells were harvested and stained for 30 min with FITC-anti-human  $\gamma\delta$  TCR antibody (BD Pharmingen, Clone: B1) or FITC-anti-human V $\delta$ 2 TCR antibody.

### **2.2.10.3 IFN- $\gamma$ Secretion Assay by Flow-cytometry**

$1 \times 10^5$  effector cells were cocultured with the same number of target cells in 96 wells tissue culture plates. After 16~18 hours incubation, cells were harvested and washed once with PBS. Cells were stained with a FITC conjugated monoclonal antibody against

## MATERIALS AND METHODS

human V $\delta$ 2 TCR. To fix anti-V $\delta$ 2 staining, solution were prepared with mixture of 1 part Fixation/Permeabilization Concentrate and 3 parts Fixation/Permeabilization Diluent (ebioscience, #005123). After the last wash, 100 $\mu$ l of prepared solution were added. Afterwards cells were incubated in the dark at room temperature for 20 minutes. Cells were washed twice with 1ml of 1 $\times$ Permeabilization Buffer (ebioscience, #008333). Subsequently were resuspended in 100 $\mu$ l of 1 $\times$ Permeabilization Buffer and stained with PE-labeled anti-IFN- $\gamma$  mAb. After incubation in the dark at room temperature for 20 minutes, cells were washed twice with 1ml of Permeabilization. The cell pellet was resuspended in 0.5ml of PBS with 0.1% BSA. Samples were analyzed on a flow-cytometer.

## 3 RESULTS

### 3.1 Generation of V $\gamma$ 9V $\delta$ 2 TCR Transduced BW58 Reporter Cell Lines

#### 3.1.1 Cell surface expression of $\gamma\delta$ TCR and mouse CD3 in TCR<sup>-</sup> hybridoma BW58 cells

Classically, in vitro expanded  $\gamma\delta$  line or V $\gamma$ 9V $\delta$ 2 TCR transduced TCR<sup>-</sup> Jurkat cells (29, 66) were used as tools for analysis of the V $\gamma$ 9V $\delta$ 2 T cells reactivity. However, both cell types have the disadvantage that specific responses are interfered either by other innate immune receptors or by self-presentation of the antigens. In our group, Matthias Kreiss (115, 117) had cloned and transduced a V $\gamma$ 9V $\delta$ 2 TCR (designated as  $\gamma\delta$ Mop) into the TCR<sup>-</sup> mouse T lymphoma hybridoma 58C (108, 118) (designated as BW58 in this dissertation). By specific MoAb staining, he demonstrated cell surface expression of  $\gamma\delta$  TCR and mouse CD3 in transduced BW58 cells. Our present study used two different strategies to transfer genes. As shown in Figure 3-1A, TCR- $\gamma$  and TCR- $\delta$  were respectively inserted into the multiple cloning sites of retroviral vectors pEGN and pIZ. Thereafter two recombinant constructs were co-transduced into BW58 cells. On the other hand, we attempted to transfer  $\gamma$  gene and  $\delta$  gene with a single retroviral vector by incorporated 2A-like sequence derived from insect virus *Thosea asigna* (T2A). As shown in Figure 3-1B, the nucleotide fragment containing V $\gamma$ 9-T2A-V $\delta$ 2 sequences in the same open reading frame was inserted into pEGN which contains downstream of the inserted gene an IRES and a EGFP- neomycin resistance fusion protein, which were used as selection markers (Figure 3-1A). Stable transductants were selected by neomycin. The cell surface expression of human  $\gamma\delta$  TCR and mouse CD3 complex was verified by FACS staining with anti-mouse CD3 $\epsilon$  and anti-human V $\delta$ 2 monoclonal antibodies in

## RESULTS

comparison to the negative control with isotype MoAb staining. A representative staining by CD3 and V $\delta$ 2 specific MoAb by CD3 and V $\delta$ 2 specific MoAb before and after transduction of  $\gamma\delta$  TCR is shown in Figure 3-1C-H.

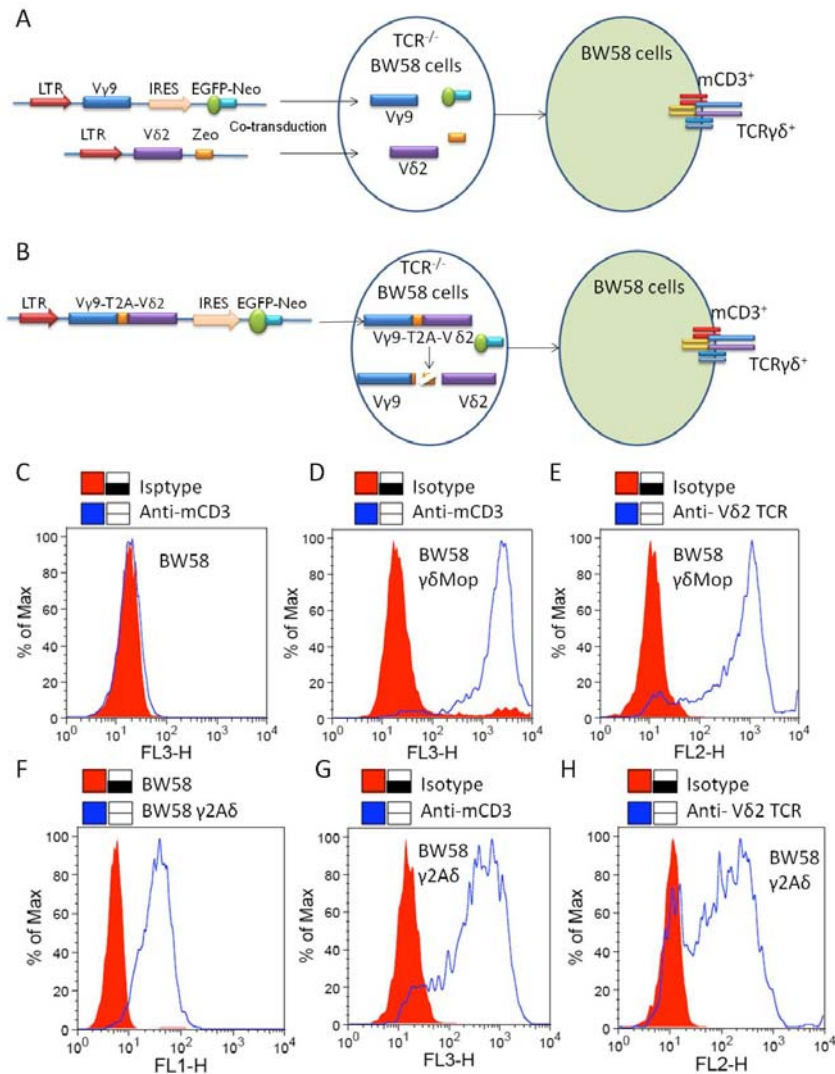


**Figure 3-1 Cells surface expression of mCD3 $\epsilon$  and V $\delta$ 2 TCR after BW58 transduction of V $\gamma$ 9V $\delta$ 2 TCR.** A) Operating principle of gene-transduction with two retroviral vectors. B) Operating principle of gene-transduction with bicistronic-retroviral vector encoding 2A-linked  $\gamma$  gene and  $\delta$  gene and a EGFP-neomycin construct. C), D) and G) show that indicated BW58 cells were stained with anti-mouse CD3 $\epsilon$  bio MoAb followed by Streptavidin-PE.Cy5. Histograms displayed specific staining (blue lines) versus isotype control (red solid). E) and H) show that transduced BW58 cells were stained with PE conjugated anti-V $\delta$ 2 TCR MoAb. Histograms displayed specific staining (blue lines) versus isotype control (red solid). F) FACS analysis of EGFP fluorescence intensity of  $\gamma$ 2A $\delta$ /pEGN transduced BW58 cells (blue line) versus wild type BW58 cells (red solid).

## RESULTS

### 3.1.2 Activation of BW58 $\gamma\delta$ T cells by phosphoantigens or aminobisphosphonates depends on CD28 mediated signal.

After generation of  $\gamma\delta$  TCR transduced cells, Matthias Kreiss further analyzed their functional characteristics (117). Initially, transductants, although were readily activated by CD3 specific monoclonal antibodies, failed to react to V $\gamma$ 9V $\delta$ 2 specific activators, but responded after co-transduction with a chimeric rat/mouse CD28 construct (109). Our present work explored whether human CD28 molecular can provide similar co-stimulatory signal. To this end, we cloned and transduced full length of human CD28 DNA into BW58 $\gamma\delta$  cells. We tested the IL-2 production after overnight stimulation. As shown in Figure 3-2, although  $\gamma\delta$  TCR expressing BW58, BW58r/mCD28 and BW58huCD28 cells produced similar amounts of IL-2 when stimulated with anti-mouse CD3 $\epsilon$  antibody, only BW58r/mCD28 cells responded to BrHPP and zoledronate(Zol) in the presence of RAJI cells.

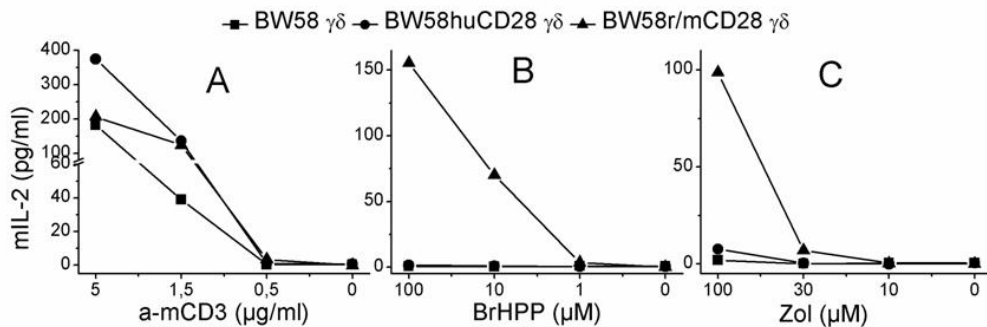


**Figure 3-2 ELISA analysis of IL-2 production by BW58 cells expressing  $\gamma\delta$  TCR.** A)  $5 \times 10^4$  indicated BW58 cells were added after 2 hours pre-coated with anti-mCD3 $\epsilon$  MoAb; B) and C)  $5 \times 10^4$  indicated BW58 cells co-incubated with  $5 \times 10^4$  RAJI cells in the presence of BrHPP or zoledronate. After overnight incubation, the supernatants were harvested and IL-2 concentrations were analyzed by IL-2 ELISA kit.

It is likely that r/mCD28 interacted with human CD80 on the surface of RAJI to generate co-stimulatory signal for BW58 cells activation, while human CD28 was unable to transfer the signal due to the difference with mouse CD28 in cytoplasmic domain despite certainly reacting with human CD80. To test this possibility, we generated Jurkat cell lines expressing rat CD80 or human CD80, respectively. FACS analysis indicated successful surface expression of rCD80 and huCD80 (Figure 3-3A). ELISA analysis showed that Jurkat/rCD80 and Jurkat/huCD80 stimulated BW58r/mCD28  $\gamma\delta$  T cells

## RESULTS

produced increasing amounts of IL-2 in response to titrated BrHPP or zoledronate (Figure 3-3B). The results verified the interaction between r/mCD28 and huCD80 as well as the indispensability of CD28-CD80 signal in activation of BW58 cells expressing  $\gamma\delta$  TCR.

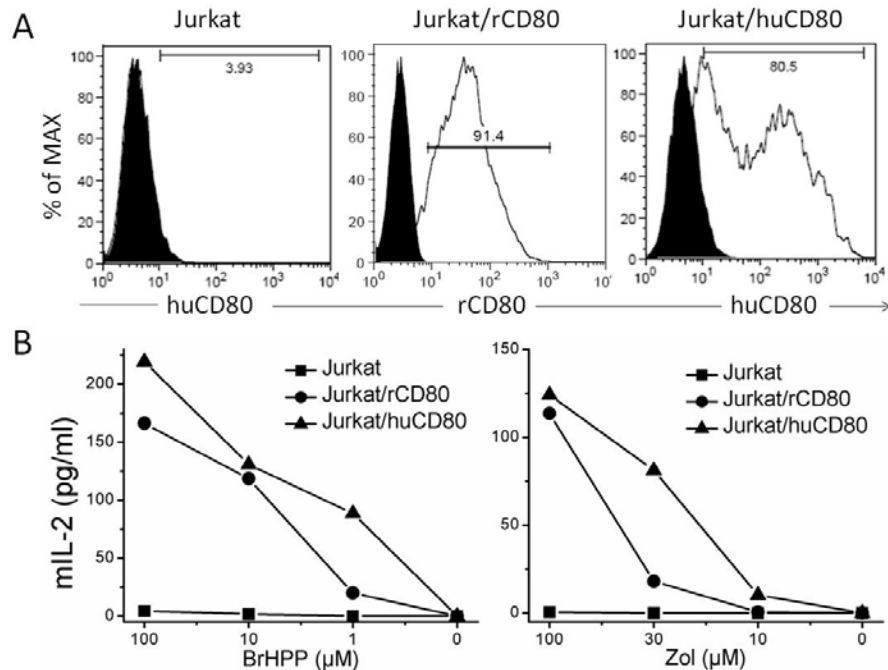


**Figure 3-3** BW58r/mCD28 cells expressing  $\gamma\delta$  TCR response to Jurkat, Jurkat/rCD80 or Jurkat/huCD80. **A)** Flow cytometry analysis of CD80 expression. Histograms present specific staining with huCD80 or rCD80 MoAbs (open curves) compared to the relevant isotype control (filled curves). **B)** Analysis of the CD80 (CD28 ligand) dependence of phosphoantigen mediated activation of  $\gamma\delta$  TCR expressing BW58r/mCD28 cells. Overnight incubation of  $5 \times 10^4$  BW58r/mCD28  $\gamma\delta$  T cells with  $5 \times 10^4$  indicated CD80 trasduced or untransduced Jurkat cells in the presence of BrHPP (left) or zoledronate (right).

### 3.1.3 The activation of BW58r/mCD28 $\gamma\delta$ cells requires presentation of the TCR-ligands by human cells

As shown above, BW58r/mCD28  $\gamma\delta$  cells were activated by BrHPP or zoledronate in the presence of human lymphomas RAJI and Jurkat expressing rat or human CD80 (Figure 3-2 and Figure 3-3). Established knowledge for  $V\gamma9V\delta2$  T cells activation by phosphoantigens is the requirement of species-specific interactions. To detect the application of this principle in our  $V\gamma9V\delta2$  TCR transduced system, we tested the capacity of other tumor lines originating from either human or non-human tissues to

## RESULTS

activate BW58r/mCD28  $\gamma\delta$  T cells in the presence of BrHPP. As shown in Figure 3-4, in presence of BrHPP, human cell lines 721.221 (natural expression of huCD80), K562/rCD80 or 293T/rCD80 were able to induce IL-2 production by BW58r/mCD28  $\gamma\delta$  T cells while cell lines from other species such as LBB (mouse B lymphoma, naturally expressing mouse CD80) or L929/rCD80 (mouse fibrosarcoma cells) or O30-D/rCD80 (canine cell line) did not.

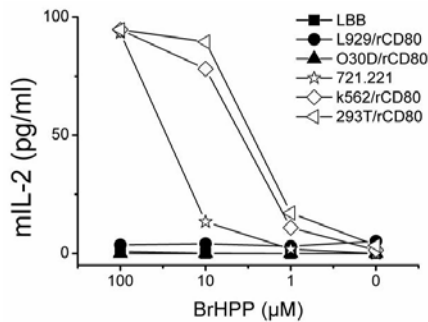


**Figure 3-4** BW58r/mCD28  $\gamma\delta$  T cells respond only to BrHPP presented by cell lines of human origin.  $5 \times 10^4$  BW58r/mCD28  $\gamma\delta$  T cells with  $5 \times 10^4$  indicated cell lines (see also Figure 3-2) were cocultured with BrHPP and tested for IL-2 production.

### 3.1.4 Mevastatin blocks the response of BW58r/mCD28 $\gamma\delta$ T cells to aminobisphosphonates but not to phosphoantigens

One explanation for  $V\gamma 9V\delta 2$  T cell activation by aminobisphosphonates is their capacity to block FPPS in the target cell, which then leads to the accumulation and subsequent “presentation” of IPP to the  $V\gamma 9V\delta 2$  T cells. To test this hypothesis, we performed the stimulation experiments in the presence of mevastatin, which lowers IPP levels as a

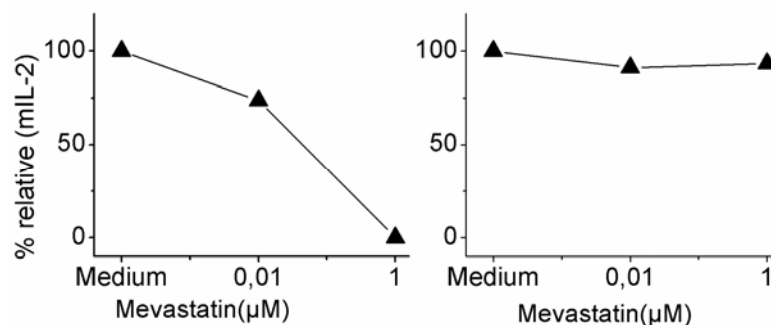


**Figure 3-5** Mevastatin reduced IL-2 production of BW58r/mCD28  $\gamma\delta$ Mop in the response to aminobisphosphonates, but not to phosphoantigens.  $5 \times 10^4$  BW58r/mCD28  $\gamma\delta$ Mop cells and  $5 \times 10^4$  RAJI cells were co-incubated with indicated concentration of Mevastatin as well as 100 $\mu$ M zoledronate (left) or 10 $\mu$ M BrHPP (right). Values in y-axis present the percentages of the control without Mevastatin (64,1 pg/ml for zoledronate and 164,9 pg/ml for BrHPP).



## RESULTS

consequence of blocking HMG-CoA reductase activity. The amounts of IL-2 secretion induced by zoledronate treatment were significantly inhibited by mevastatin (left of Figure 3-5). Conversely, in the BrHPP stimulation (right of Figure 3-5), no inhibiting effects were observed which also excluded the possibility that decline of IL-2 secretion was caused by cytotoxicity of mevastatin.

### ***3.1.5 Mutations in V $\delta$ 2 region abrogate the reactivity of the TCR transductants***

To verify whether the IL-2 production by BW58r/mCD28  $\gamma\delta$  cells was dependent on specific interaction of V $\gamma$ 9V $\delta$ 2TCR with BrHPP or endogenous IPP, we established two mutants based on  $\delta$ Mop DNA at positions proposed to be crucial for the binding of V $\gamma$ 9V $\delta$ 2TCR with phospho-ligands (67, 119). One mutation replaced the Arginine (R) residue at position 51 with Alanine (A) which is located in CDR2 region of TCR- $\delta$  chain ( $\delta$ R51A); another one changed the CDR3 in length and hydrophobicity via removing hydrophobic amino acids ( $\delta$ 96). By gene transfer, we generated BW58r/mCD28  $\gamma\delta$ R51A and BW58r/mCD28  $\gamma\delta$ 96 cell lines which are designated as D51 and D96, respectively. FACS analysis revealed that both mutants did not affect the surface expression of  $\gamma\delta$  TCR and mCD3 on the surface of BW58 cells (data not shown). Further analysis of IL-2 production proved that D51 and D96 completely abrogated the responsiveness to either BrHPP or zoledronate, while no negative effects were found on IL-2 production in response to the stimulations with anti-mCD3 or anti- $\gamma\delta$  TCR MoAbs (Figure 3-6).

## RESULTS

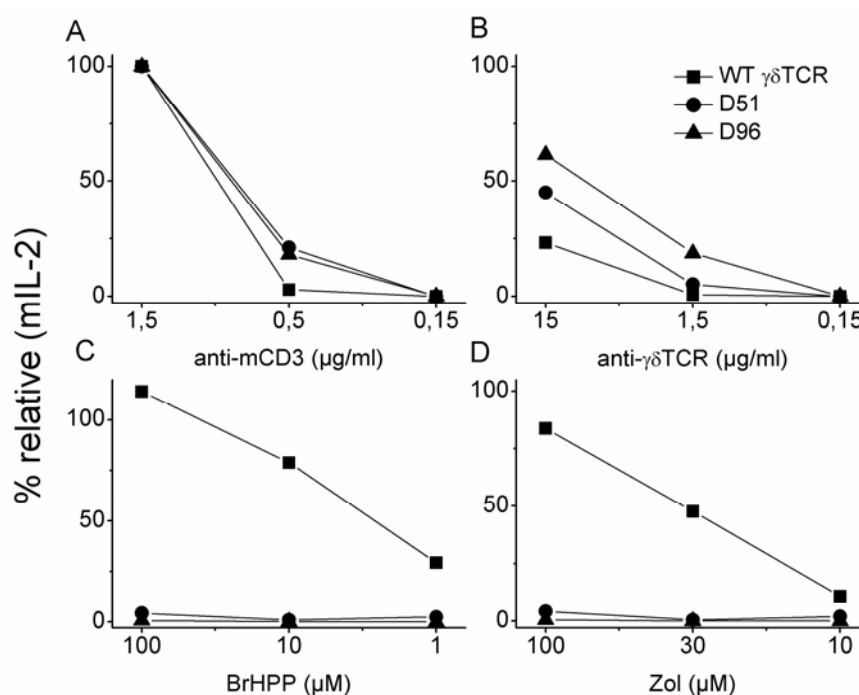


**Figure 3-6 Comparison of the IL-2 production by WT  $\gamma\delta$ Mop, D51 and D96 in response to different stimuli.**  $5 \times 10^4$  of the indicated lines were cultured overnight in presence of following stimuli: A) Culture plates coated for 2 hours with anti-mCD3 MoAb. B) Culture plates coated for 2 hours anti- $\gamma\delta$  TCR MoAb. C) and D)  $5 \times 10^4$  effectors plus  $5 \times 10^4$  RAJI in the presence of BrHPP or zoledronate. Values in y-axis were calculated as percentages of control with 1, 5 $\mu\text{g/ml}$  anti-mCD3 MoAb stimulation. The amounts of IL-2 produced by stimulation of 1, 5 $\mu\text{g/ml}$  anti-mCD3 MoAb were 124,6 pg/ml (wild type), 21,3 pg/ml (D51) and 1718,5 pg/ml (D96), respectively.

### **3.1.6 Comparison of the response of short term $\gamma\delta$ T cell lines and $\gamma\delta$ TCR transduced BW58 cells to different V $\gamma$ 9V $\delta$ 2 activators**

To learn to what extent factors other than V $\gamma$ 9V $\delta$ 2 TCR recognition of phosphoantigens affect the activation of V $\gamma$ 9V $\delta$ 2 T lymphocytes, the response of  $\gamma\delta$  TCR transduced cells and human primary  $\gamma\delta$  T cells to different types of putative V $\gamma$ 9V $\delta$ 2 TCR ligands was compared. To this end IFN- $\gamma$  production by a BrHPP plus IL-2 expanded  $\gamma\delta$  line was tested with an ELISpot assay. At the time of the experiments, cell lines contained 40–70% V $\gamma$ 9V $\delta$ 2 T cells (data not shown).

A comparison of the response of primary and transduced  $\gamma\delta$  T cells is shown in Figure 3-7. “% IFN- $\gamma$ ” presents the efficiency of activation of short term enriched primary  $\gamma\delta$  T

## RESULTS

cells while “% mIL-2” presents the efficiency of activation of  $\gamma\delta$  TCR expressing BW58r/mCD28 cells. The former showed nearly one thousand times higher sensitivity to the exogenous phospholigands (HMBPP and BrHPP) than latter (A). However, for the response to aminobisphosphonates which by blocking FPPS lead to the accumulation and subsequent “presentation” of endogenous IPP to  $\gamma\delta$  TCR, the sensitivity differs only by a factor of 10 (B). The transduced cells showed no response to exogenous IPP. Since concentrations of IPP higher than 1mM turned out to be toxic, the capacity of transductants to respond a higher concentration could not be tested.

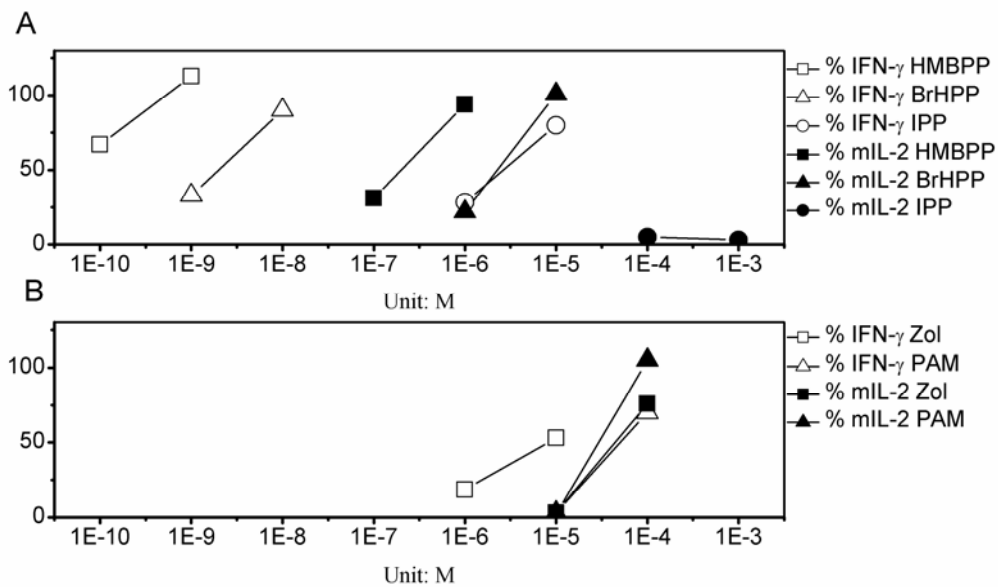


**Figure 3-7 A comparison of the response of BW58r/mCD28  $\gamma\delta$  T cells and enriched short-term  $\gamma\delta$  lines.** ELISPOT IFN- $\gamma$  assays were performed by overnight incubation of  $3 \times 10^3$   $\gamma\delta$  T cells of short term  $\gamma\delta$  lines with  $2.5 \times 10^4$  RAJI cells in the presence of indicated stimuli. ELISA assays of IL-2 were carried out with the supernatants of overnight culture of  $5 \times 10^4$  BW58r/mCD28  $\gamma\delta$  T cells and  $5 \times 10^4$  RAJI cells in the presence of indicated stimulators. Symbols in A represents the relative percent of IFN- $\gamma$  secretion (open) and IL-2 production (closed) in the response to soluble phosphoantigens: HMBPP (square), BrHPP (triangle), IPP (circle); Symbols in B represents the relative percent of IFN- $\gamma$  secretion (open) and IL-2 production (closed) in the response to aminobisphosphonates: Zol (square), PAM (triangle). X-axis shows the corresponding concentration for different stimulators. PAM: pamidronate; Zol: zoledronate.

## RESULTS

### 3.1.7 Daudi cells alone do not induce IL-2 production by BW58r/mCD28 $\gamma\delta$ cells

It is established knowledge that Daudi cells but not RAJI cells are good activators of V $\gamma$ 9V $\delta$ 2 T cells. Therefore we tested the IL-2 production by  $\gamma\delta$  TCR Mop transduced BW58r/mCD28 cells in response to Daudi cells alone. Unexpectedly, the IL-2 production in response to Daudi cells was not higher than that in response to RAJI cells (Figure 3-8 C). In order to exclude the possibility that only  $\gamma\delta$  TCR Mop were incapable to respond to Daudi alone, we established cell lines transduced with two other V $\gamma$ 9V $\delta$ 2 TCR DNAs, BW58r/mCD28  $\gamma\delta$ Buk and BW58r/mCD28  $\gamma\delta$ G115. Amino acid sequence difference between  $\gamma\delta$  TCR Mop, Buk and G115 was aligned with software DNAMAN. Alignment results are shown as Figure 3-9. FACS assays showed also similar surface co-expression of  $\gamma\delta$  TCR and mCD3 as with  $\gamma\delta$ Mop transduced BW58 cells (data not shown). Next, we tested their response to RAJI cells treated by BrHPP or zoledronate. ELISA results showed a very similar IL-2 production (Figure 3-8A, B). Similarly with  $\gamma\delta$  TCR Mop, Buk and G115 indicated very poor responsiveness to Daudi cells without BrHPP or zoledronate. To be noted,  $\gamma\delta$ Buk produced higher amounts of IL-2 than  $\gamma\delta$ Mop and  $\gamma\delta$ G115 when stimulated by either Daudi or RAJI/AS (Figure 3-8C).

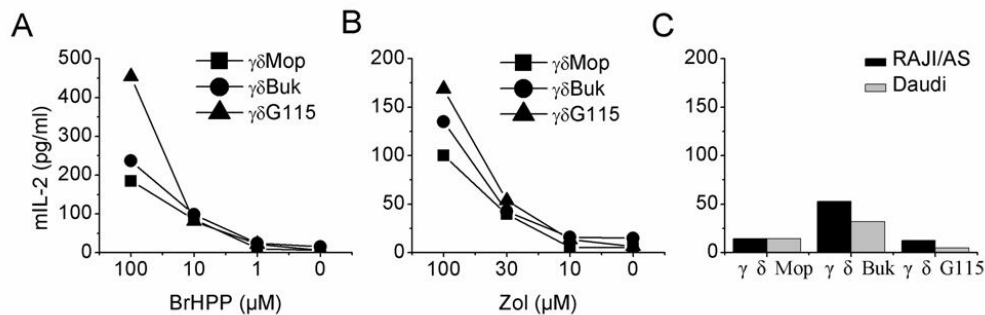


**Figure 3-8 BW58r/mCD28 cells expressing  $\gamma\delta$  TCR Mop, Buk and G115 indicated no response to Daudi cells alone.**  $5 \times 10^4$  of indicated TCR expressing BW58r/mCD28 and  $5 \times 10^4$  RAJI were cultured in the presence of BrHPP (A) or zoledronate (B) or with  $5 \times 10^4$  Daudi cells (C). Culture supernatants were analyzed by mIL-2 ELISA kit.

## RESULTS

	<-L----- --L-><-V-----		<-L----- --L-><-V-----		
Gamma_Buk.pro	MISIIHASTLAVIGALCVYGPAGHLECFQISSTRTISPTA	40	Delta_Buk.pro	MQRIESLIHISIFWAGVMSAIEIVFEHQTVFVSIQVPEPTL	40
Gamma_G115.pro	MISIIHASTLAVIGALCVYGPAGHLECFQISSTRTISPTA	39	Delta_G115.pro	MQRIESLIHISIFWAGVMSAIEIVFEHQTVFVSIQVPEPTL	40
Gamma_Mop.pro	MISIIHASTLAVIGALCVYGPAGHLECFQISSTRTISPTA	40	Delta_Mop.pro	. . MISLIHISIFWAGVMSAIEIVFEHQTVFVSIQVPEPTL	38
-----					
Gamma_Buk.pro	RLECVVSGITISPTSVYWYREFEFGVEVIQFIVSISYDGTVR	80	Delta_Buk.pro	RCSMPGEAIGNYYINWYRKTQGNMTFIYFEKLIYGFQFK	80
Gamma_G115.pro	RLECVVSGITISPTSVYWYREFEFGVEVIQFIVSISYDGTVR	79	Delta_G115.pro	RCSMPGEAIGNYYINWYRKTQGNMTFIYFEKLIYGFQFK	80
Gamma_Mop.pro	RLECVVSGITISPTSVYWYREFEFGVEVIQFIVSISYDGTVR	80	Delta_Mop.pro	RCSMPGEAIGNYYINWYRKTQGNMTFIYFEKLIYGFQFK	78
-----					
-----V->					
Gamma_Buk.pro	KESGIFSGKFEVIRIFETSTSTLTIHNVFQDIATYYCAL	120	Delta_Buk.pro	DNEQCDILIAKNIHAVIKILAFSEERDEGSYYCACDIIIVS..	118
Gamma_G115.pro	KESGIFSGKFEVIRIFETSTSTLTIHNVFQDIATYYCAL	119	Delta_G115.pro	DNEQCDILIAKNIHAVIKILAFSEERDEGSYYCACDIIIVS..	120
Gamma_Mop.pro	KESGIFSGKFEVIRIFETSTSTLTIHNVFQDIATYYCAL	120	Delta_Mop.pro	DNEQCDILIAKNIHAVIKILAFSEERDEGSYYCACDFFVWIGD	118
-----					
-----D51↑					
-----V-><-D-----					
-----					
-----D96					
-----D-><-J-----J-><-C-----					
Gamma_Buk.pro	...FEIGKIKIIGWVPGTKLIITDRQILDVSEKFTIIFL	156	Delta_Buk.pro	...TIKLIIFGKGRVTVVEFRSCEHTKFSVFMKNGTIVAC	155
Gamma_G115.pro	WEAQCCEIGKIKI.VEGPCTKLIITDRQILDVSEKFTIIFL	158	Delta_G115.pro	E.YTIKLIIFGKGRVTVVEFRSCEHTKFSVFMKNGTIVAC	159
Gamma_Mop.pro	...FEIGKIKI.VEGPCTKLIITDRQILDVSEKFTIIFL	155	Delta_Mop.pro	<u>IC</u> YTIKLIIFGKGRVTVVEFRSCEHTKFSVFMKNGTIVAC	158
-----					
Gamma_Buk.pro	FSIAETRLQKAGTYICLLEKFFEFVIRIHWQEKRSNTIILG	196	Delta_Buk.pro	IVKEFYFKDIRINIVSSRKITEFDFFAIVISFSGKYNAVKL	195
Gamma_G115.pro	FSIAETRLQKAGTYICLLEKFFEFVIRIHWQEKRSNTIILG	198	Delta_G115.pro	IVKEFYFKDIRINIVSSRKITEFDFFAIVISFSGKYNAVKL	199
Gamma_Mop.pro	FSIAETRLQKAGTYICLLEKFFEFVIRIHWQEKRSNTIILG	195	Delta_Mop.pro	IVKEFYFKDIRINIVSSRKITEFDFFAIVISFSGKYNAVKL	198
-----					
Gamma_Buk.pro	SQEGNTMKTNDTYMKFSWITVVEKSLKKEHRCIVRHENNK	236	Delta_Buk.pro	GRYEISNSVICSVQCHENRTVHSTLDFEVKTIESTLHVKEPET	235
Gamma_G115.pro	SQEGNTMKTNDTYMKFSWITVVEKSLKKEHRCIVRHENNK	238	Delta_G115.pro	GRYEISNSVICSVQCHENRTVHSTLDFEVKTIESTLHVKEPET	239
Gamma_Mop.pro	SQEGNTMKTNDTYMKFSWITVVEKSLKKEHRCIVRHENNK	235	Delta_Mop.pro	GRYEISNSVICSVQCHENRTVHSTLDFEVKTIESTLHVKEPET	238
-----					
Gamma_Buk.pro	NGVDCETIIFFPIFTIVITMDFEENC SRLANETILLQIINT	276	Delta_Buk.pro	ENTKCFESKSKHKERAIVHTEKVNMMSITVIGLRMIFAFIV	275
Gamma_G115.pro	NGVDCETIIFFPIFTIVITMDFEENC SRLANETILLQIINT	278	Delta_G115.pro	ENTKCFESKSKHKERAIVHTEKVNMMSITVIGLRMIFAFIV	279
Gamma_Mop.pro	NGVDCETIIFFPIFTIVITMDFEENC SRLANETILLQIINT	275	Delta_Mop.pro	ENTKCFESKSKHKERAIVHTEKVNMMSITVIGLRMIFAFIV	278
-----					
-----C->					
Gamma_Buk.pro	SAYYMYLLLLLKVYVYFAIITCCILRRTAFCCNGEK	312	Delta_Buk.pro	AVNFILITAKLFF	287
Gamma_G115.pro	SAYYMYLLLLLKVYVYFAIITCCILRRTAFCCNGEK	314	Delta_G115.pro	AVNFILITAKLFF	291
Gamma_Mop.pro	SAYYMYLLLLLKVYVYFAIITCCILRRTAFCCNGEK	311	Delta_Mop.pro	AVNFISTAKLFF	290

**Figure 3-9** Amino acid sequence alignment of TCR- $\gamma$  chain (left) and TCR- $\delta$  chain (right) from different  $\gamma\delta$ TCR genes Buk, G115 and Mop. The variable residues are indicated by shadows or dots. The different TCR- $\gamma$  or TCR- $\delta$  domains are also indicated. L: leader region; V: variable gene segments encoded region; D: diversity gene segments encoded region; J: joining gene segments encoded region; C: constant gene segments encoded region. The mutant sites of D51 and D96 on  $\delta$ Mop chain are marked with red arrow or red line.

## RESULTS

### 3.1.8 Primary $\gamma\delta$ T cells and $\gamma\delta$ TCR transductants differ in their response to Ecto-ATPase coated beads

We investigated the responsiveness of  $\gamma\delta$  TCR transduced cells as well as primary  $\gamma\delta$  T cells to the postulated V $\gamma$ 9 $\delta$ 2 TCR ligand, extracellular ATP synthase (Ecto-ATPase) (80). Beads coated with F1-ATPase (F1) or F1Fo-ATPase (F1Fo) and control beads coated with unrelated peptide (Ctl) were kindly provided by Prof. Champagne (Toulouse, France). IFN- $\gamma$  ELISPOT analysis shows that F1-ATPase coated beads directly stimulated primary  $\gamma\delta$  T cells to secrete IFN- $\gamma$  with an efficacy which was about half of that found for with RAJI cells plus 100nM BrHPP. After addition of RAJI cells to the beads, the response was further increased. Beads coated with F1Fo-ATPase induced only a very weak response (8%), which again was increased by addition of RAJI cells (30%) (Figure 3-10A, B). In contrast to these results, beads did not induce IL-2 production of

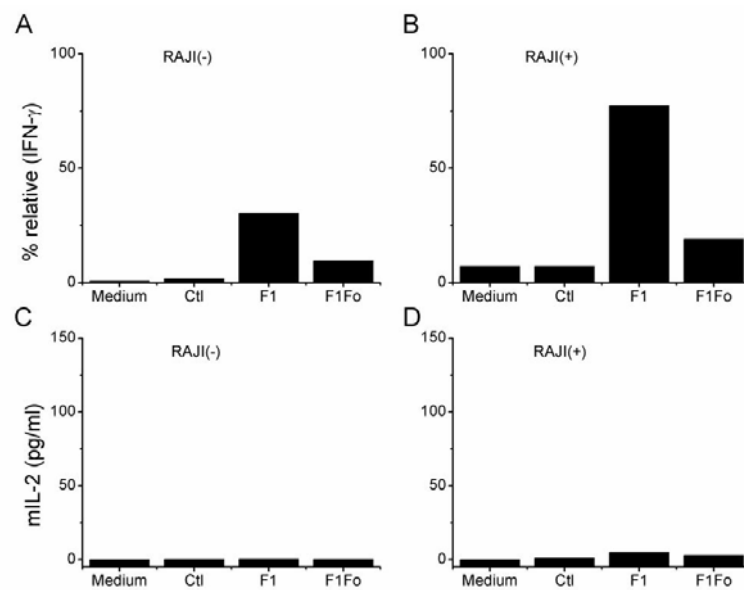


**Figure 3-10 activation analysis of primary  $\gamma\delta$  T cells and  $\gamma\delta$  TCR transduced cells by Ecto-ATPase coated beads.** A) and B) show results of IFN- $\gamma$  ELISPOT assays.  $3 \times 10^3$  enriched primary  $\gamma\delta$  T cells were incubated overnight with of the  $2, 5 \times 10^4$  indicated beads (A) or  $2, 5 \times 10^4$  RAJI cells (B). Values were calculated as percentages of stimulation obtained with RAJI plus 100nM BrHPP (168 spots). C) and D) show results of IL-2 ELISA assays.  $5 \times 10^4$  BW58r/mCD28  $\gamma\delta$ Mop cells were incubated overnight with  $1 \times 10^5$  beads (C),  $1 \times 10^5$  beads plus  $5 \times 10^4$  RAJI cells (D). Ctl: beads coated with unrelated peptide; F1: beads coated with F1-ATPase; F1Fo: beads coated with F1Fo-ATPase.

## RESULTS

BW58r/mCD28  $\gamma\delta$ Mop cells and addition of RAJI cells had hardly any effect (Figure 3-10 C and D).

### **3.2 Reduced FPPS Expression Unveils Recognition of Tumor Cells by V $\gamma$ 9V $\delta$ 2 T Cells**

#### ***3.2.1 Reduction of FPPS expression in RAJI cells by retrovirally expressed shRNAs***

We next investigated the effects of FPPS knockdown in tumor cells on the activation of V $\gamma$ 9V $\delta$ 2 T cells. To this end, RAJI cells stably expressing both FPPS-EYFP fusion protein (RAJI-FPPSYFP) and FPPS specific shRNA constructs were established. We tested the efficacy of different shRNAs to reduce FPPS expression by flow cytometry analysis, Figure 3-11A shows similar expression of shRNA constructs in the different cell lines generated as indicated by equally high AsRed fluorescence in FL3 (AsRed), and widely varying levels of FL1-fluorescence (EYFP) (Figure 3-11B). Cells transduced with FPPS-targeting vectors AS11 and AS22 showed a 5-10 fold reduction of FL1, compared to cells transduced with empty vector (AS) or a vector comprising an unrelated shRNA control vector (ASGR2). Additionally, we tested for specificity of the shRNA construct by generating cells expressing the prenyltransferase GGPPS as EYFP fusion protein. In contrast to the FPPS-EYFP the AS22 vector had no effect of the GGPPS-EYFP expression (data not shown). This is of especial interest since aminobisphosphonates bind and inhibit not only FPPS but also GGPPS (45). It also suggests that shRNA knockdown of the different enzymes of isoprenoid synthesis may provide feasible tools in further dissecting their role in cellular functions.

After interference with FPPS had been demonstrated by flow cytometry, AS22 and AS11 were used to target wild type RAJI cells. As shown by immunoblot, AS22 and AS11 significantly reduce FPPS expression compared to empty vector control AS (Figure 3-11C). Densitometric analysis revealed a relative reduction of FPPS protein by 90% for RAJI/AS22, by 62% for RAJI/AS11 cells, respectively.

## RESULTS

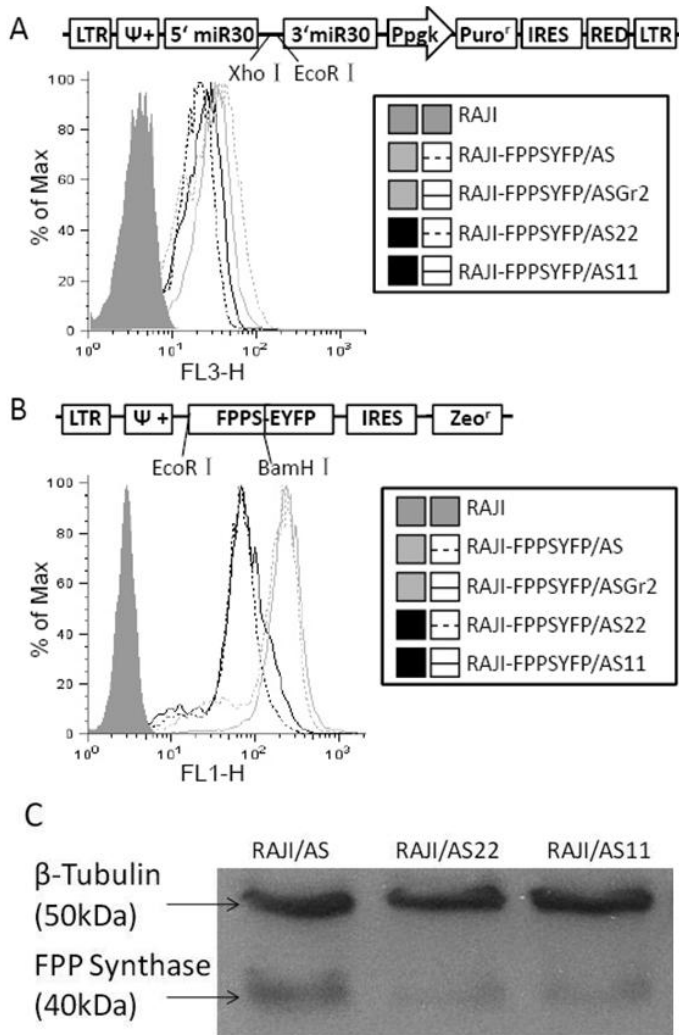


**Figure 3-11** The RAJI cell line expressing FPPS-EYFP fusion protein (RAJI-FPPSYFP) was transfected, with either empty vector control (AS) or control shRNA (ASGr2) or FPPS-specific shRNA (AS22 or AS11). After 2 weeks of puromycin selection, expression of shRNA constructs (A), and FPPS-YFP were tested by FACS analysis (B). Panel (C) shows an immunoblot analysis of FPPS expression levels in wild type RAJI cells stably expressing empty vector AS or FPPS-specific shRNA AS22 and AS11. Blots were probed with beta-tubulin to verify equal loading. Results are representative of three independent experiments.

### 3.2.2 FPPS knockdown in RAJI cells induces activation of primary Vγ9Vδ2 T cells

To investigate the capacity of FPPS knockdown cells to activate primary γδ T cells, total PBMC from healthy donors were stimulated in co-cultures with different target cells as described in Materials and Methods. Subsequently cells were stained for CD69, CD107a and tested in an IFN-γ secretion assay. The proportion of activated Vγ9Vδ2 T cells was tested by electronically gating on Vδ2 TCR positive cells, which varied between 1 and 3% of total PBMC (data not shown). The frequency was determined by expression of the early activation marker CD69, CD107a as marker for the active cytolytic machinery and



## RESULTS

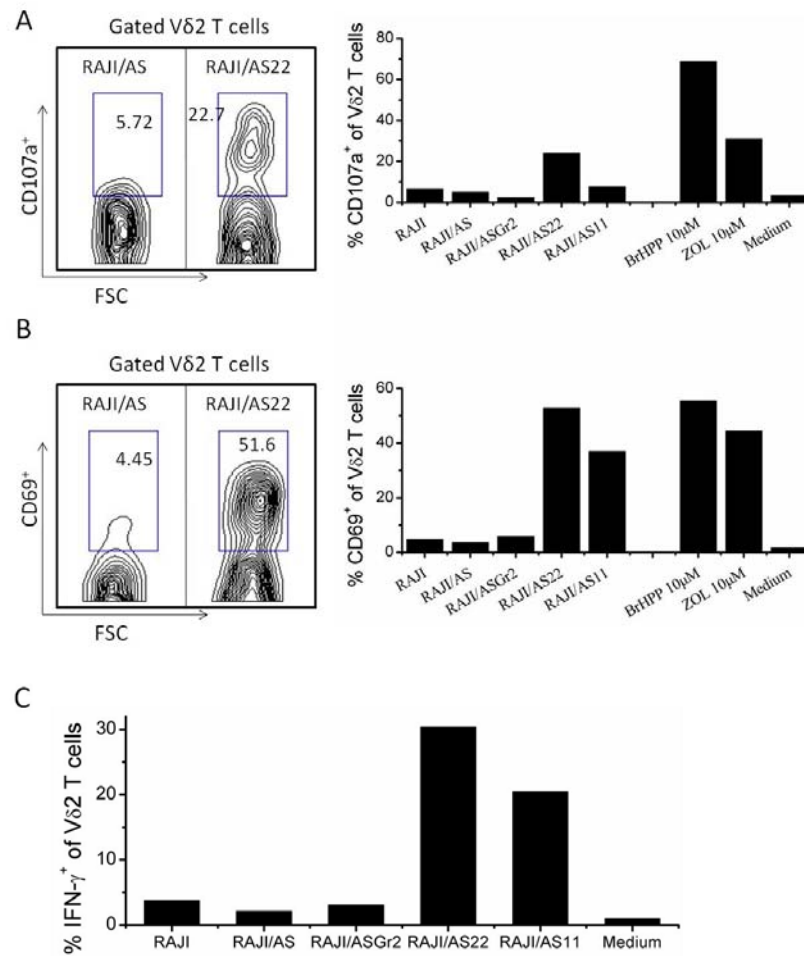


**Figure 3-12 FPPS knockdown in RAJI cells increases CD69 and CD107a expression and IFN- $\gamma$  production by primary V $\delta$ 2 T cells.** The contour plots depict the gating strategy used to generate the data depicted in the bar histograms. A) Representative FACS analysis of CD107a induction after coculture of PBL with indicated RAJI cells, BrHPP, zoledronate or medium alone. B) Representative FACS analysis of CD69 induction after cocultures of PBL with indicated RAJI cells, BrHPP, zoledronate or medium alone. C) Proportion of IFN- $\gamma$  secreting cells among V $\delta$ 2 TCR-positive PBL. (Data of Figure C was generated by group of Dr. Kunzmann).

of IFN- $\gamma$  secreting cells as is described in materials and methods. Figure 3-12A and B show the induction of CD69 and CD107a by RAJI-FPPS knockdown cells as well as by aminobisphosphonates and phosphoantigen, but not by cells expressing only control vector constructs (RAJI/AS and RAJI/ASGr2). In three out of three experiments, RAJI/AS22 shRNA knockdown cells induced upregulation of CD69 and CD107a expression, which was always stronger than by RAJI/AS11 cells. AS11 cells always

## RESULTS

induced CD69 expression by the V $\gamma$ 9V $\delta$ 2 T cells but varied with respect to induction of CD107a expression between hardly detectable induction (data not shown) or induction reaching about half of that found with RAJI/AS22 cells (Figure 3-12B). IFN- $\gamma$  secretion was tested in three experiments and was, again, more efficient with RAJI/AS22 than with RAJI/AS11 cells (Figure 3-12C). The differential degree of activation by both types of FPPS knockdown cells correlates with the differential reduction of FPPS (Figure 3-11C). Cells transduced with vector controls (RAJI/AS and RAJI/ASGr2) did not activate V $\gamma$ 9V $\delta$ 2 T cells. Finally, RAJI-FPPS knockdown cells induced no significant upregulation of CD69 and CD107a on NK cells and  $\gamma\delta$  T cells, indicating specific activation of the  $\gamma\delta$  T cells (data not shown).

### ***3.2.3 RAJI-FPPS knockdown cells induce activation of V $\gamma$ 9V $\delta$ 2 T cell lines***

RAJI-FPPS knockdown cells were also tested for their capacity to induce CD107a upregulation as well as IFN- $\gamma$  production in polyclonal V $\gamma$ 9V $\delta$ 2 T cell enriched cell lines. CD107a surface expression of the  $\gamma\delta$  TCR positive cells was assessed by electronically gating on the  $\gamma\delta$  TCR positive cells and the proportion of CD107a positive cells was determined. Figure 3-13A shows that CD107a surface expression was strongly upregulated after over-night coculture with AS22 cells. Furthermore, we observed an increased size of CD107a positive V $\gamma$ 9V $\delta$ 2 cells, compared to cocultures with control RAJI cells. We tested the capacity of FPPS knockdown cells to induce IFN- $\gamma$  secretion. Figure 3-13B depicts a drastic increase in the frequency of IFN- $\gamma$  secreting cells, in an ELISPOT assay of co-cultures of a short term  $\gamma\delta$  T cell line with FPPS knockdown cells, but not in the negative control cultures. The activation by AS22-transduced cells was more efficient than that by AS11-transduced FPPS knockdown cells, which, again, inversely, relates with the different levels of residual FPPS reached by the knockdown constructs. The figure is representative of 3 independent experiments.

## RESULTS

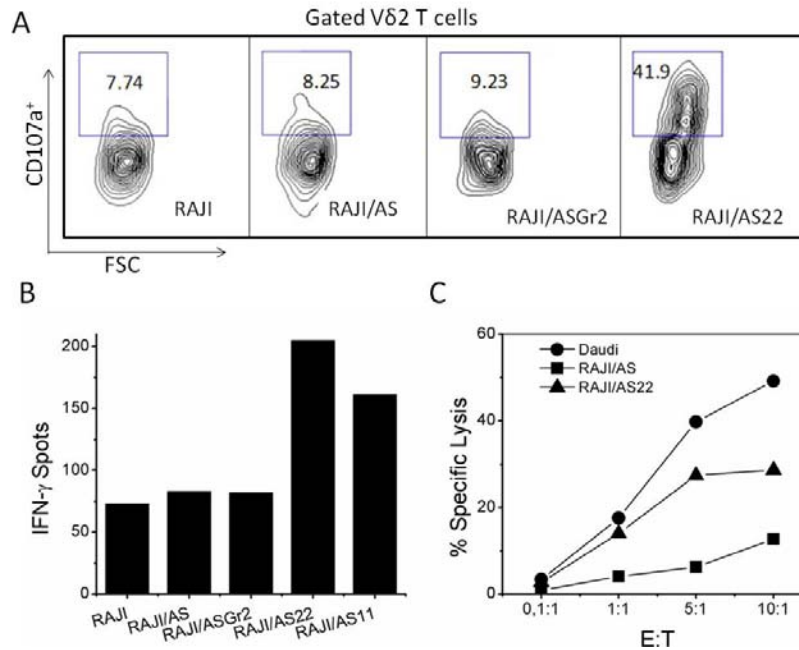


**Figure 3-13 FPPS knockdown in RAJI cells induces effector-functions in V $\gamma$ 9V $\delta$ 2 T cells.** A) FACS analysis of CD107a surface expression in V $\gamma$ 9V $\delta$ 2 T cells.  $3 \times 10^4$  cells of a V $\gamma$ 9V $\delta$ 2 T cell line were incubated overnight with  $10^5$  cells of the indicated RAJI lines in the presence of PE-anti-CD107a antibody. Thereafter cells were harvested and co-stained with FITC-anti- $\gamma\delta$  TCR antibody. Events shown are gated on the  $\gamma\delta$  TCR positive population. The numbers represent the percent of CD107a positive cells in the  $\gamma\delta$  T cell gate. B) ELISPOT IFN- $\gamma$  assays of overnight cocultures of  $3 \times 10^3$  V $\gamma$ 9V $\delta$ 2 T cells with  $2,5 \times 10^4$  of the indicated RAJI cells. C) A V $\gamma$ 9V $\delta$ 2 T cell enriched cell line was tested for cytotoxic activity against RAJI cells transduced with control vector (RAJI/AS; squares), transduced with FPPS knockdown vector (RAJI/AS22; triangles) or Daudi cells (circles) as described in material and methods. Effector : target ratios are indicated. Duration of the assay was 4h. (Data of Figure C was generated by group of Dr. Kunzmann).

Next we tested V $\gamma$ 9V $\delta$ 2 T cell enriched lines for their capacity to mediate a dose dependent killing of FPPS knockdown cells in comparison to control vector-transduced cells and Daudi cells. C shows killing of AS22 transduced RAJI cells, AS control RAJI cells and Daudi by a V $\gamma$ 9V $\delta$ 2 T cell-enriched cell line. The killing of AS22 cells, as measured on a per cell basis, was about 10-fold more efficient than killing of untransduced cells, but still less efficient than that of Daudi cells. The figure is representative for three independent experiments.

## RESULTS

To exclude that observed effects were indirect and do not result from activation of other cell populations such as  $\alpha\beta$  T cells, NK cells or monocytes, which then may provide “help” to the  $\gamma\delta$  T cells, CD107a upregulation and IFN- $\gamma$  secretion was also tested using highly purified V $\gamma$ 9V $\delta$ 2 T cells. Figure 3-14 shows for both assays specific activation of the highly purified  $\gamma\delta$  T cell lines (> 98% purity) by FPPS knock down cells.

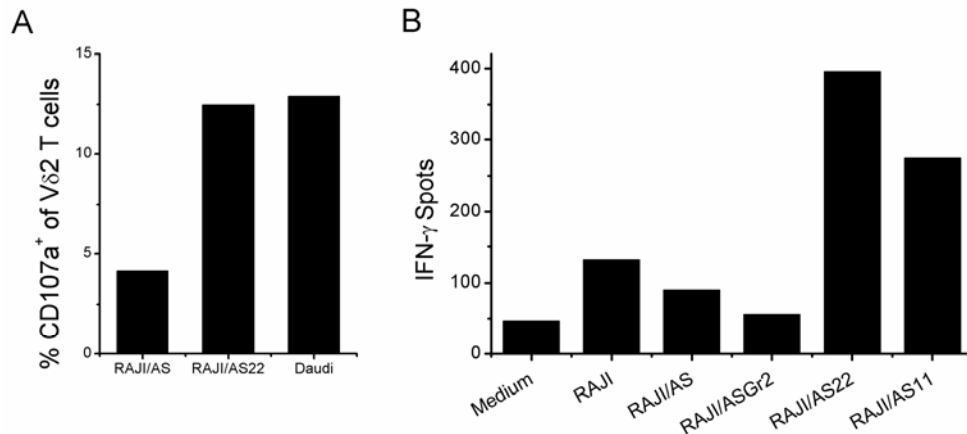


**Figure 3-14 FPPS knockdown in RAJI cells induces effector-functions in highly purified V $\gamma$ 9V $\delta$ 2 T cells.** Highly purified short term  $\gamma\delta$  T cells lines were enriched by MACS for  $\gamma\delta$  T cells (> 98% purity), rested for 1 d (A) or 3 d (B) and tested for CD107a surface expression or frequency of IFN- $\gamma$  secreting cells, respectively. A)  $3 \times 10^4$  cells of purified V $\gamma$ 9V $\delta$ 2 line T cells were incubated overnight with  $10^5$  cells of the indicated cell lines in the presence of PE-anti-CD107a antibody. Thereafter cells were harvested and co-stained with FITC-anti- $\gamma\delta$  TCR antibody. The numbers represent the percent of CD107a positive  $\gamma\delta$  T cells. B) shows results of an ELISPOT IFN- $\gamma$  assay of overnight cocultures of  $5 \times 10^3$  purified V $\gamma$ 9V $\delta$ 2 line T cells with  $2.5 \times 10^4$  of the indicated RAJI cells.

### ***3.2.4 Activation of V $\gamma$ 9V $\delta$ 2 T cells by aminobisphosphonates and RAJI-FPPS knockdown cells is inhibited by mevastatin***

One explanation for V $\gamma$ 9V $\delta$ 2 T cell activation by aminobisphosphonates is their capacity to block FPPS in the target cell leading to the accumulation and subsequent “presentation” of IPP to the V $\gamma$ 9V $\delta$ 2 T cells. To test this hypothesis we treated FPPS knockdown cells with mevastatin, which lowers IPP levels as a consequence of blocking HMG-CoA reductase activity. IFN- $\gamma$  secretion induced by both types of FPPS knockdown cells was significantly inhibited by mevastatin (Figure 3-15). Similarly we observed reduced induction of IFN- $\gamma$  secretion induced by aminobisphosphonate

## RESULTS

zoledronate treated cells. Addition of the exogenous ligand BrHPP to mevastatin treated cells reversed the block and led to efficient IFN- $\gamma$  production.

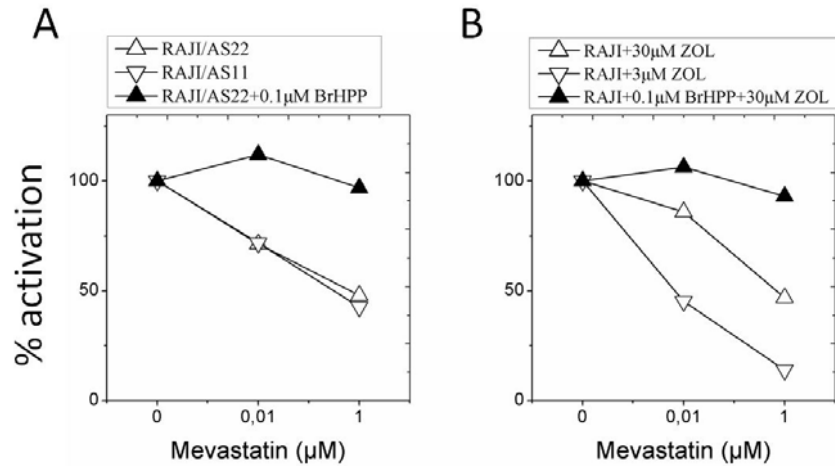


**Figure 3-15 Effects of mevastatin treatment on induction of IFN- $\gamma$  secretion by FPPS knockdown RAJI and zoledronate-treated RAJI cells.** ELISPOT IFN- $\gamma$  assays of overnight cocultures of  $3 \times 10^3$   $\gamma\delta$  T cells with  $2.5 \times 10^4$  of the indicated RAJI cells were performed in the presence of the given concentrations of mevastatin. % percent activation indicates the activation in comparison to activation without mevastatin which is set as 100% activation. The symbols indicate following stimuli in the left panel: RAJI/AS22 (304); open triangle, RAJI/AS11 (121); inverted open triangle, RAJI/AS22 + 0.1  $\mu$ M BrHPP (321); full triangle. The symbols indicate following stimuli in the right panel: RAJI + 30  $\mu$ M zoledronate (192); open triangle, RAJI + 3  $\mu$ M zoledronate (86); inverted open triangle, RAJI + 30  $\mu$ M zoledronate and 0.1  $\mu$ M BrHPP (282); full triangle. The numbers in brackets indicate the spots found for 100% activation with the respective stimulus.

### 3.2.5 FPPS knockdown in RAJI directly activated $\gamma\delta$ TCR transduced BW58r/mCD28 cells

To determine whether AS22 transduced RAJI cells also directly induced activation of  $\gamma\delta$  TCR transduced cells, we tested the responsiveness of BW58r/mCD28  $\gamma\delta$ Mop to RAJI, RAJI/AS, RAJI/AS22 and RAJI/AS11. As shown in Figure 3-16A, RAJI/AS22 induced a remarkable degree of IL-2 production, while IL-2 levels found after co/culture with RAJI/AS11 were only slightly above those found with the negative controls RAJI and RAJI/AS. In order to exclude the possibility that IL-2 production was caused by other factors than the TCR-CD3 signal, we tested the reaction of the established BW58r/mCD28 V $\alpha$ 14(CDR2+4) transductant cells (118) to the superantigen YPM,

## RESULTS

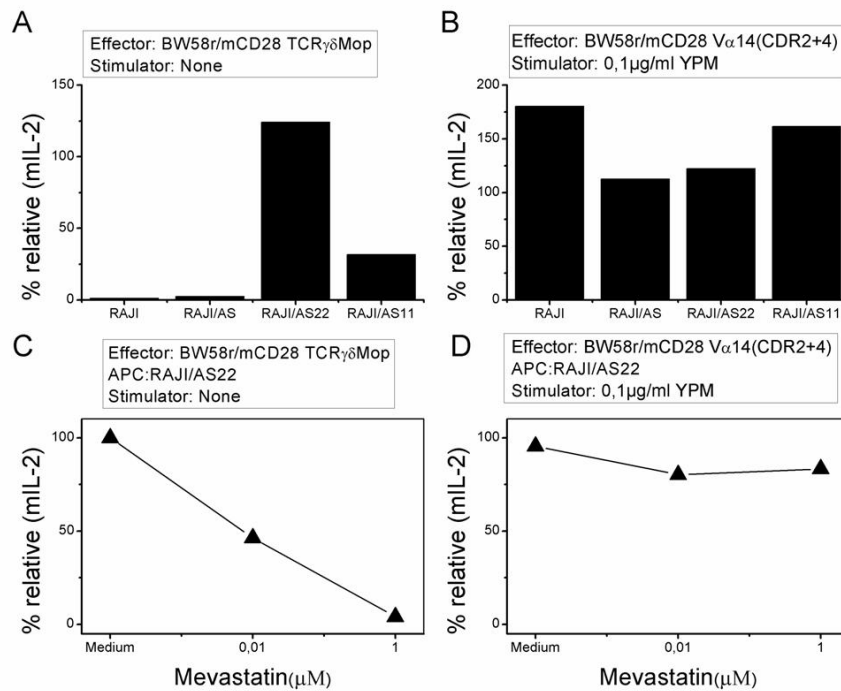


**Figure 3-16 FPPS knockdown in RAJI cells induces IL-2 production by BW58r/mCD28  $\gamma\delta$  cells.** A) Overnight co-culture of  $5 \times 10^4$  BW58r/mCD28  $\gamma\delta$ Mop cells with indicated  $5 \times 10^4$  RAJI cells. B)  $5 \times 10^4$  BW58r/mCD28 V $\alpha$ 14(CDR2+4) overnight co-culture with YPM treated RAJI cells. C) Overnight co-culture of  $5 \times 10^4$  BW58r/mCD28  $\gamma\delta$ Mop cells with  $5 \times 10^4$  RAJI/AS cells in the presence of mevastatin. D)  $5 \times 10^4$  BW58r/mCD28 V $\alpha$ 14(CDR2+4) overnight co-culture with YPM treated RAJI/AS22 cells in the presence of mevastatin. Values in A and B were calculated as the relative percentage of the control stimulated by  $10 \mu\text{M}$  BrHPP and RAJI. Values in C and D were calculated as the relative percentages of the control without Mevastatin. YPM: Yersinia pseudotuberculosis mitogen.

which was presented by RAJI, RAJI/AS, RAJI/AS22, RAJI/AS11, respectively (Figure 3-16B). Results did not show more IL-2 production when stimulation by RAJI/AS22 or RAJI/AS11 than RAJI and RAJI/AS. Additionally, we observed that the response of  $\gamma\delta$  TCR transduced BW58r/mCD28 cells to RAJI/AS22 alone was dramatically inhibited by mevastatin (Figure 3-16C) while the response of BW58r/mCD28 V $\alpha$ 14(CDR2+4) cells to RAJI/AS22 plus YPM was not affected.

### 3.2.6 FPPS knockdown in RAJI had no effects on Ecto-ATPase expression

To investigate whether FPPS knockdown would affect the expression of the postulated V $\gamma$ 9V $\delta$ 2 TCR ligand F1-ATPase, we performed staining with the F1-ATPase  $\beta$ -chain

## RESULTS

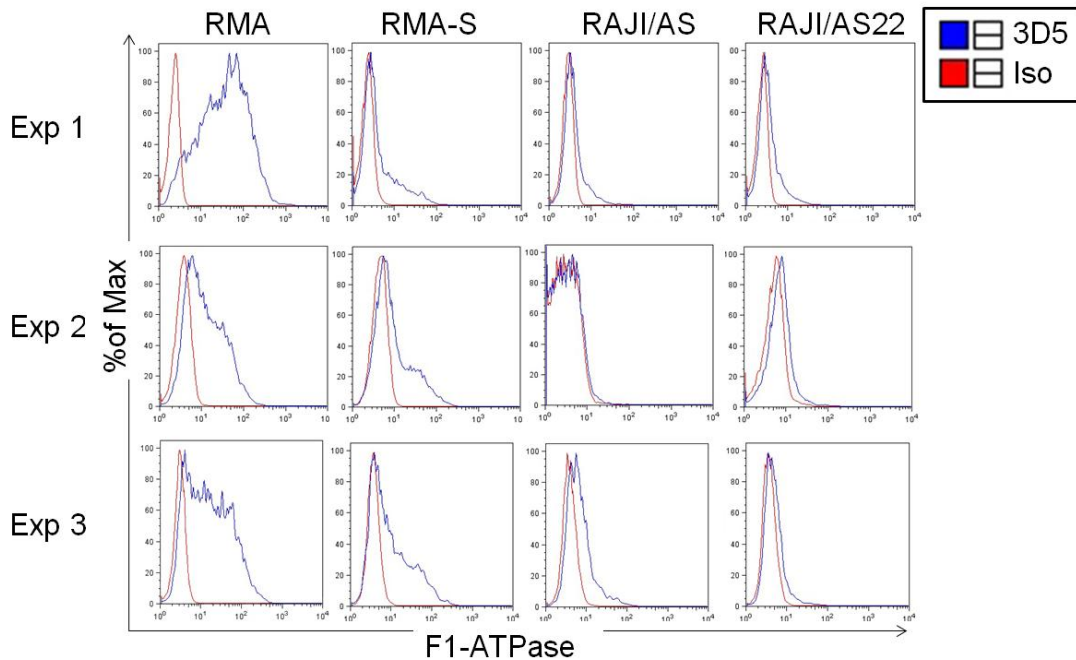


**Figure 3-17 FACS staining with F1-ATPase MoAb.**  $1 \times 10^5$  RMA, RMA-S, RAJI/AS or RAJI/AS22 were stained with F1-ATPase  $\beta$ -chain specific MoAb, 3D5 (1:1000 dilution) followed by FITC-anti mIgG MoAb. Histograms represented three times staining results.

specific mAb 3D5, which has been reported to stain also mouse cell lines RMA and RMAS. We confirmed staining of these cells, but different to what has been reported RMA cells stained better than MHC class I negative RMAS cells. In parallel, we stained RAJI/AS control cells and RAJI FPPS knock down AS22. In one experiment which was shown in the first row of Figure 3-17, both cells presented the same staining. Then we repeated the experiment twice. FPPS knockdown cells showed once better staining and once weaker staining than empty vector control. It is important to emphasize that  $V\gamma 9V\delta 2$  T cell activation by RAJIAS22 was always reproducible. So far we do not see how to connect these results with a role of F1-ATPase in  $V\gamma 9V\delta 2$  T cell activation by FPPS knockdown cells.

### ***3.2.7 FPPS knockdown in RAJI cells had no effects on growth of tumor cells***

We next investigated whether FPPS knockdown affects growth of tumor cells. To this end, we quantified the cell numbers of RAJI, RAJI/AS and RAJI/AS22 by FACS after

## RESULTS

overnight culture. As shown in Figure 3-18, no big differences between RAJI, RAJI/AS and RAJI/AS22 were observed. In our subsequent work, Martina Roilo from our laboratory further investigated the effects of FPPS knockdown in tumor cell growth in her master's work (120). The results always showed even better growth of RAJI/AS22 than RAJI/AS.

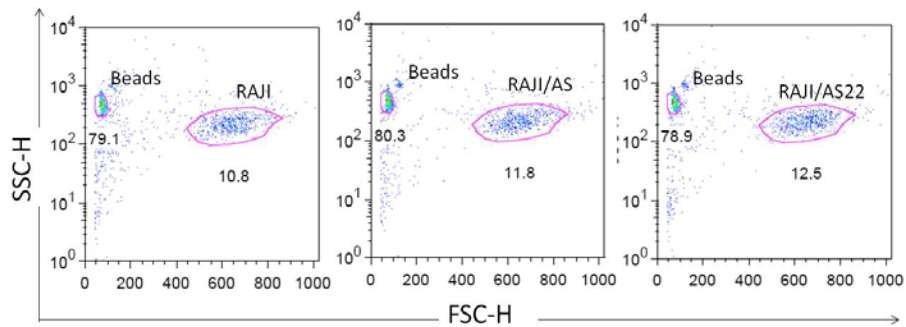


**Figure 3-18 Flow cytometry analysis of cell growth.**  $1 \times 10^5$  RAJI, RAJI/AS and RAJI/AS22 cells were overnight cultured in a 96 well plate. All cells were harvested and washed twice with FACS buffer, thereafter were resuspended in 500 $\mu$ l buffer. Before measurement by flow cytometry, the same number of counting beads was added to each sample. The dot plots show the percentages of the gated beads and indicated RAJI cells in the total events (5, 000), respectively.

### 3.2.8 FPPS specific shRNA converts Jurkat cells to $V\gamma 9V\delta 2$ T cell activators

To test whether FPPS specific shRNA induces a  $V\gamma 9V\delta 2$  T cell activating phenotype in other tumors of hematopoietic origin, AS and AS22 transduced Jurkat cells were also tested for their  $V\gamma 9V\delta 2$  T cell activating properties. Co-incubated with short term  $\gamma\delta$  T cell line, AS22 transduced Jurkat clearly induced IFN- $\gamma$  release (245 spots) while AS transduced cells did not (1 spot) (Figure 3-19A). Jurkat/AS22 treated with 10nM mevastatin reduced IFN- $\gamma$  release over 60% compared with without mevastatin treatment (Figure 3-19B). Similarly, AS22 transduced Jurkat induced more CD107a surface mobilization than AS transduced cells and mevastatin treatment blocked around 50% of CD107a expression.



## RESULTS

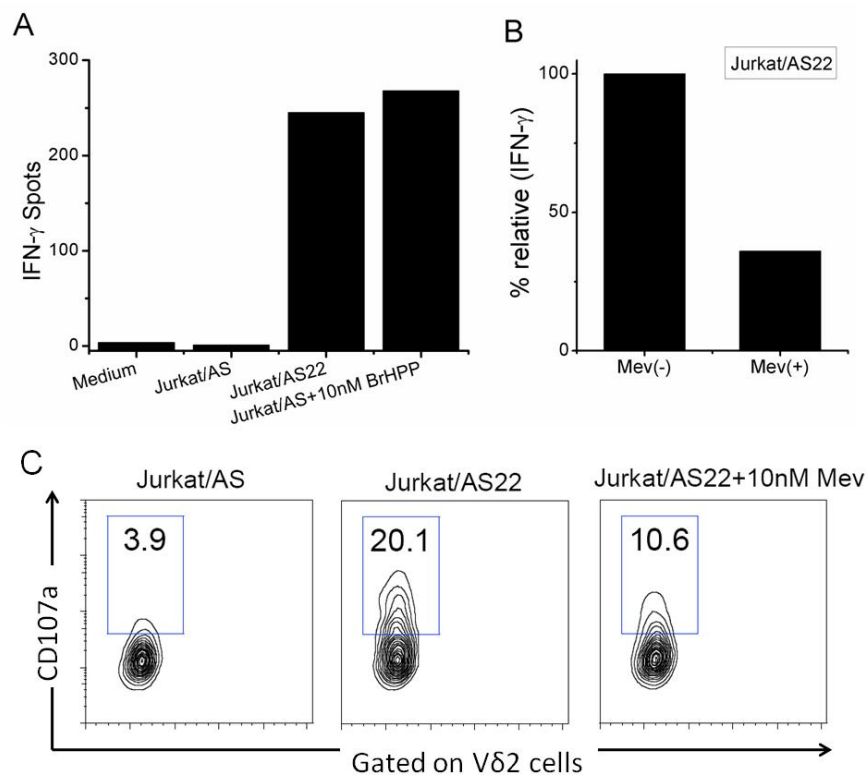


**Figure 3-19 FPPS knockdown in Jurkat cells increase the IFN- $\gamma$  secretion and CD107a expression by short-term enriched  $\gamma\delta$  line while both were reduced by 10nM mevastatin.** A) ELISPOT IFN- $\gamma$  assays of overnight cocultures of  $3 \times 10^3$  V $\gamma$ 9V $\delta$ 2 T cells with  $2.5 \times 10^4$  of the indicated Jurkat cells and stimulators; B) values represent the percentage of IFN- $\gamma$  spots in the presence of 10nM mevastatin in comparison to the control of without mevastatin; C) FACS analysis of CD107a surface expression in V $\gamma$ 9V $\delta$ 2 T cells.  $3 \times 10^4$  cells of V $\gamma$ 9V $\delta$ 2 T cell line were incubated overnight with  $5 \times 10^4$  cells Jurkat/AS or Jurkat/AS22 with or without 10nM mevastatin in the presence of PE-anti-CD107a antibody. Thereafter cells were harvested and co-stained with FITC-anti-V $\delta$ 2 TCR antibody. Events shown are gated on the V $\delta$ 2 TCR positive population. The numbers in boxes indicate percentages of CD107a positive cells in the V $\delta$ 2 T cell gate.

### ***3.2.9 FPPS specific shRNA converts also tumor cells of non-hematopoietic origin to V $\gamma$ 9V $\delta$ 2 T cell activators***

To test whether FPPS specific shRNA induces a V $\gamma$ 9V $\delta$ 2 T cell activating phenotype in cell lines derived from non-hematopoietic tumors, following cell lines were transduced with AS or AS22, respectively: AsPC-1 (human pancreatic adenocarcinoma), HepG2 (human hepatocellular carcinoma), 293T cells (human embryonic kidney cell line

## RESULTS

expressing large T antigen) and A549 (human alveolar basal epithelial carcinomic). Analysis of CD107a mobilization was shown in Figure 3-20. In the absence of stimulators, AS22 transduced AsPC-1, HepG2 and 293T cells induced to various extent up-regulation of CD107a surface staining while it was not obvious in A549/AS22 cells. When treated with 0,1 $\mu$ M BrHPP, either AS or AS22 transduced cells showed a clear increase of CD107a<sup>+</sup> V $\delta$ 2<sup>+</sup> cells but the activation was always stronger in co-cultures with AS22 transduced cells than with AS transduced cells.

Next, we analyzed the expression of early activation marker CD69 by V $\gamma$ 9V $\delta$ 2 T cells found in fresh isolated PBLs. Again, activation by AS22 transduced cells was always stronger than by AS transduced cells (Figure 3-21).

## RESULTS

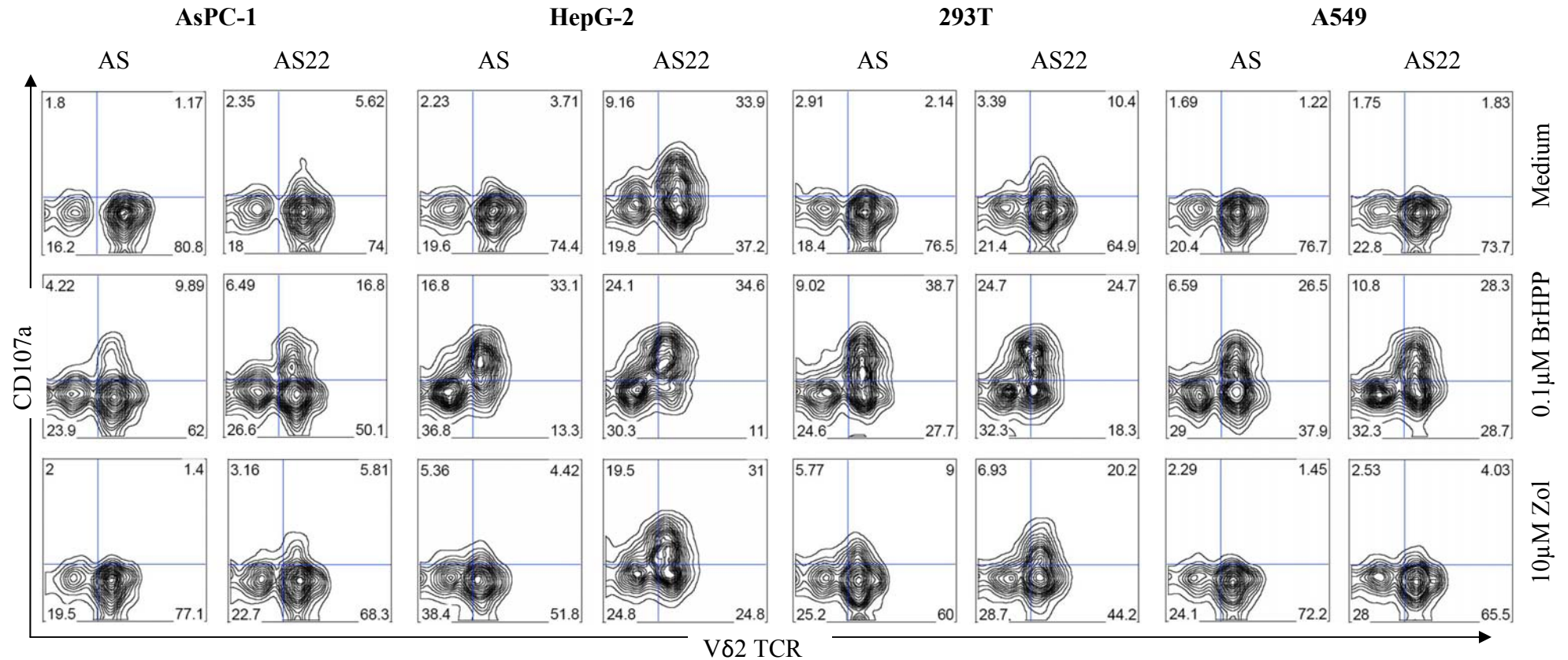


**Figure 3-20 FACS analysis of CD107a expression in short-term enriched  $\gamma\delta$  T cell line in response to various non-hematopoietic tumor targets transduced with AS or AS22.**  $3 \times 10^4$   $V\gamma 9V\delta 2$  T cells of short term  $\gamma\delta$  T cell line were incubated for 5 hours with  $10^5$  cells of the indicated cell lines with medium, 0,1µM BrHPP or 10µM zoledronate in the presence of PE.Cy5-anti-CD107a antibody. Thereafter cells were harvested and co-stained with FITC-anti- $\gamma\delta$  TCR antibody. Numbers of the top right in quadrants indicate percentages of  $V\delta 2$  TCR<sup>+</sup> CD107a<sup>+</sup> cells.

## RESULTS

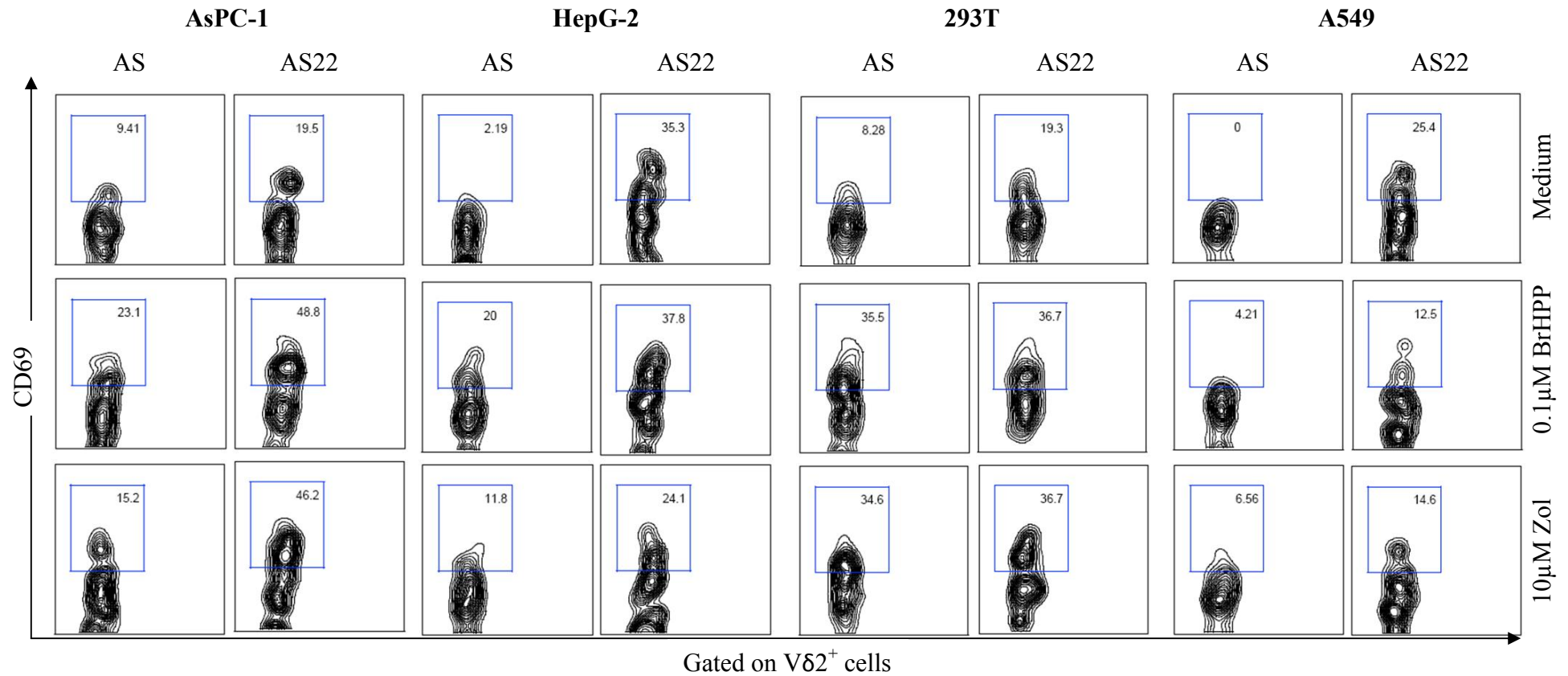


**Figure 3-21 FACS analysis of CD69 upregulation in fresh isolated PBLs in response to various non-hematopoietic tumor lines transduced with AS or AS22.**  $1 \times 10^5$  fresh isolated PBLs were incubated overnight with  $5 \times 10^4$  cells of the indicated cell lines in the presence of medium, 0,1μM BrHPP or 10μM zoledronate. Thereafter cells were harvested and co-stained with FITC-anti-CD69 MoAb and PE-anti-Vδ2TCR MoAb. Events shown are gated on the Vδ2 TCR positive population. Numbers in boxes indicate percentages of CD69<sup>+</sup> cells in Vδ2TCR<sup>+</sup> cell gate.

## RESULTS

### 3.2.10 Comparison of $\gamma\delta$ -T-cell activation by FPPS knockdown cells versus Daudi cells

The analysis of IFN- $\gamma$  spots indicated that Daudi cells, as well as AS22 transduced RAJI, Jurkat, AsPC-1 and 293T cells, activated a short term  $\gamma\delta$  T cell line to secrete more IFN- $\gamma$  than AS transduced cells (Figure 3-22A). In addition, mevastatin blocked the activation of  $\gamma\delta$  T cells by Daudi cells or AS22 transduced cells to various extent. To be noted, Daudi cells showed lower sensitivity to mevastatin blocking than AS22 transduced cells (Figure 3-22B).

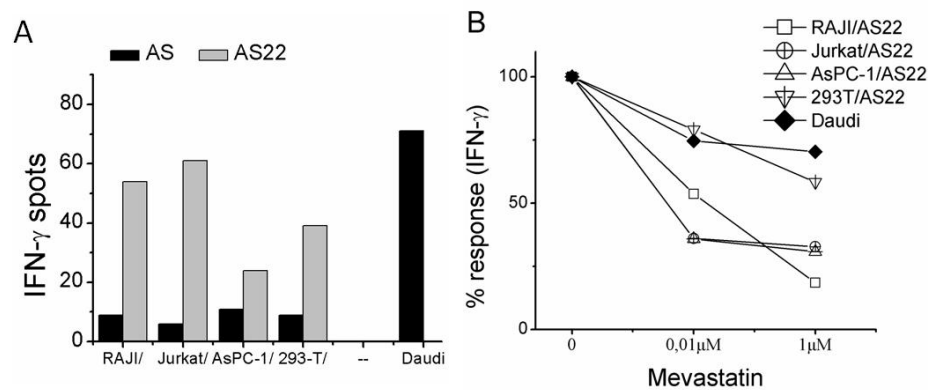


**Figure 3-22 Comparison of the response of a short term  $\gamma\delta$  T cell line to Daudi and FPPS knockdown cells.** A)  $3 \times 10^3$   $\gamma\delta$  T cells were overnight co-cultured with  $2.5 \times 10^4$  Daudi cells, or AS transduced (black bar) and AS22 transduced (grey bar) RAJI, Jurkat, AsPC-1, 293T cells, respectively. B) Mevastatin was added during the overnight culture. The shown values represented the percentages of control without mevastatin treatment.

### 3.3 Conditional Knockdown of FPPS by a Tet-Inducible Lentiviral shRNA Expression System

Unlike many retroviral vectors which require replicating DNA to insert them into the host genome, lentiviral vectors offer the advantage to also non-proliferating cells. In addition, it would be of large interest to get the opportunity to modulate temporarily knockdown FPPS expression. To this end, a Tet-inducible shRNA expressing lentiviral vector FH1tUTG (107) was investigated, which has been shown previously to fulfill this promise in primary cells as well as in an animal model. This vector was kindly provided

## RESULTS

by Dr. Herold. Operating principle of the lentiviral construct is shown in Figure 3-23A. A FPPS specific construct containing the same target sequence with AS22, designated as sequence of the rat Insulin/receptor were transduced into RAJI cells. Although flow cytometry analysis of GFP reporter expression indicated that not all RAJI cells were transfected with lentivirus FH1t(SR22)UTG (Figure 3-23B), immunoblot results still show remarkable inhibition of FPPS expression after doxycyclin treatment (Figure 3-23C). Densitometric analysis revealed a relative reduction of FPPS protein by 35% for FH1t(SR22)UTG transduced RAJI cells than FH1t(INSR)UTG transduced cells.

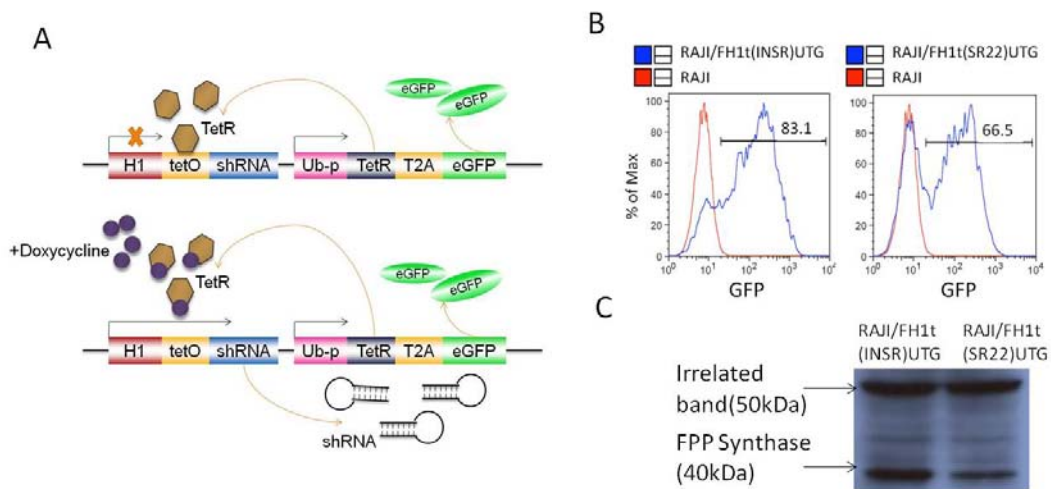


**Figure 3-23 Lentiviral system for inducible FPPS knockdown.** A) The vector FH1tUTG contains one cassette consisting of a shRNA regulated by the H1 promoter with tetO and a second cassette consisting of the tetR linked to EGFP by the viral T2A peptide under the control of the ubiquitin C promoter (Ub-p). In the absence of doxycyclin, the tetR binds to tetO and blocks shRNA transcription. After addition of doxycyclin, the tetR is released, facilitating the onset of shRNA expression. EGFP is constitutively expressed under both conditions. B) EGFP expression after viral package and infection in RAJI cells. C) Immunoblot of indicated RAJI cells after 2 days treatment with 0,1 $\mu$ g/ml doxycyclin. RAJI/FH1t(INSR)UTG represent RAJI cells infected with lentiviral construct containing unrelated shRNA sequence; RAJI/FH1t(SR22)UTG represent RAJI cells infected with lentiviral construct containing target sequence of AS22 in shRNA specific for FPPS.

Next, we analyzed the inducible and reversible activation of  $\gamma\delta$  TCR transduced cells. The results showed that 48 hours 0,1 $\mu$ g/ml doxycyclin treatment successfully converted FH1t(SR22)UTG transduced RAJI cells to activators of BW58r/mCD28  $\gamma\delta$  T cells while FH1t(INSR)UTG transduced RAJI cells or RAJI alone not (Figure 3-24A). The same

## RESULTS

degree of activation was seen with 100 fold lower concentration of doxycyclin and the threshold for induction of IL-2 production was between 0,01 and 0,1 ng/ml of the antibiotic (Figure 3-24B). Activation of the  $\gamma\delta$  TCR transductants by FH1t(SR22)UTG transduced RAJI cells was effectively blocked by mevastatin (Figure 3-24C). Finally, the inducible capacity of activation was almost completely reversed after 8 days of doxycyclin removal and decreased to 20% after 4 days of doxycyclin removal (Figure 3-24D).

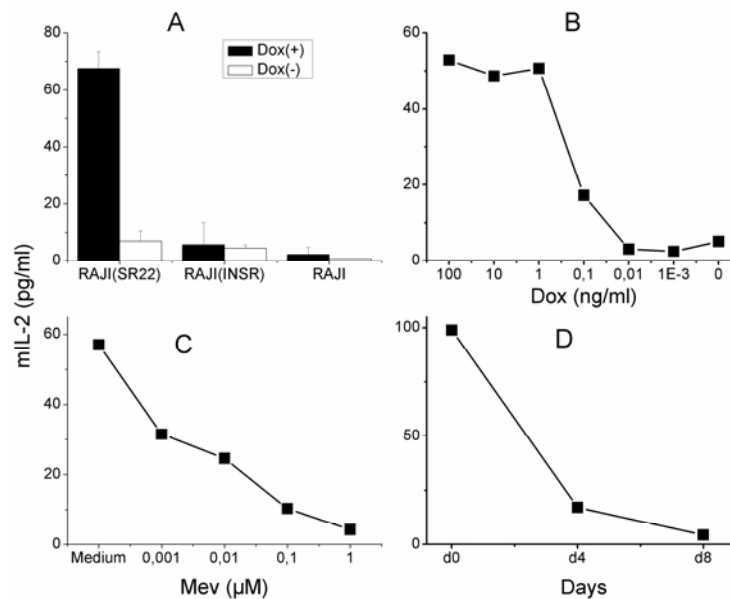


**Figure 3-24 Inducible and reversible IL-2 production of BW58r/mCD28  $\gamma\delta$  TCR in response to RAJI/FH1t(SR22)UTG cells.** A) FH1t(SR22)UTG transduced RAJI cells, FH1t(INSR)UTG transduced RAJI and RAJI cells were treated with 0,1 $\mu$ g/ml doxycyclin (closed bar) or without treatment (open bar). Thereafter cells were harvested and centrifuged once for removal of doxycyclin. The graph shows IL-2 production of  $5 \times 10^4$  BW58r/mCD28  $\gamma\delta$ Mop cells overnight co-culture with same numbers treated RAJI transductants. B) FH1t(SR22)UTG transduced RAJI cells were treated with titrated doxycyclin (100-0 ng/ml) for 48 hours. The graph shows IL-2 production of BW58r/mCD28  $\gamma\delta$ Mop cells overnight co-culture with treated RAJI transductants. C) FH1t(SR22)UTG transduced RAJI cells were treated with 0,1 $\mu$ g/ml doxycyclin for 48 hours, washed once and counted, and cells were incubated for 2 hours with mevastatin. Thereafter BW58r/mCD28  $\gamma\delta$  T cells were added, and the IL-2 production was measured after overnight incubation. Mevastatin remained present during the period of co-culture. D) H1t(SR22)UTG transduced RAJI cells were treated with 0,1 $\mu$ g/ml doxycyclin for 48 hours. Cells were harvested and washed twice for removal of doxycyclin. Overnight co-culture of transduced RAJI cells with BW58r/mCD28  $\gamma\delta$ Mop cells was carried out immediately (d0) or after continually cultured 4 days (d4) or 8 days (d8) with RPMI1640 without doxycyclin. The graph shows IL-2 production at different time points.

## RESULTS

### 3.4 Regulating Expression of Other Enzymes of Isoprenoid Synthesis

In addition to the knockdown of FPPS, we also over-expressed FPPS in RAJI cells with two different strategies; one was over-expression of a FPPS-YFP fusion protein using the retroviral vector pIZ, another one was over-expression of FPPS with an EGFP reporter using IRES bicistronic retroviral vector. FPPS expression was compared by immunoblot-analysis with that of untransduced RAJI cells and effects of AS22 on the FPPS transduced cells was also tested. Up-regulation of FPPS protein was shown in both systems (Figure 3-25). FPPSpIZYFP construct-transduced RAJI cells indicated a specific band in around 65KD position which presented the successful expression of fusion protein, FPPSYFP, but interestingly a 30% increase of density was also found for the (endogenous) FPPS band in comparison to RAJI cells. Both FPPSYFP and FPPS bands were effectively inhibited by AS22 transduction (A). In figure B, we also detected around 40% increasing density in FPPSEGZ transduced RAJI/AS cells to RAJI/AS cells. AS22 effectively inhibited the expression of FPPS protein in the RAJI/FPPSEGZ cells.

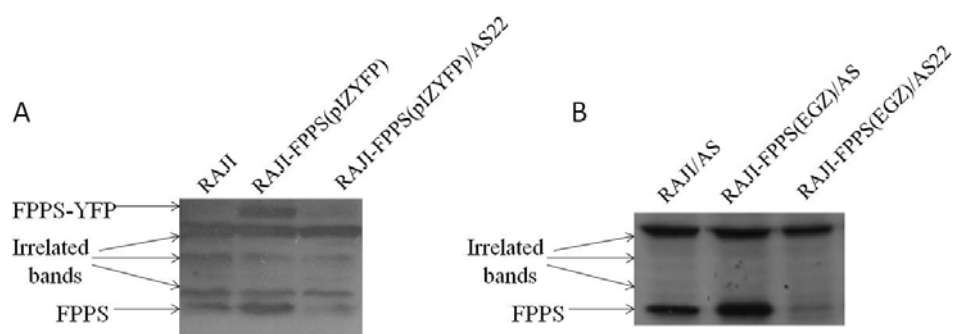


**Figure 3-25 Immunoblot analysis of FPPS expression levels.** Rabbit anti-human FPP synthase Polyclonal antibody were used as specific binding with FPPS or FPPSYFP. Unrelated bands represented the unspecific protein binding with this Polyclonal Ab.

Following the same strategy, we also transduced RAJI cells with GGPPS, IDI, MVD and HMGR, respectively. The idea of this experiment was to test whether over-expression of enzymes in RAJI cells, which participate in synthesis or consumption of IPP, would somehow affect the  $\gamma\delta$  T cell activation. The specific primers for different constructs are



## RESULTS

shown in Table 2-4. Stably transduced cells were selected with antibiotic treatment and gene expression was verified by flow cytometry analysis of expression of fluorescence reporter EGFP or EYFP. Subsequently we compared their capacity to activate  $\gamma\delta$  TCR transduced BW58r/mCD28 cells. As shown in Figure 3-26, RAJI cells transduced with those enzymes did not induce IL-2 production by BW58r/mCD28  $\gamma\delta$  cells. Addition of BrHPP or zoledronate to the different RAJI cells differentially affected IL-2 production by BW58r/mCD28  $\gamma\delta$  cells. In parallel, as control for possible  $\gamma\delta$  TCR independent effects on the presenting RAJI-transductants the response of by BW58r/mCD28  $V\alpha 14$ (CDR2+4) to the superantigen YPM was tested and some variation in this response was seen as well. The significance of this variation remains to be elucidated.

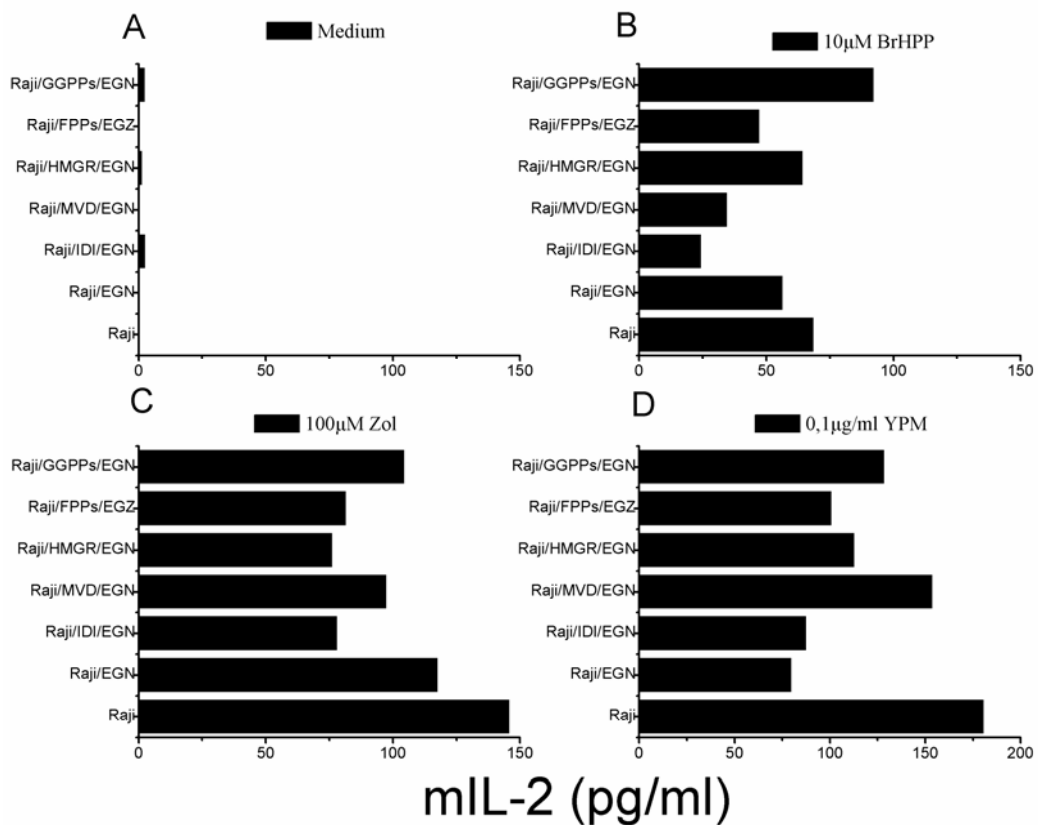


**Figure 3-26 Comparing analysis of IL-2 production by transduced BW58 cells in response to RAJI cells up-regulating different enzymes.** A,B,C)  $5 \times 10^4$  BW58r/mCD28  $\gamma\delta$  T cells were co-cultured with  $5 \times 10^4$  indicated RAJI cells and marked stimulators. D)  $5 \times 10^4$  BW58r/mCD28  $V\alpha 14$ (CDR2+4) cells were co-cultured with  $5 \times 10^4$  indicated RAJI cells in the presence of 0,1 $\mu$ g/ml YPM.

## RESULTS

Finally, we tested whether knockdown of enzymes other than FPPS would significantly affect  $V\gamma 9V\delta 2$  T cells activation. To this end, generated RAJI cell lines were transduced with respective LMP/Asred derived vectors containing specific shRNA of GGPPS, IDI, MVD and HMGR. Following the flow-cytometry screening strategy as described in Figure 3-11, we verified the successful knockdown of IDI and GGPPS by flow cytometry analysis (data not shown) while knockdown efficacy of MVD and HMGR still remains to be proven. The various knockdowns were tested for their capacity to induce IFN- $\gamma$  secretion by a short term  $\gamma\delta$  T cell line in response to different RAJI cell line. As shown in Figure 3-27, there was a slight increase in the phosphoantigen-dependent and phosphoantigen-independent response for all shRNA knock-down cells different from the ASGR2, but this activation was rather small and its significance remains to be proven.

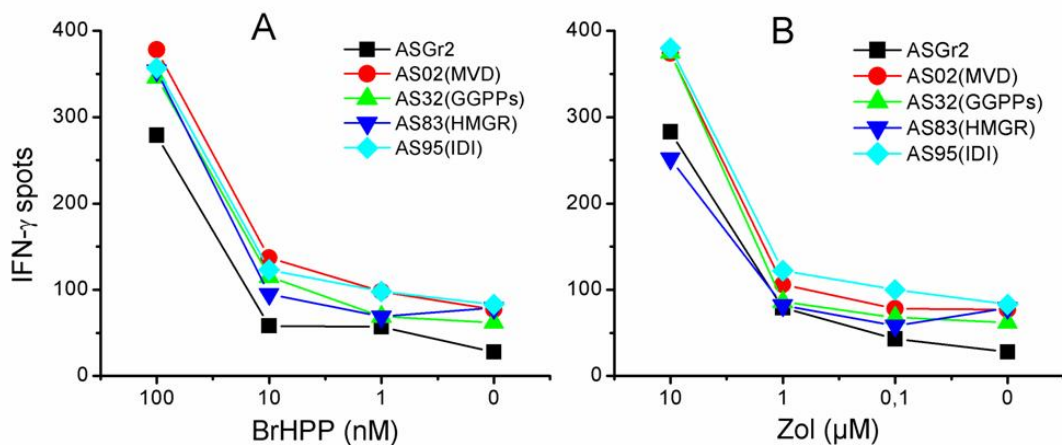


**Figure 3-27 Comparison of induction of IFN $\gamma$  in a short term  $\gamma\delta$  T cell line by RAJI cells transduced with constructs containing different shRNAs.** A IFN- $\gamma$  ELISPOT was performed of  $3 \times 10^3$  enriched  $\gamma\delta$  T cells co-cultured overnight with  $2,5 \times 10^4$  of the indicated shRNA transduced RAJI cells with indicated BrHPP and zoledronate. AS02: RAJI cells with MVD specific shRNA; AS32: RAJI cells with GGPPS specific shRNA; AS83: RAJI cells with HMGR specific shRNA; AS95: RAJI cells with IDI specific shRNA.

## **4 DISCUSSION**

### **4.1 A new tool for the analysis of ligand recognition by V $\gamma$ 9V $\delta$ 2 TCR**

The classical way to analyze ligand recognition by human V $\gamma$ 9V $\delta$ 2 T cells is the analysis of in vitro propagated antigen specific T cell lines or clones, respectively. Such cells can be generated rather easily by in vitro culture of human PBL with phosphoantigens such as BrHPP or IPP, which allows an expansion from 0.5-5% of total T cells to 60-80% after 10 days in vitro culture. Also a further purification to more than 99% by positive selection with TCR specific antibodies is possible, although this raises problems due to an additional activation by the TCR specific antibodies, and finally V $\gamma$ 9V $\delta$ 2 T cell clones can be used to study V $\gamma$ 9V $\delta$ 2 TCR mediated activation, which allows a functional characterization of a clonotypic V $\gamma$ 9V $\delta$ 2 TCR. The analysis of all these cell types is complicated by the pronounced effects of innate receptors, especially of receptors which are also found on NK cells such as Killer Inhibitory Receptors (KIRs) as well as the activating receptor NKG2D. The interference of TCR mediated activation by such receptors can be partially circumvented by expression of the V $\gamma$ 9V $\delta$ 2 TCR in a TCR- $\beta$  deficient clone of the human T cell leukemia Jurkat, but these lines are often difficult to activate and notorious for the instability response to V $\gamma$ 9V $\delta$ 2 TCR ligands. The other problem, which is common to V $\gamma$ 9V $\delta$ 2 TCR transduced Jurkat cells and primary human V $\gamma$ 9V $\delta$ 2 T cells, is the capacity of essentially all human cell lines to present V $\gamma$ 9V $\delta$ 2 TCR ligands, which makes it difficult to dissect presenting and recognition functions of these cells.

## DISCUSSION

To circumvent these problems, we have generated V $\gamma$ 9V $\delta$ 2 TCR transduced mouse cells with the capacity to respond to bona fide V $\gamma$ 9V $\delta$ 2 TCR ligands such as soluble phosphoantigens and human (tumor) cells, which have been treated either with aminobisphosphonates or which have been transduced with vectors encoded for FPPS specific shRNA. In the following part the generation of such cells and the features contributing to their V $\gamma$ 9V $\delta$ 2 TCR reactivity will be discussed and compared with that of primary V $\gamma$ 9V $\delta$ 2 T cells. To refrain from the alternation by such self-presentation, an ideal alternative recipient of TCR gene transfer is TCR<sup>-</sup> mouse T cell hybridoma 58C (BW58) (108). In our previous work, BW58 cells were used as recipients of a rat myelin basic protein-specific TCR (118) and various mouse and rat iNKT TCR (121). TCRs transduction conferred upon BW58 cells the capability to produce IL-2 in response to corresponding antigens MBP or  $\alpha$ -GalCer. To be noted is that activation and subsequent IL-2 production of the TCR transduced BW58 cells was considerably improved by expressing a transgenic chimeric rat/mouse CD28 molecule (109) and its interaction with CD80/86 on the presenting cell (122). Similarly, Matthias Kreiss from our laboratory cloned and transduced a phosphoantigens reactive V $\gamma$ 9V $\delta$ 2 TCR into BW58r/mCD28 cells subsequently proved the responsiveness of transductants to phosphoantigens in the presence of RAJI cells (115, 117). Our present work extended the observation of V $\gamma$ 9V $\delta$ 2 TCR transductants.

In our newly developed V $\gamma$ 9V $\delta$ 2 TCR transductants, r/mCD28 expression is essential in response to BrHPP or zoledronate in the presence of RAJI cells while expression of human CD28 has no effect (Figure 3-2) which suggests: 1). The extracellular region of the rat CD28 molecule cross-reacts with human CD80 or CD86 of RAJI cells; 2). the human CD28 cannot transfer the activating signal generated by its binding to the human CD80/CD86 due to impaired interaction of the cytoplasmic part of the CD28 with species specific intracellular signaling molecules. The latter surprises to some extent since certain motifs of CD28-cytoplasmic part known to be involved in signal transduction are conserved between all three species such as the phosphorylated tyrosines of YMNM motif and two proline-rich regions (Figure 4-1) (122). The validity of the first hypothesis

## DISCUSSION

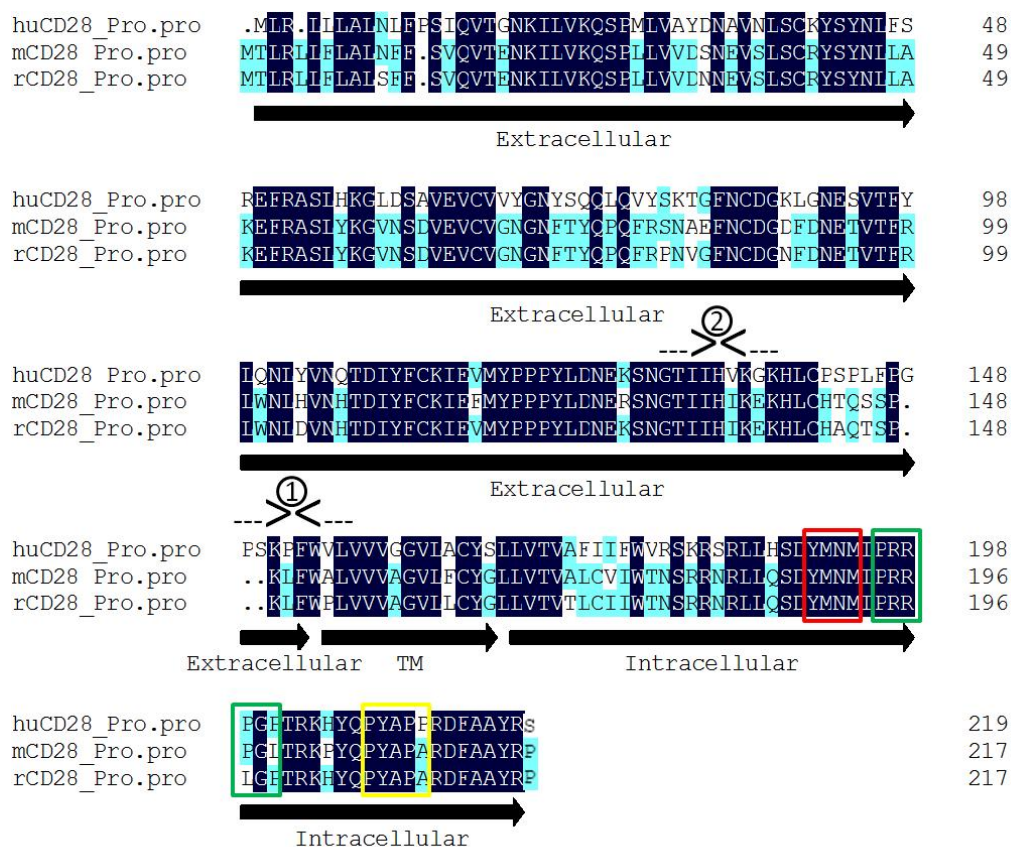


**Figure 4-1 Amino acid sequence alignment of human, mouse and rat CD28 and crucial cytoplasmic tails for signal transduction.** The black shadow represent identical, the blue shadow represent partially identical amino acid residues. Black arrows indicate the extracellular, transmembrane (TM) and intracellular regions of CD28. The blue line depicts the 40-residue signal tails of CD28 containing the Tyr-Met-Asn-Met (YMNMM) motif (red box) and two proline-rich regions (green and yellow boxes). The site “①” represents the boundary of chimeric constructs of r/m CD28 and the first hu/mCD28; the site “②” represents the boundary of new hu/mCD28 construct.

was demonstrated by the capacity to “present” phosphoantigens and aminobisphosphonates to V $\gamma$ 9V $\delta$ 2 TCR expressing BW58r/mCD28 cells (Figure 3-3). The successful presentation was measured as response of V $\gamma$ 9V $\delta$ 2 TCR expressing BW58r/mCD28 cells, and was found irrespective whether the Jurkat transductants expressed rat CD80 or human CD80 (Figure 3-3). These results provide a direct functional evidence of a cross-reaction between rat CD28 and human CD80. To evaluate the second hypothesis, we generated new chimeric molecules. We aligned the whole

## DISCUSSION

amino acid sequences of human CD28 and mouse CD28 (Figure 4-1) and chimeric molecules were expressed containing the extracellular region of human CD28 (amino acid residues 1-154) and intracellular and transmembrane regions of mouse CD28 (amino acid residues 153-218). However V $\gamma$ 9V $\delta$ 2 TCR expressing BW58 cells transduced with such chimera, respond but only very poorly to BrHPP or zoledronate whatever cells were used as presenters (RAJI, Jurkat/rCD80 or Jurkat/huCD80; data not shown). The same was true for another construct which contained aa1-125 residues of huCD28 and aa127-218 residues of mCD28. Based on this result, one may hypothesize that the extracellular region of CD28 may not only serve as CD80/86 binding module of the CD28 molecule but may also interact with additional species specific compounds on the cell surface which may be essential for its proper function. Another possibility is that the signal strength generated by the interaction of humanCD28 and CD80 is weaker than by the interaction of rat CD28 and CD80 or that the chimeric proteins may fail to form a stable and functional CD28 homo-dimer. To define the crucial extracellular factors which determine IL-2 signal transduction or signal strength, more chimeric human/mouse CD28 constructs are required as well as detailed studies on their signaling and CD80/86 binding properties.

As we will discuss later, the fact that BW58r/mCD28 cells after transduction of the V $\gamma$ 9V $\delta$ 2 TCR acquire the capacity to produce IL-2 in response to BrHPP or RAJI cells treated with aminobisphosphonate alone is not sufficient to prove that a recognition of phosphoantigens or aminobisphosphonates by the transduced TCR has been taken place. A support that such a cognate antigen recognition has taken place comes from the analysis of the TCR mutants (Figure 3-6). These mutants have been generated based on the proposed putative phosphoantigens binding sites in TCR- $\delta$  chain (67, 119) and lost their reactivity for phosphoantigens and aminobisphosphonates but not for stimulation by anti-CD3 or anti- $\gamma\delta$  TCR antibodies. This finding strongly suggests that these cells, or the phosphoantigens presented by them, are recognized as cognate antigens by the TCR.

Species-specific cell-cell contact has been well documented as an essential requirement for V $\gamma$ 9V $\delta$ 2 T cell activation by phosphoantigens. However, the interacting mechanisms

## DISCUSSION

are poorly understood. This species-specificity could relate to the antigen presentation and/or the co-stimulatory signal. It is of especial interests to know whether this species-specific reaction is dependent on V $\gamma$ 9V $\delta$ 2 TCR. Previous experiments with primary  $\gamma\delta$  T cells or TCR transduced Jurkat cells could not provide the answer since the responder cells themselves had antigen presenting capacity. This problem seems not to occur with the transduced BW58 cells, since only (CD80 transduced) human cells but not CD80 transduced BW58 cells or any other kind of CD80 transduced or CD80 positive cell of rat, mouse, cow or dog origin presented phosphoantigens (Figure 3-4 and data not shown). The lacking response of the V $\gamma$ 9V $\delta$ 2 TCR transduced BW58r/mCD28 cells to phosphoantigens plus various non-human presenting cells and cell lines is not due to a general deficit in interaction with these cells. This was shown by testing BW58r/mCD28 derived reporter cell lines, expressing mouse iNKT TCR transductants (121) or a MBP specific  $\alpha\beta$  TCR (118) which responded to the TCR ligands such as  $\alpha$ -GalCer, MBP or superantigens irrespective of the species origin of the presenting cell as long as the suitable antigen-presenting molecule and a CD28 ligand has been provided. Therefore we propose that the species-specificity of the antigen recognition by the V $\gamma$ 9V $\delta$ 2 T cells is at least in part a consequence of a species-specific interaction of the TCR with a hypothetical antigen-presenting molecule, and that this response may be abrogated either by a lack of such a molecule in the tested non-human cells (mouse, rat, dog and cow) or a species-specificity in the TCR-interaction with this molecule.

The BW58 reporter cell lines are also helpful to test for possible unknown factors contributing to the specific activation of V $\gamma$ 9V $\delta$ 2 T cells. We compared the response of TCR transduced BW58 cells and enriched short-term  $\gamma\delta$  T cells to phosphoantigens and aminobisphosphonates, respectively (Figure 3-7). In the case of phosphoantigens, TCR transductants showed around 1, 000 times lower sensitivity than primary  $\gamma\delta$  T cell lines while the response to aminobisphosphonates was at maximum 10 fold less sensitive. Sofar this difference is not understood. It could either indicate that V $\gamma$ 9V $\delta$ 2 TCR transductants lack peculiar compounds required for the response to exogenous phosphoantigen which are not required for the recognition of and/or activation by, respectively, endogenously produced phosphoantigens. Alternatively, treatment with

## DISCUSSION

aminobisphosphonate may induce cofactors which specifically act on the TCR transductants. Another, mutually non-exclusive possibility is that at a certain concentration of aminobisphosphonate or FPPS knockdown the overall reduction in FPPS activity may lead to a massive accumulation of intracellular IPP (or related substances), which binds intracellularly to a substantial proportion of the presumed phosphoantigen presenting molecules, which may be sufficient to activate primary as well as TCR transduced BWr/mCD28 cells.

More difficult to explain is the differential activation of TCR transductants and primary V $\gamma$ 9V $\delta$ 2 T cells by Daudi cells. Theoretically, one could imagine that in general Daudi cells could present phosphoantigens not as efficiently as RAJI cells, and therefore the endogenous phosphoantigens of the Daudi cells may fail to activate the TCR transductants. This possibility seems unlikely, since in experiments not shown in the section of results, Daudi cells presented BrHPP as well as aminobisphosphonates at least as well RAJI cells. Therefore it is more likely that the activation signal provided by the presumed endogenous phosphoantigens of the Daudi cells is just lower than the basic threshold needed for activation of BW58 reporter cell lines.

In this context it is of interest that to our knowledge a response has been reported of V $\gamma$ 9V $\delta$ 2 TCR transduced Jurkat cells to Daudi cells only in the original description of the V $\gamma$ 9V $\delta$ 2 TCR transduct but never since then (66). Therefore, although very provocative, it may be considered that V $\gamma$ 9V $\delta$ 2 T cell response to Daudi cells does not result from an antigen-specific recognition by the TCR but by activation via another molecule which is preferentially expressed on V $\gamma$ 9V $\delta$ 2 T cells and which is ligated by a molecule expressed on Daudi cell.

In any case, new experimental approaches are needed to identify the exact factors leading to these pronounced differences in the response of V $\gamma$ 9V $\delta$ 2 TCR transduced BW58 cells to FPPS knock downs or aminobisphosphonates on the one hand and to soluble phosphoantigens or Daudi cells on the other hand. Some hints may come from experiments with V $\gamma$ 9V $\delta$ 2 TCR transduced mouse or rat T cell hybridomas or primary



## DISCUSSION

$\alpha\beta$  or  $\gamma\delta$  T cells, provided that the transduced TCR are expressed as functional cell surface receptors. Similarly, the analysis of  $V\gamma9V\delta2$  TCR transduced primary human  $\alpha\beta$  T cells could also be helpful to elucidate whether these presumed additional factors are species specific. For both types of experiments, the newly generated 2A peptide linked  $V\gamma9V\delta2$  TCR constructs will be advantageous since it permits successful gene transduction for both TCR proteins in a single experiment. In case that TCR transduction renders cells to become responsive to Daudi cells, it will be interesting to test the TCR mutants, in order to gain further insights whether there is cognate antigen recognition by the TCR or whether expression of  $V\gamma9V\delta2$  TCR is just a prerequisite for the function of other Daudi specific molecules. An example for such TCR dependent activation, which does not result from cognate antigen recognition, is the activation of r/m CD28 transduced BW58 cells by superagonist MoAb for which expression of a transduced  $\alpha\beta$  TCR is mandatory (109).

Nevertheless, despite the above discussed differences in the antigen response of the  $V\gamma9V\delta2$  TCR transduced BW58 cells and primary  $V\gamma9V\delta2$  T cells, the  $V\gamma9V\delta2$  TCR transduced BW58r/mCD28 cells provide a valuable and robust tool to study the molecular and cellular basis of  $V\gamma9V\delta2$  TCR mediated cell activation and for a direct comparison with activation by  $\alpha\beta$  TCR, namely by MHC class II presented peptide antigens (118) and CD1d presented glycopeptides (121).

### **4.2 Reduced expression of the farnesylpyrophosphate synthase unveils recognition of tumor cells by $V\gamma9V\delta2$ T cells**

The second part of this thesis demonstrated that shRNA mediated inhibition of FPPS expression is sufficient to induce a  $V\gamma9V\delta2$  T cell stimulatory activity in otherwise non-stimulatory tumor cells. The data provide independent support of the concept that increased intracellular IPP levels are instrumental in  $V\gamma9V\delta2$  T cell activation by tumor lines, which so far is based on the detection of rather high IPP levels in  $V\gamma9V\delta2$  T cell activating tumors as well as by observations with enzyme inhibitors, such as HMG-CoA reductase inhibitors (e.g. mevastatin) and FPPS inhibitors (e.g. aminobisphosphonates) (53).

## DISCUSSION

However, both pharmacological inhibitors provide only indirect evidence that phosphorylated metabolites generated in the mevalonate pathway are the stimulatory antigens of tumor cells. As the mevalonate pathway is fundamental for cell survival and growth of all eukaryotic cells, inhibition of this pathway might interfere with function and growth of lymphocytes themselves, including the targeted V $\gamma$ 9V $\delta$ 2 T cells (123). Increased IPP levels have also been claimed as reason for the formation of toxic ATP-analogs (ApppI) after aminobisphosphonate treatment (124). It will be interesting to learn whether similar observations on IPP and ApppI levels will be made with the FPPS knock down cells. Especially, since in contrast to aminobisphosphonates, which exert also effects on tumor cell growth and survival, there were no overt differences in this respect between FPPS and control-knockdowns at least not under culture conditions used (high glucose and glutamine, saturating oxygen) (Li, Herrmann, Kunzmann; unpublished data). Noteworthy is also that different to aminobisphosphonates, which bind and inhibit not only FPPS but also GGPPS (45), the shRNA constructs used in this paper showed no effect on GGPPS expression, indicating: 1) that reduced FPPS alone is sufficient for generation or accumulation, respectively, of V $\gamma$ 9V $\delta$ 2 T cell ligands 2) that shRNA knock-downs of the different enzymes of isoprenoidsynthesis may provide feasible tools in further dissecting their role in cellular functions.

In any case, the V $\gamma$ 9V $\delta$ 2 T cell activation by the FPPS knock-down cells, strongly supports the current hypothesis that intracellular accumulation of phosphorylated mevalonate metabolites (such as IPP) allows identification of stressed (e.g. infected) (53) or transformed cells (125) and show that reduced FPPS activity is a key mechanism in stimulation of V $\gamma$ 9V $\delta$ 2 T cells by tumor cells. Indeed, it is tempting to speculate that V $\gamma$ 9V $\delta$ 2 T cell mediated immuno-surveillance may continuously act on tumors with aberrant isoprenoid metabolism, and thereby contribute to the rather small number of human tumors exerting V $\gamma$ 9V $\delta$ 2 T cell activating properties found so far.

However, the exact mode of recognition of tumor cells and IPP, respectively, by V $\gamma$ 9V $\delta$ 2 T cells remains still unclear. Besides overproduction of phosphorylated metabolites

## DISCUSSION

generated from the mevalonate pathway recognition of tumor cells by V $\gamma$ 9V $\delta$ 2 T cells requires not only the expression of the V $\gamma$ 9V $\delta$ 2 TCR, as indicated by antibody blocking and gene transfer approaches (66) but probably also species-specific interactions of adhesion - (i.e. LFA-1/ICAM-1) and co-stimulatory signals (64) or even a species-specific V $\gamma$ 9V $\delta$ 2 T cell antigen presenting molecule (126).

In addition to B lymphomas, we had performed a more extensive analysis of FPPS knockdown in other hematological and solid tumor cell lines. Almost all the investigated tumor cells were callable of directly activating V $\gamma$ 9V $\delta$ 2 T cells to different extents after FPPS knockdown.

In conclusion, our present strategy demonstrates a “proof of concept” that mevalonate pathway dysregulation in tumor cells is sufficient to activate immune-surveillance by V $\gamma$ 9V $\delta$ 2 T cells and may provide a strategic platform to develop novel compounds for immunotherapy of human malignancies.

### 4.3 Work in progress and outlook

How far other molecules such as the ectopically expressed F1-ATPase (80), which has been claimed to serve as the V $\gamma$ 9V $\delta$ 2 TCR ligand expressed by Daudi tumor cells, are involved in IPP recognition remains unclear, but we observed neither after treatment with aminobisphosphonates nor in FPPS knock-down cells an increased binding of  $\beta$ -chain F1-ATPase specific monoclonal antibodies (Figure 3-17). We are also trying to find the associations between another most recently reported V $\gamma$ 9V $\delta$ 2 TCR ligand ULBP4 (81) and IPP recognition.

It has been reported that inhibition of mevalonate pathway caused cell apoptosis through loss or decrease of prenylated small signaling proteins (Rho, Ras) (38, 39) or the accumulation of a cytotoxic ATP analog, APPPi (40, 41). We also predict that FPPS knockdown would affect the normal tumor cells growth. Unexpectedly, however, our observation does not support this perspective (Figure 3-18). In our subsequent work, Martina Roilo found even better growth of RAJI/AS22 than RAJI/AS (120). The reason

## DISCUSSION

remains to be investigated. A possible explanation is that knockdown cells got used to the long phase low level metabolism of mevalonate pathway. The new generated inducible and reversible knockdown system would be a promising tool to solve this problem.

Besides FPPS, several other enzymes may also play important role in regulation of IPP production. Therefore regulating their expression in tumor cells may also changes the activating capacity to V $\gamma$ 9V $\delta$ 2 T cells but as shown in Figure 3-26 and Figure 3-27, neither the upregulation nor the inhibition of expression of those enzymes has obvious effects on V $\gamma$ 9V $\delta$ 2 T cells activation. Particularly, over-expression of FPPS in tumor cells seems not to affect on activation of V $\gamma$ 9V $\delta$ 2 T cells too. The exact reason that inhibiting expression of FPPS plays a more crucial role than other enzymes in V $\gamma$ 9V $\delta$ 2 T cells activation is still unclear.

Here our work developed two promising tools for the study of V $\gamma$ 9V $\delta$ 2 T cells activation and phosphoantigen recognition: 1) the V $\gamma$ 9V $\delta$ 2 TCR transduced mouse reporter cell line, a robust responsive effector; 2) FPPS knockdown cell lines, the stable direct activators of V $\gamma$ 9V $\delta$ 2 T cells. Additionally, very recently, some other new tools have been generated (60, 61). Altogether, these tools open the door wide on promising perspective to finally lift the mysterious veil of V $\gamma$ 9V $\delta$ 2 T cells activation and phosphoantigen recognition.

## REFERENCE

1. Hayday, A. C. 2000.  $\gamma\delta$  cells: a right time and a right place for a conserved third way of protection. *Annu Rev Immunol* 18:975-1026.
2. Adams, E. J., Y. H. Chien, and K. C. Garcia. 2005. Structure of a gammadelta T cell receptor in complex with the nonclassical MHC T22. *Science* 308:227-231.
3. Groh, V., A. Steinle, S. Bauer, and T. Spies. 1998. Recognition of stress-induced MHC molecules by intestinal epithelial gammadelta T cells. *Science* 279:1737-1740.
4. Poggi, A., C. Venturino, S. Catellani, M. Clavio, M. Miglino, M. Gobbi, A. Steinle, P. Ghia, S. Stella, F. Caligaris-Cappio, and M. R. Zocchi. 2004. Vdelta1 T lymphocytes from B-CLL patients recognize ULBP3 expressed on leukemic B cells and up-regulated by trans-retinoic acid. *Cancer Res* 64:9172-9179.
5. Collins, M. K., P. N. Goodfellow, M. J. Dunne, N. K. Spurr, E. Solomon, and M. J. Owen. 1984. A human T-cell antigen receptor beta chain gene maps to chromosome 7. *Embo J* 3:2347-2349.
6. Chien, Y. H., M. Iwashima, K. B. Kaplan, J. F. Elliott, and M. M. Davis. 1987. A new T-cell receptor gene located within the alpha locus and expressed early in T-cell differentiation. *Nature* 327:677-682.
7. Hata, S., M. B. Brenner, and M. S. Krangel. 1987. Identification of putative human T cell receptor delta complementary DNA clones. *Science* 238:678-682.
8. Takihara, Y., J. Reimann, E. Michalopoulos, E. Ciccone, L. Moretta, and T. W. Mak. 1989. Diversity and structure of human T cell receptor delta chain genes in peripheral blood gamma/delta-bearing T lymphocytes. *J Exp Med* 169:393-405.
9. Guglielmi, P., F. Davi, L. d'Auriol, J. C. Bories, J. Dausset, and A. Bensussan. 1988. Use of a variable alpha region to create a functional T-cell receptor delta chain. *Proc Natl Acad Sci U S A* 85:5634-5638.
10. Arden, B., S. P. Clark, D. Kabelitz, and T. W. Mak. 1995. Human T-cell receptor variable gene segment families. *Immunogenetics* 42:455-500.
11. Migone, N., S. Padovan, C. Zappador, C. Giachino, M. Bottaro, G. Matullo, C. Carbonara, G. D. Libero, and G. Casorati. 1995. Restriction of the T-cell receptor V delta gene repertoire is due to preferential rearrangement and is independent of antigen selection. *Immunogenetics* 42:323-332.
12. Murre, C., R. A. Waldmann, C. C. Morton, K. F. Bongiovanni, T. A. Waldmann, T. B. Shows, and J. G. Seidman. 1985. Human gamma-chain genes are rearranged in leukaemic T cells and map to the short arm of chromosome 7. *Nature* 316:549-552.

## REFERENCE

13. Lefranc, M. P., and T. H. Rabbitts. 1990. A nomenclature to fit the organization of the human T-cell receptor gamma and delta genes. *Res Immunol* 141:615-618.
14. Davis, M. M., and P. J. Bjorkman. 1988. T-cell antigen receptor genes and T-cell recognition. *Nature* 334:395-402.
15. Hata, S., K. Satyanarayana, P. Devlin, H. Band, J. McLean, J. L. Strominger, M. B. Brenner, and M. S. Krangel. 1988. Extensive junctional diversity of rearranged human T cell receptor delta genes. *Science* 240:1541-1544.
16. Dik, W. A., K. Pike-Overzet, F. Weerkamp, D. de Ridder, E. F. de Haas, M. R. Baert, P. van der Spek, E. E. Koster, M. J. Reinders, J. J. van Dongen, A. W. Langerak, and F. J. Staal. 2005. New insights on human T cell development by quantitative T cell receptor gene rearrangement studies and gene expression profiling. *J Exp Med* 201:1715-1723.
17. Goodman, T., and L. Lefrancois. 1988. Expression of the gamma-delta T-cell receptor on intestinal CD8+ intraepithelial lymphocytes. *Nature* 333:855-858.
18. Jameson, J., and W. L. Havran. 2007. Skin gammadelta T-cell functions in homeostasis and wound healing. *Immunol Rev* 215:114-122.
19. Legrand, F., V. Driss, G. Woerly, S. Loiseau, E. Hermann, J. J. Fournie, L. Heliot, V. Mattot, F. Soncin, M. L. Gougeon, D. Dombrowicz, and M. Capron. 2009. A functional gammadeltaTCR/CD3 complex distinct from gammadeltaT cells is expressed by human eosinophils. *PLoS One* 4:e5926.
20. Kuhnlein, P., J. H. Park, T. Herrmann, A. Elbe, and T. Hunig. 1994. Identification and characterization of rat gamma/delta T lymphocytes in peripheral lymphoid organs, small intestine, and skin with a monoclonal antibody to a constant determinant of the gamma/delta T cell receptor. *J Immunol* 153:979-986.
21. Straube, F., and T. Herrmann. 2001. Differential modulation of CD8beta by rat gammadelta and alphabeta T cells after activation. *Immunology* 104:252-258.
22. Straube, F., and T. Herrmann. 2000. Expression of functional CD8alpha Beta heterodimer on rat gamma delta T cells does not correlate with the CDR3 length of the TCR delta chain predicted for MHC class I-restricted antigen recognition. *Eur J Immunol* 30:3562-3568.
23. Wilson, E., M. K. Aydintug, and M. A. Jutila. 1999. A circulating bovine gamma delta T cell subset, which is found in large numbers in the spleen, accumulates inefficiently in an artificial site of inflammation: correlation with lack of expression of E-selectin ligands and L-selectin. *J Immunol* 162:4914-4919.
24. Berndt, A., J. Pieper, and U. Methner. 2006. Circulating gamma delta T cells in response to *Salmonella enterica* serovar enteritidis exposure in chickens. *Infect Immun* 74:3967-3978.
25. Urban, E. M., H. Li, C. Armstrong, C. Focaccetti, C. Cairo, and C. D. Pauza. 2009. Control of CD56 expression and tumor cell cytotoxicity in human Vgamma2Vdelta2 T cells. *BMC Immunol* 10:50.
26. Ribot, J. C., A. deBarros, D. J. Pang, J. F. Neves, V. Peperzak, S. J. Roberts, M. Girardi, J. Borst, A. C. Hayday, D. J. Pennington, and B. Silva-Santos. 2009. CD27 is a thymic determinant of the balance between interferon-gamma- and interleukin 17-producing gammadelta T cell subsets. *Nat Immunol* 10:427-436.
27. Pfeffer, K., B. Schoel, H. Gulle, S. H. Kaufmann, and H. Wagner. 1990. Primary

## REFERENCE

- responses of human T cells to mycobacteria: a frequent set of gamma/delta T cells are stimulated by protease-resistant ligands. *Eur J Immunol* 20:1175-1179.
28. Tanaka, Y., S. Sano, E. Nieves, G. De Libero, D. Rosa, R. L. Modlin, M. B. Brenner, B. R. Bloom, and C. T. Morita. 1994. Nonpeptide ligands for human gamma delta T cells. *Proc Natl Acad Sci U S A* 91:8175-8179.
  29. Tanaka, Y., C. T. Morita, Y. Tanaka, E. Nieves, M. B. Brenner, and B. R. Bloom. 1995. Natural and synthetic non-peptide antigens recognized by human gamma delta T cells. *Nature* 375:155-158.
  30. Rohmer, M. 1999. The discovery of a mevalonate-independent pathway for isoprenoid biosynthesis in bacteria, algae and higher plants. *Nat Prod Rep* 16:565-574.
  31. Hintz, M., A. Reichenberg, B. Altincicek, U. Bahr, R. M. Gschwind, A. K. Kollas, E. Beck, J. Wiesner, M. Eberl, and H. Jomaa. 2001. Identification of (E)-4-hydroxy-3-methyl-but-2-enyl pyrophosphate as a major activator for human gammadelta T cells in *Escherichia coli*. *FEBS Lett* 509:317-322.
  32. Eberl, M., B. Altincicek, A. K. Kollas, S. Sanderbrand, U. Bahr, A. Reichenberg, E. Beck, D. Foster, J. Wiesner, M. Hintz, and H. Jomaa. 2002. Accumulation of a potent gammadelta T-cell stimulator after deletion of the *lytB* gene in *Escherichia coli*. *Immunology* 106:200-211.
  33. Espinosa, E., C. Belmant, F. Pont, B. Luciani, R. Poupot, F. Romagne, H. Brailly, M. Bonneville, and J. J. Fournie. 2001. Chemical synthesis and biological activity of bromohydrin pyrophosphate, a potent stimulator of human gamma delta T cells. *J Biol Chem* 276:18337-18344.
  34. Morita, C. T., C. Jin, G. Sarikonda, and H. Wang. 2007. Nonpeptide antigens, presentation mechanisms, and immunological memory of human Vgamma2Vdelta2 T cells: discriminating friend from foe through the recognition of prenyl pyrophosphate antigens. *Immunol Rev* 215:59-76.
  35. Sacchettini, J. C., and C. D. Poulter. 1997. Creating isoprenoid diversity. *Science* 277:1788-1789.
  36. Buhaescu, I., and H. Izzedine. 2007. Mevalonate pathway: a review of clinical and therapeutical implications. *Clin Biochem* 40:575-584.
  37. Morita, C. T., R. A. Mariuzza, and M. B. Brenner. 2000. Antigen recognition by human gamma delta T cells: pattern recognition by the adaptive immune system. *Springer Semin Immunopathol* 22:191-217.
  38. Benford, H. L., J. C. Frith, S. Auriola, J. Monkkonen, and M. J. Rogers. 1999. Farnesol and geranylgeraniol prevent activation of caspases by aminobisphosphonates: biochemical evidence for two distinct pharmacological classes of bisphosphonate drugs. *Mol Pharmacol* 56:131-140.
  39. Luckman, S. P., D. E. Hughes, F. P. Coxon, R. Graham, G. Russell, and M. J. Rogers. 1998. Nitrogen-containing bisphosphonates inhibit the mevalonate pathway and prevent post-translational prenylation of GTP-binding proteins, including Ras. *J Bone Miner Res* 13:581-589.
  40. Monkkonen, H., S. Auriola, P. Lehenkari, M. Kellinsalmi, I. E. Hassinen, J. Vepsalainen, and J. Monkkonen. 2006. A new endogenous ATP analog (ApppI) inhibits the mitochondrial adenine nucleotide translocase (ANT) and is responsible for the apoptosis induced by nitrogen-containing bisphosphonates. *Br*

## REFERENCE

- J Pharmacol* 147:437-445.
41. Mitrofan, L. M., J. Pelkonen, and J. Monkkonen. 2009. The level of ATP analog and isopentenyl pyrophosphate correlates with zoledronic acid-induced apoptosis in cancer cells in vitro. *Bone*.
  42. Thompson, K., J. Rojas-Navea, and M. J. Rogers. 2006. Alkylamines cause Vgamma9Vdelta2 T-cell activation and proliferation by inhibiting the mevalonate pathway. *Blood* 107:651-654.
  43. Kunzmann, V., E. Bauer, and M. Wilhelm. 1999. Gamma/delta T-cell stimulation by pamidronate. *N Engl J Med* 340:737-738.
  44. Russell, R. G. 2006. Bisphosphonates: from bench to bedside. *Ann N Y Acad Sci* 1068:367-401.
  45. Guo, R. T., R. Cao, P. H. Liang, T. P. Ko, T. H. Chang, M. P. Hudock, W. Y. Jeng, C. K. Chen, Y. Zhang, Y. Song, C. J. Kuo, F. Yin, E. Oldfield, and A. H. Wang. 2007. Bisphosphonates target multiple sites in both cis- and trans-prenyltransferases. *Proc Natl Acad Sci U S A* 104:10022-10027.
  46. Dunford, J. E., K. Thompson, F. P. Coxon, S. P. Luckman, F. M. Hahn, C. D. Poulter, F. H. Ebetino, and M. J. Rogers. 2001. Structure-activity relationships for inhibition of farnesyl diphosphate synthase in vitro and inhibition of bone resorption in vivo by nitrogen-containing bisphosphonates. *J Pharmacol Exp Ther* 296:235-242.
  47. Zhang, Y., R. Cao, F. Yin, M. P. Hudock, R. T. Guo, K. Krysiak, S. Mukherjee, Y. G. Gao, H. Robinson, Y. Song, J. H. No, K. Bergan, A. Leon, L. Cass, A. Goddard, T. K. Chang, F. Y. Lin, E. Van Beek, S. Papapoulos, A. H. Wang, T. Kubo, M. Ochi, D. Mukkamala, and E. Oldfield. 2009. Lipophilic bisphosphonates as dual farnesyl/geranylgeranyl diphosphate synthase inhibitors: an X-ray and NMR investigation. *J Am Chem Soc* 131:5153-5162.
  48. Wilhelm, M., V. Kunzmann, S. Eckstein, P. Reimer, F. Weissinger, T. Ruediger, and H. P. Tony. 2003. Gammadelta T cells for immune therapy of patients with lymphoid malignancies. *Blood* 102:200-206.
  49. Kunzmann, V., E. Bauer, J. Feurle, F. Weissinger, H. P. Tony, and M. Wilhelm. 2000. Stimulation of gammadelta T cells by aminobisphosphonates and induction of antiplasma cell activity in multiple myeloma. *Blood* 96:384-392.
  50. Kavanagh, K. L., K. Guo, J. E. Dunford, X. Wu, S. Knapp, F. H. Ebetino, M. J. Rogers, R. G. Russell, and U. Oppermann. 2006. The molecular mechanism of nitrogen-containing bisphosphonates as antiosteoporosis drugs. *Proc Natl Acad Sci U S A* 103:7829-7834.
  51. Rondeau, J. M., F. Bitsch, E. Bourgier, M. Geiser, R. Hemmig, M. Kroemer, S. Lehmann, P. Ramage, S. Rieffel, A. Strauss, J. R. Green, and W. Jahnke. 2006. Structural basis for the exceptional in vivo efficacy of bisphosphonate drugs. *ChemMedChem* 1:267-273.
  52. Hosfield, D. J., Y. Zhang, D. R. Dougan, A. Broun, L. W. Tari, R. V. Swanson, and J. Finn. 2004. Structural basis for bisphosphonate-mediated inhibition of isoprenoid biosynthesis. *J Biol Chem* 279:8526-8529.
  53. Gober, H. J., M. Kistowska, L. Angman, P. Jenö, L. Mori, and G. De Libero. 2003. Human T cell receptor gammadelta cells recognize endogenous mevalonate metabolites in tumor cells. *J Exp Med* 197:163-168.



## REFERENCE

54. Thompson, K., and M. J. Rogers. 2004. Statins prevent bisphosphonate-induced gamma,delta-T-cell proliferation and activation in vitro. *J Bone Miner Res* 19:278-288.
55. Das, H., L. Wang, A. Kamath, and J. F. Bukowski. 2001. Vgamma2Vdelta2 T-cell receptor-mediated recognition of aminobisphosphonates. *Blood* 98:1616-1618.
56. Bukowski, J. F., C. T. Morita, and M. B. Brenner. 1999. Human gamma delta T cells recognize alkylamines derived from microbes, edible plants, and tea: implications for innate immunity. *Immunity* 11:57-65.
57. Kamath, A. B., L. Wang, H. Das, L. Li, V. N. Reinhold, and J. F. Bukowski. 2003. Antigens in tea-beverage prime human Vgamma 2Vdelta 2 T cells in vitro and in vivo for memory and nonmemory antibacterial cytokine responses. *Proc Natl Acad Sci U S A* 100:6009-6014.
58. Morita, C. T., E. M. Beckman, J. F. Bukowski, Y. Tanaka, H. Band, B. R. Bloom, D. E. Golan, and M. B. Brenner. 1995. Direct presentation of nonpeptide prenyl pyrophosphate antigens to human gamma delta T cells. *Immunity* 3:495-507.
59. Lang, F., M. A. Peyrat, P. Constant, F. Davodeau, J. David-Ameline, Y. Poquet, H. Vie, J. J. Fournie, and M. Bonneville. 1995. Early activation of human V gamma 9V delta 2 T cell broad cytotoxicity and TNF production by nonpeptidic mycobacterial ligands. *J Immunol* 154:5986-5994.
60. Sarikonda, G., H. Wang, K. J. Puan, X. H. Liu, H. K. Lee, Y. Song, M. D. Distefano, E. Oldfield, G. D. Prestwich, and C. T. Morita. 2008. Photoaffinity antigens for human gammadelta T cells. *J Immunol* 181:7738-7750.
61. Wei, H., D. Huang, X. Lai, M. Chen, W. Zhong, R. Wang, and Z. W. Chen. 2008. Definition of APC presentation of phosphoantigen (E)-4-hydroxy-3-methyl-but-2-enyl pyrophosphate to Vgamma2Vdelta 2 TCR. *J Immunol* 181:4798-4806.
62. Das, H., V. Groh, C. Kuijl, M. Sugita, C. T. Morita, T. Spies, and J. F. Bukowski. 2001. MICA engagement by human Vgamma2Vdelta2 T cells enhances their antigen-dependent effector function. *Immunity* 15:83-93.
63. Rincon-Orozco, B., V. Kunzmann, P. Wrobel, D. Kabelitz, A. Steinle, and T. Herrmann. 2005. Activation of V gamma 9V delta 2 T cells by NKG2D. *J Immunol* 175:2144-2151.
64. Kato, Y., Y. Tanaka, H. Tanaka, S. Yamashita, and N. Minato. 2003. Requirement of species-specific interactions for the activation of human gamma delta T cells by pamidronate. *J Immunol* 170:3608-3613.
65. Kato, Y., Y. Tanaka, M. Hayashi, K. Okawa, and N. Minato. 2006. Involvement of CD166 in the activation of human gamma delta T cells by tumor cells sensitized with nonpeptide antigens. *J Immunol* 177:877-884.
66. Bukowski, J. F., C. T. Morita, Y. Tanaka, B. R. Bloom, M. B. Brenner, and H. Band. 1995. V gamma 2V delta 2 TCR-dependent recognition of non-peptide antigens and Daudi cells analyzed by TCR gene transfer. *J Immunol* 154:998-1006.
67. Yamashita, S., Y. Tanaka, M. Harazaki, B. Mikami, and N. Minato. 2003. Recognition mechanism of non-peptide antigens by human gammadelta T cells. *Int Immunol* 15:1301-1307.
68. Kroca, M., A. Tarnvik, and A. Sjostedt. 2000. The proportion of circulating

## REFERENCE

- gammadelta T cells increases after the first week of onset of tularaemia and remains elevated for more than a year. *Clin Exp Immunol* 120:280-284.
69. Morita, C. T., S. Verma, P. Aparicio, C. Martinez, H. Spits, and M. B. Brenner. 1991. Functionally distinct subsets of human gamma/delta T cells. *Eur J Immunol* 21:2999-3007.
  70. Garcia, V. E., P. A. Sieling, J. Gong, P. F. Barnes, K. Uyemura, Y. Tanaka, B. R. Bloom, C. T. Morita, and R. L. Modlin. 1997. Single-cell cytokine analysis of gamma delta T cell responses to nonpeptide mycobacterial antigens. *J Immunol* 159:1328-1335.
  71. Cipriani, B., G. Borsellino, F. Poccia, R. Placido, D. Tramonti, S. Bach, L. Battistini, and C. F. Brosnan. 2000. Activation of C-C beta-chemokines in human peripheral blood gammadelta T cells by isopentenyl pyrophosphate and regulation by cytokines. *Blood* 95:39-47.
  72. Hara, T., Y. Mizuno, K. Takaki, H. Takada, H. Akeda, T. Aoki, M. Nagata, K. Ueda, G. Matsuzaki, Y. Yoshikai, and et al. 1992. Predominant activation and expansion of V gamma 9-bearing gamma delta T cells in vivo as well as in vitro in Salmonella infection. *J Clin Invest* 90:204-210.
  73. Ottonnes, F., J. Dornand, A. Naroeni, J. P. Liautard, and J. Favero. 2000. V gamma 9V delta 2 T cells impair intracellular multiplication of *Brucella suis* in autologous monocytes through soluble factor release and contact-dependent cytotoxic effect. *J Immunol* 165:7133-7139.
  74. Dieli, F., M. Troye-Blomberg, J. Ivanyi, J. J. Fournie, A. M. Krensky, M. Bonneville, M. A. Peyrat, N. Caccamo, G. Sireci, and A. Salerno. 2001. Granulysin-dependent killing of intracellular and extracellular *Mycobacterium tuberculosis* by Vgamma9/Vdelta2 T lymphocytes. *J Infect Dis* 184:1082-1085.
  75. Wang, L., A. Kamath, H. Das, L. Li, and J. F. Bukowski. 2001. Antibacterial effect of human V gamma 2V delta 2 T cells in vivo. *J Clin Invest* 108:1349-1357.
  76. Shen, Y., D. Zhou, L. Qiu, X. Lai, M. Simon, L. Shen, Z. Kou, Q. Wang, L. Jiang, J. Estep, R. Hunt, M. Clagett, P. K. Sehgal, Y. Li, X. Zeng, C. T. Morita, M. B. Brenner, N. L. Letvin, and Z. W. Chen. 2002. Adaptive immune response of Vgamma2Vdelta2+ T cells during mycobacterial infections. *Science* 295:2255-2258.
  77. Fisch, P., M. Malkovsky, S. Kovats, E. Sturm, E. Braakman, B. S. Klein, S. D. Voss, L. W. Morrissey, R. DeMars, W. J. Welch, and et al. 1990. Recognition by human V gamma 9/V delta 2 T cells of a GroEL homolog on Daudi Burkitt's lymphoma cells. *Science* 250:1269-1273.
  78. Selin, L. K., S. Stewart, C. Shen, H. Q. Mao, and J. A. Wilkins. 1992. Reactivity of gamma delta T cells induced by the tumour cell line RPMI 8226: functional heterogeneity of clonal populations and role of GroEL heat shock proteins. *Scand J Immunol* 36:107-117.
  79. McClanahan, J., P. I. Fukushima, and M. Stetler-Stevenson. 1999. Increased peripheral blood gamma delta T-cells in patients with lymphoid neoplasia: A diagnostic dilemma in flow cytometry. *Cytometry* 38:280-285.
  80. Scotet, E., L. O. Martinez, E. Grant, R. Barbaras, P. Jenou, M. Guiraud, B. Monsarrat, X. Saulquin, S. Maillet, J. P. Esteve, F. Lopez, B. Perret, X. Collet, M.

## REFERENCE

- Bonneville, and E. Champagne. 2005. Tumor recognition following Vgamma9Vdelta2 T cell receptor interactions with a surface F1-ATPase-related structure and apolipoprotein A-I. *Immunity* 22:71-80.
81. Kong, Y., W. Cao, X. Xi, C. Ma, L. Cui, and W. He. 2009. The NKG2D ligand ULBP4 binds to TCRgamma9/delta2 and induces cytotoxicity to tumor cells through both TCRgammadelta and NKG2D. *Blood* 114:310-317.
  82. Chen, H., X. He, Z. Wang, D. Wu, H. Zhang, C. Xu, H. He, L. Cui, D. Ba, and W. He. 2008. Identification of human T cell receptor gammadelta-recognized epitopes/proteins via CDR3delta peptide-based immunobiochemical strategy. *J Biol Chem* 283:12528-12537.
  83. Brandes, M., K. Willimann, and B. Moser. 2005. Professional antigen-presentation function by human gammadelta T Cells. *Science* 309:264-268.
  84. Brandes, M., K. Willimann, G. Bioley, N. Levy, M. Eberl, M. Luo, R. Tampe, F. Levy, P. Romero, and B. Moser. 2009. Cross-presenting human gammadelta T cells induce robust CD8+ alphabeta T cell responses. *Proc Natl Acad Sci U S A* 106:2307-2312.
  85. Brandes, M., K. Willimann, A. B. Lang, K. H. Nam, C. Jin, M. B. Brenner, C. T. Morita, and B. Moser. 2003. Flexible migration program regulates gamma delta T-cell involvement in humoral immunity. *Blood* 102:3693-3701.
  86. Eberl, M., G. W. Roberts, S. Meuter, J. D. Williams, N. Topley, and B. Moser. 2009. A rapid crosstalk of human gammadelta T cells and monocytes drives the acute inflammation in bacterial infections. *PLoS Pathog* 5:e1000308.
  87. Dieli, F., N. Gebbia, F. Poccia, N. Caccamo, C. Montesano, F. Fulfaro, C. Arcara, M. R. Valerio, S. Meraviglia, C. Di Sano, G. Sireci, and A. Salerno. 2003. Induction of gammadelta T-lymphocyte effector functions by bisphosphonate zoledronic acid in cancer patients in vivo. *Blood* 102:2310-2311.
  88. Dieli, F., D. Vermijlen, F. Fulfaro, N. Caccamo, S. Meraviglia, G. Cicero, A. Roberts, S. Buccheri, M. D'Asaro, N. Gebbia, A. Salerno, M. Eberl, and A. C. Hayday. 2007. Targeting human {gamma}delta T cells with zoledronate and interleukin-2 for immunotherapy of hormone-refractory prostate cancer. *Cancer Res* 67:7450-7457.
  89. J. Bennouna, J. M., F. Rolland, J. L. Misset, M. Campone, H. Sicard, J. Tiollier, F. Romagne, J. Y. Douillard, F. Calvo 2005. Phase I clinical trial of BromoHydrin PyroPhosphate, BrHPP (Phosphostim), a Vg9Vd2 T lymphocytes agonist in combination with low dose Interleukin-2 in patients with solid tumors. In *2005 ASCO Annual Meeting*. Journal of Clinical Oncology.
  90. Kobayashi, H., Y. Tanaka, J. Yagi, Y. Osaka, H. Nakazawa, T. Uchiyama, N. Minato, and H. Toma. 2007. Safety profile and anti-tumor effects of adoptive immunotherapy using gamma-delta T cells against advanced renal cell carcinoma: a pilot study. *Cancer Immunol Immunother* 56:469-476.
  91. Bennouna, J., E. Bompas, E. M. Neidhardt, F. Rolland, I. Philip, C. Galea, S. Salot, S. Saiagh, M. Audrain, M. Rimbart, S. Lafaye-de Micheaux, J. Tiollier, and S. Negrier. 2008. Phase-I study of Innacell gammadelta, an autologous cell-therapy product highly enriched in gamma9delta2 T lymphocytes, in combination with IL-2, in patients with metastatic renal cell carcinoma. *Cancer Immunol Immunother* 57:1599-1609.

## REFERENCE

92. Beck, B. H., H. G. Kim, H. Kim, S. Samuel, Z. Liu, R. Shrestha, H. Haines, K. Zinn, and R. D. Lopez. 2009. Adoptively transferred ex vivo expanded gammadelta-T cells mediate in vivo antitumor activity in preclinical mouse models of breast cancer. *Breast Cancer Res Treat*.
93. Fire, A., S. Xu, M. K. Montgomery, S. A. Kostas, S. E. Driver, and C. C. Mello. 1998. Potent and specific genetic interference by double-stranded RNA in *Caenorhabditis elegans*. *Nature* 391:806-811.
94. Hammond, S. M. 2005. Dicing and slicing: the core machinery of the RNA interference pathway. *FEBS Lett* 579:5822-5829.
95. Hannon, G. J., and J. J. Rossi. 2004. Unlocking the potential of the human genome with RNA interference. *Nature* 431:371-378.
96. Fewell, G. D., and K. Schmitt. 2006. Vector-based RNAi approaches for stable, inducible and genome-wide screens. *Drug Discov Today* 11:975-982.
97. Elbashir, S. M., J. Harborth, W. Lendeckel, A. Yalcin, K. Weber, and T. Tuschl. 2001. Duplexes of 21-nucleotide RNAs mediate RNA interference in cultured mammalian cells. *Nature* 411:494-498.
98. Silva, J. M., M. Z. Li, K. Chang, W. Ge, M. C. Golding, R. J. Rickles, D. Siolas, G. Hu, P. J. Paddison, M. R. Schlabach, N. Sheth, J. Bradshaw, J. Burchard, A. Kulkarni, G. Cavet, R. Sachidanandam, W. R. McCombie, M. A. Cleary, S. J. Elledge, and G. J. Hannon. 2005. Second-generation shRNA libraries covering the mouse and human genomes. *Nat Genet* 37:1281-1288.
99. Cleary, M. A., K. Kilian, Y. Wang, J. Bradshaw, G. Cavet, W. Ge, A. Kulkarni, P. J. Paddison, K. Chang, N. Sheth, E. Leproust, E. M. Coffey, J. Burchard, W. R. McCombie, P. Linsley, and G. J. Hannon. 2004. Production of complex nucleic acid libraries using highly parallel in situ oligonucleotide synthesis. *Nat Methods* 1:241-248.
100. Boden, D., O. Pusch, R. Silbermann, F. Lee, L. Tucker, and B. Ramratnam. 2004. Enhanced gene silencing of HIV-1 specific siRNA using microRNA designed hairpins. *Nucleic Acids Res* 32:1154-1158.
101. Soneoka, Y., P. M. Cannon, E. E. Ramsdale, J. C. Griffiths, G. Romano, S. M. Kingsman, and A. J. Kingsman. 1995. A transient three-plasmid expression system for the production of high titer retroviral vectors. *Nucleic Acids Res* 23:628-633.
102. Cockrell, A. S., and T. Kafri. 2007. Gene delivery by lentivirus vectors. *Mol Biotechnol* 36:184-204.
103. Aagaard, L., M. Amarzguioui, G. Sun, L. C. Santos, A. Ehsani, H. Prydz, and J. J. Rossi. 2007. A facile lentiviral vector system for expression of doxycycline-inducible shRNAs: knockdown of the pre-miRNA processing enzyme Drosha. *Mol Ther* 15:938-945.
104. Shin, K. J., E. A. Wall, J. R. Zavzavadjian, L. A. Santat, J. Liu, J. I. Hwang, R. Rebres, T. Roach, W. Seaman, M. I. Simon, and I. D. Fraser. 2006. A single lentiviral vector platform for microRNA-based conditional RNA interference and coordinated transgene expression. *Proc Natl Acad Sci U S A* 103:13759-13764.
105. Szulc, J., M. Wiznerowicz, M. O. Sauvain, D. Trono, and P. Aebischer. 2006. A versatile tool for conditional gene expression and knockdown. *Nat Methods* 3:109-116.

## REFERENCE

106. Amar, L., M. Desclaux, N. Faucon-Biguët, J. Mallet, and R. Vogel. 2006. Control of small inhibitory RNA levels and RNA interference by doxycycline induced activation of a minimal RNA polymerase III promoter. *Nucleic Acids Res* 34:e37.
107. Herold, M. J., J. van den Brandt, J. Seibler, and H. M. Reichardt. 2008. Inducible and reversible gene silencing by stable integration of an shRNA-encoding lentivirus in transgenic rats. *Proc Natl Acad Sci U S A* 105:18507-18512.
108. Letourneur, F., and B. Malissen. 1989. Derivation of a T cell hybridoma variant deprived of functional T cell receptor alpha and beta chain transcripts reveals a nonfunctional alpha-mRNA of BW5147 origin. *Eur J Immunol* 19:2269-2274.
109. Luhder, F., Y. Huang, K. M. Dennehy, C. Guntermann, I. Müller, E. Winkler, T. Kerkau, S. Ikemizu, S. J. Davis, T. Hanke, and T. Hunig. 2003. Topological requirements and signaling properties of T cell-activating, anti-CD28 antibody superagonists. *J Exp Med* 197:955-966.
110. Nicolas, J. F., D. Wegmann, P. Lebrun, D. Kaiserlian, J. Tovey, and A. L. Glasebrook. 1987. Relationship of B cell Fc receptors to T cell recognition of Mls antigen. *Eur J Immunol* 17:1561-1565.
111. Pietschmann, T., M. Heinkelein, M. Heldmann, H. Zentgraf, A. Rethwilm, and D. Lindemann. 1999. Foamy virus capsids require the cognate envelope protein for particle export. *J Virol* 73:2613-2621.
112. Dull, T., R. Zufferey, M. Kelly, R. J. Mandel, M. Nguyen, D. Trono, and L. Naldini. 1998. A third-generation lentivirus vector with a conditional packaging system. *J Virol* 72:8463-8471.
113. Lindemann, D., M. Bock, M. Schweizer, and A. Rethwilm. 1997. Efficient pseudotyping of murine leukemia virus particles with chimeric human foamy virus envelope proteins. *J Virol* 71:4815-4820.
114. Li, J., M. J. Herold, B. Kimmel, I. Müller, B. Rincon-Orozco, V. Kunzmann, and T. Herrmann. 2009. Reduced expression of the mevalonate pathway enzyme farnesyl pyrophosphate synthase unveils recognition of tumor cells by Vgamma9Vdelta2 T cells. *J Immunol* 182:8118-8124.
115. Kreiss, M. 1998. Gene transfer and functional characteristic of a microbial phospholigands specific reactive gammadelta TCR. *Diploma Thesis*. University bibliothek der University Wuerzburg, Wuerzburg.
116. Davodeau, F., M. A. Peyrat, I. Houde, M. M. Hallet, G. De Libero, H. Vie, and M. Bonneville. 1993. Surface expression of two distinct functional antigen receptors on human gamma delta T cells. *Science* 260:1800-1802.
117. Kreiss, M. 2004. T-cell receptor binding and modulation of the T-cell activation through autoantigens of the rat. *PhD Thesis*. University bibliothek der University Wuerzburg, Wuerzburg.
118. Kreiss, M., A. Asmuss, K. Krejci, D. Lindemann, T. Miyoshi-Akiyama, T. Uchiyama, L. Rink, C. P. Broeren, and T. Herrmann. 2004. Contrasting contributions of complementarity-determining region 2 and hypervariable region 4 of rat BV8S2+ (Vbeta8.2) TCR to the recognition of myelin basic protein and different types of bacterial superantigens. *Int Immunol* 16:655-663.
119. Allison, T. J., C. C. Winter, J. J. Fournie, M. Bonneville, and D. N. Garboczi. 2001. Structure of a human gammadelta T-cell antigen receptor. *Nature* 411:820-824.

## REFERENCE

120. Roilo, M. 2009. The response of tumor cells to the inhibition of the mevalonate pathway. *Master Thesis*. University of Padua Padua, Italy.
121. Pyz, E., O. Naidenko, S. Miyake, T. Yamamura, I. Berberich, S. Cardell, M. Kronenberg, and T. Herrmann. 2006. The complementarity determining region 2 of BV8S2 (V beta 8.2) contributes to antigen recognition by rat invariant NKT cell TCR. *J Immunol* 176:7447-7455.
122. Acuto, O., and F. Michel. 2003. CD28-mediated co-stimulation: a quantitative support for TCR signalling. *Nat Rev Immunol* 3:939-951.
123. Kurakata, S., M. Kada, Y. Shimada, T. Komai, and K. Nomoto. 1996. Effects of different inhibitors of 3-hydroxy-3-methylglutaryl coenzyme A (HMG-CoA) reductase, pravastatin sodium and simvastatin, on sterol synthesis and immunological functions in human lymphocytes in vitro. *Immunopharmacology* 34:51-61.
124. Monkkonen, H., J. Kuokkanen, I. Holen, A. Evans, D. V. Lefley, M. Jauhiainen, S. Auriola, and J. Monkkonen. 2008. Bisphosphonate-induced ATP analog formation and its effect on inhibition of cancer cell growth. *Anticancer Drugs* 19:391-399.
125. Kistowska, M., E. Rossy, S. Sansano, H. J. Gober, R. Landmann, L. Mori, and G. De Libero. 2008. Dysregulation of the host mevalonate pathway during early bacterial infection activates human TCR gamma delta cells. *Eur J Immunol* 38:2200-2209.
126. Green, A. E., A. Lissina, S. L. Hutchinson, R. E. Hewitt, B. Temple, D. James, J. M. Boulter, D. A. Price, and A. K. Sewell. 2004. Recognition of nonpeptide antigens by human V gamma 9V delta 2 T cells requires contact with cells of human origin. *Clin Exp Immunol* 136:472-482.

## ABBREVIATION

Ab	Antibody
Ag	Antigen
$\alpha$ -GalCer	A-Galactosylceramide (2S, 3S, 4R)-1-O-( $\alpha$ -D-galactopyranosyl)-N-hexacosanoyl-2-amino-1,3,4-octadecanetriol)
ANT	Adenine nucleotide translocase
APC	Antigen presenting cell
BCG	Bacillus calmetteguerin
BCR	B cell receptor
BrHPP	Phosphorylated bromohydrin
BSA	Bovine serum albumin
BSS	Balanced salt solution
CD	Cluster of differentiation
cDNA	Complementary dna
CDR	Complementary determining region
DC	Dendritic cell
DEPC	Diethylpyrocarbonate
DETCs	Dendritic epidermal T cells
DMSO	Dimethyl sulfoxide
DNA	Deoxyribonucleic acid
dNTP	100 mm solution of each dATP, dCTP, dGTP, dTTP
DP	Double positive
dsRNA	Double-stranded RNA
EDTA	Ethylendiamintetracetic acid
FACS	Fluorescence activated cell scan

## ABBREVIATION

FCS	Fetal calf serum
FcεR	Fc epsilon receptor
FITC	Fluorescein isothiocyanate
FL	Fluorescence
FPP	Farnesyl pyrophosphate
FPPS	Farnesyl pyrophosphate synthase
FSC	Forward scatter
G418	Geneticin
GGPP	Geranyl-geranyl pyrophosphate
GGPPS	Geranyl-geranyl pyrophosphate synthase
GR	Glucocorticoid receptor
h	Hour
HMBPP	(E)-4-Hydroxy-3-methyl-but-2-enyl pyrophosphate
HMGR	HMG-CoA reductase
IDI	Isopentenyl pyrophosphate isomerase
IELs	Intraepithelial lymphocytes
IFN	Interferon
Ig	Immunoglobulin
IL	Interleukin
IPP	Isopentenyl pyrophosphate
kDa	Kilo dalton
LN	Lymph node
LTRs	Long terminal repeats
M	Molar
mAb	Monoclonal antibody
MBP	Myelin basic protein
Mev	Mevastatin
MHC	Major histocompatibility complex
MICA/B	MHC class I chain-related gene A/B
min	Minutes
miRNA	MicroRNA



## ABBREVIATION

mRNA	Messenger RNA
MVD	Mevalonate pyrophosphate decarboxylase
N-BPs	Aminobisphosphonates
NK	Natural Killer cell
NMR	Nuclear magnetic resonance
PAM	Pamidronate
PBS	Phosphate buffered saline
PCR	Polymerase chain reaction
PE	Phycoerythrin
RISC	RNA-induced silencing complex
RNA	Ribonucleic acid
RNAase	Ribonuclease
RNAi	RNA interference
RT	Room temperature
SCID	Severe combined immunodeficiency
sec	Seconds
shRNA	Short hairpin RNA
shRNAmir	Microna-adapted short hairpin RNA
siRNAs	Short interfering RNAs
SSC	Side scatter
TCR	T cell receptor
Tdt	Terminal deoxynucleotidyl transferase
TLR	Toll-like receptor
TNF	Tumor necrosis factor
TRIS	N, n, n', n'-tetramethylethylenediamine
ULBPs	UL16-binding proteins
V	Variable segment of the T cell receptor variable domain
YPM	Yersinia pseudotuberculosis mitogen
Zol	Zoledronate

# CURRICULUM VITAE

Jianqiang Li

---

*Signature*

**Date** November, 2009

## **Personal Dates**

- Place and date of birth: Hebei, China, 13 Aug. 1973
- Nationality: P. R. China
- Familiar Status: Married; One daughter.

## **Contact Information**

- Address: Versbacherstr. 7, D-97078 Würzburg, Germany
- Phone: +49-931-20149124
- Fax : +49-931-20149243
- e-mail: [limmune@gmail.com](mailto:limmune@gmail.com)

## **Education**

- M.B., Sept. 1991-Jul. 1996, Zhangjiakou Medical College, Clinical Laboratory Medicine.
- M.Sc, Sept. 2003-Jul. 2006, Peking Union Medical College, Immunology.  
Thesis title: The mechanism of  $\gamma\delta$  T cell activation via interaction between MICA and NKG2D.  
Advisor: Prof. Wei He

## CURRICULUM VITAE

- PhD, Oct. 2006-Now, University of Wuerzburg, Immunology.

Thesis title: Modulating expression of enzymes of isoprenoid metabolism: effects on V $\gamma$ 9V $\delta$ 2 T cells activation and tumor cell growth.

Advisor: Prof. Thomas Herrmann.

### **Employment History**

#### **Academic Appointments**

- Sept. 1996-Jul. 2001, Teaching Assistant, Yanjing Medical School, Capital University of Medical Sciences, Beijing, China.
- Aug. 2002-Oct. 2006, Lecturer/Instructor, Yanjing Medical School, Capital University of Medical Sciences, Beijing, China.

#### **Intern**

- May. 1995-Jun. 1996, Intern doctor, Clinical Immunology Laboratory, Beijing 302 Military Hospital, Beijing, China.

### **Professional Society Memberships**

- 1998-2006, Member of Chinese Society of Immunology.

### **Honors and Awards**

- Associated member of the Graduiertenkolleg “Immunomodulation”. Würzburg, Germany. 2007-2009.
- Travel awards of the 2rd international gammadelta T cell conference. Marseille, France (2008)

### **Publications**

#### **Peer-reviewed journal articles**

## CURRICULUM VITAE

1. **Li JQ**, Cui LX, He W: Distinct Pattern of Human Vdelta1 gammadelta T Cells Recognizing MICA (review). Cell Mol Immunol 2005, 2:253-258.
2. [CUI Yong-chun & **LI Jian-qiang**: The Research Progress of CD1 Molecules]. International Journal of Immunology [Chinese] 2006, 3, 129-132.
3. **Li, J.**, Herold, M.J., Kimmel, B., Muller, I., Rincon-Orozco, B., Kunzmann, V., and Herrmann, T. (2009). Reduced expression of the mevalonate pathway enzyme farnesyl pyrophosphate synthase unveils recognition of tumor cells by Vgamma9Vdelta2 T cells. J Immunol 182, 8118-8124.

### **Abstracts and/or Proceedings**

1. “**Li, J.**, Herold, M.J., Kimmel, B., Muller, I., Rincon-Orozco, B., Kunzmann, V., and Herrmann, T. Modulating the expression of enzymes of isoprenoid synthesis: effects on Vγ9Vδ2 T cell activation and tumor cell growth”. 2nd international gammadelta T cell conference, Marseille, France, May 21st-23rd, 2008. (Oral presentation)
2. “**Li, J.**, Herold, M.J., Kimmel, B., Muller, I., Rincon-Orozco, B., Kunzmann, V., and Herrmann, T. Reduced expression of the mevalonate pathway enzyme farnesyl pyrophosphate synthase unveils recognition of tumor cells by Vg9Vd2 T cells”. Doctoral Students Symposium 2009, Würzburg. (Poster)
3. “**Li, J.**, Rolio M, Herold, M.J., Kimmel, B., Muller, I., Rincon-Orozco, B., Kunzmann, V., and Herrmann, T. Reduced expression of the mevalonate pathway enzyme farnesyl pyrophosphate synthase unveils recognition of tumor cells by Vg9Vd2 T cells”. 7th Annual Meeting of CIMT, Mainz, June 3rd-5th, 2009. (Poster)
4. “**Li, J.**, Rolio M, Herold, M.J., Kimmel, B., Muller, I., Rincon-Orozco, B., Kunzmann, V., and Herrmann, T. Reduced expression of the mevalonate pathway enzyme farnesyl pyrophosphate synthase unveils recognition of tumor cells by Vg9Vd2 T cells”. 2nd European Congress of Immunology, Berlin, Sept 13th-16th, 2009. (Poster)

### **Languages:**

## CURRICULUM VITAE

- Chinese Mother tongue
- English Fluent knowledge
- German Basic knowledge

### Awards

Associated member of the Graduiertenkolleg “Immunomodulation”. Würzburg, Germany. 2007-2009.

Travel awards of the 2rd international gammadelta T cell conference. Marseille, France (2008).

### Additional Training

- From Bioinformatics to rational drug design. IRTG Summer School.
- Microarray Analysis Course. IZKF, Würzburg.
- 2-D gel Training. GRK-520, Würzburg
- Applied statistics for life science. GSLS, Würzburg.
- Patent Laws. GSLS, Würzburg.
- Presentation technique. GSLS, Würzburg.

**AFFIDATIV**  
**(Eidesstattliche Erklärung)**

The experimental work described in this thesis was carried out in the Institute of Virology and Immunology, University of Würzburg, Germany, from October 2006 to November 2009, under the supervision of Prof. Dr. Thomas Herrmann.

I hereby declare that my thesis entitled *Modulating the Expression of Enzymes of Isoprenoid Synthesis: Effects on V $\gamma$ 9v $\delta$ 2 T Cell Activation and Tumor Cell Growth* is the result of my own work. I did not receive any help or support from commercial consultants. All sources and/or materials applied are listed and specified in the thesis.

Furthermore, I verify that this thesis has not yet been submitted as part of another examination process neither in identical nor in similar form.

Würzburg.....  
Date Signature